Departament d'Enginyeria Telemàtica
UNIVERSITAT POLITÈCNICA DE CATALUNYA

CTTC

Universitat Politècnica de Catalunya

PhD Thesis

Energy Sustainability of Next Generation Cellular Networks through Learning Techniques

Author:
Marco Miozzo

Director:
Dr. Paolo Dini

Tutor:
Prof. Dr. Miquel Soriano

A project thesis submitted in fulfilment of the requirements for the degree of Doctor of Philosophy in the

Department of Telematic Engineering

Barcelona, May 2018

"Don't judge each day by the harvest you reap, but by the seeds that you plant."

Robert Louis Stevenson

UNIVERSITAT POLITÈCNICA DE CATALUNYA

Abstract

Department of Telematic Engineering

Doctor of Philosophy

Energy Sustainability of Next Generation Cellular Networks through Learning Techniques

by Marco Miozzo

The trend for the next generation of cellular network, the Fifth Generation (5G), predicts a 1000x increase in the capacity demand with respect to 4G, which leads to new infrastructure deployments. To this respect, it is estimated that the energy consumption of ICT might reach the 51% of global electricity production by 2030, mainly due to mobile networks and services. Consequently, the cost of energy may also become predominant in the operative expenses of a mobile network operator (MNO). Therefore, an efficient control of the energy consumption in 5G networks is not only desirable but essential. In fact, the energy sustainability is one of the pillars in the design of the next generation cellular networks.

In the last decade, the research community has been paying close attention to the energy efficiency (EE) of the radio communication networks, with particular care on the dynamic switch ON/OFF of the Base Stations (BSs). Besides, 5G architectures will introduce the Heterogeneous Network (HetNet) paradigm, where small BSs (SBSs) are deployed to assist the standard macro BS in satisfying the high traffic demand and reduce the impact on the energy consumption. However, only with the introduction of energy harvesting (EH) capabilities the networks might reach the needed energy savings for mitigating both the high costs and the environmental impact. In the case of HetNets with EH capabilities, the erratic and intermittent nature of renewable energy sources has to be considered, which entails some additional complexity. Solar energy has been chosen as reference EH source due to its widespread adoption and its high efficiency in terms of energy produced compared to its costs. To this end, in the first part of the thesis, a harvested solar energy model has been presented based on an accurate stochastic Markov processes for the description of the energy scavenged by outdoor solar sources.

The typical HetNet scenario involves dense deployments with a high level of flexibility, which suggests the usage of distributed control systems rather than centralized, where the scalability can become rapidly a bottleneck. For this reason, in the second part of the thesis, we propose to model the SBS tier as a multi-agent reinforcement learning (MRL) system, where each SBS is an intelligent and autonomous agent, which learns by directly interacting with the environment and by properly utilizing the past experience. The agents implemented in each SBS independently learns a proper switch ON/OFF control policy, so as to jointly maximize the system performance in terms of throughput, drop rate and energy consumption, while adapting to the dynamic conditions of the environment, in terms of energy inflow and traffic demand.

However, multi-agent might suffer the problem of coordination when finding simultaneously a solution among all the agents that is good for the whole system. In consequence, the Layered Learning paradigm has been adopted to simplify the problem by decompose it in subtasks. In particular, the global solution is obtained in a hierarchical fashion: the learning process of a subtask is aimed at facilitating the learning of the next higher subtask layer. The first layer implements an MRL approach and it is in charge of the local online optimization at SBS level as function of the traffic demand and the energy incomes. The second layer is in charge of the network-wide optimization and it is based on Artificial Neural Networks (ANNs) aimed at estimating the model of the overall network.

Acknowledgements

It has been a very long journey arrive till here. When I started I was convinced that it would taken a few years at most, after many years in the ambient of the research. On the contrary, I realized soon that it would be a very tough task, especially for balancing this important work with my job and my personal life. Therefore, I would like to thanks all the people that with their great support helped me in finding that good balance both from technical and non-technical perspective.

First and foremost, I would like to thank my family, that always provided me a very important moral support during all the years that I spent in my formation. Despite of being a bit far from me, you have contributed to all the successes in my educational career. I would like to special thanks my mother, that has been always for me the most important example of effort and dedication, *grazie mamma*. Of course, thanks to all my friends, that helped me in disconnecting from the technical work and be more productive.

I would like to express my sincere gratitude to my advisor Dr. Paolo Dini for the continuous support of my Ph.D study and of all the related research. Throughout all these years, he has patiently assisted me with motivation, constructive criticism and moral support, both for my studies and my professional growth. Definitely, his guidance helped me a lot in becoming a better researcher, thanks to his unceasing work for provoking my creativity and sense of critic.

Finally, I would like to thanks all the colleagues that supported me during these years with their motivation, with their inspiring technical conversations and also with wonderful moments all around the world.

Marco Miozzo

Barcelona, September 2018

Contents

List of Figures

List of Tables

Abbreviations

3G	**3**-rd **G**eneration
3GPP	**3**-rd **G**eneration **P**artnership **P**roject
4G	**3**-th **G**eneration
5G	**5**-th **G**eneration
ACF	**A**uto **C**orrelation **F**unction
AI	**A**rtificial **I**ntelligence
ANN	**A**rtificial **N**eural **N**etwork
ARPU	**A**verage **R**evenue **P**er **U**nit
BBU	**B**ase **B**and **U**nit
BS	**B**ase **S**tation
CAGR	**C**ompound **A**nnual **G**rowth **R**ate
CAPEX	**CAP**ital **EX**penditure
CoMP	**Co**oordinated **M**ulti **P**oint
CTMC	**C**ontinous **T**ime **M**arkov **C**hain
CRAN	**C**loud **R**adio **A**ccess **T**echnology
CSI	**C**hannel **S**tate **I**nformation
DP	**D**ynamic **P**rogramming
DR	**D**emand **R**esponse
DSM	**D**emand **S**ide **M**anagement
EDS	**E**nergy **D**ependent **S**et
EPN	**E**nergy **P**acket **N**etwork
EE	**E**nergy **E**ffciency
EH	**E**nergy **H**arvesting
EDR	**E**nergy **D**epleting **R**ate
ETSI	**E**uropean **T**elecommunications **S**tandards **I**nstitute

FPGA	**Fi**eld **P**rogrammable **G**ate **A**rray
GOPS	**G**iga **O**peration **P**er **S**econd
GSMA	**G**lobal **S**ystem for **M**obile communications **A**ssociation
GPM	**G**reen **P**ower for **M**obile
HAMRL	**H**euristically **A**ccelerated **M**ulti-agent **R**einforcement **L**earning
HCRAN	**H**eteregeneous **C**loud **R**adio **A**ccess **T**echnology
HBS	**H**igh-power **B**ase **S**ation
ICIC	**I**ter **C**ell **I**nterference **C**oordination
KS	**K**ernel **S**moothing
ICT	**I**nformation and **C**ommunication **T**echnologies
LL	**L**ayered **L**earning
LTE	**L**ong **T**erm **E**volution
LBS	**L**ow-power **B**ase **S**ation
MAC	**M**edia **A**ccess **C**ontrol
MBS	**M**acro **B**ase **S**ation
MCS	**M**odulation and **C**oding **S**cheme
MDP	**M**arkov **D**ecision **P**rocess
MFNN	**M**ulti-layer **F**eedForward **N**eural **N**etworks
MISO	**M**idcontinent **I**ndependent **S**ystem **O**perator
ML	**M**achine **L**earning
MNO	**M**obile **N**etwork **O**perator
MPPT	**M**aximum **P**ower **P**oint **T**racking
MRL	**M**ult-agent **R**einforcement **L**earning
NN	**N**eural **N**etwork
NFV	**N**etwork **F**unction **V**irtualization
NREL	**N**ational **R**enewable **E**nergy **L**aboratory
OPEX	**OP**erative **EX**penditure
PA	**P**ower **A**mplifier
PDCCH	**P**hysical **D**ownlink **C**ontrol **C**hannel
PPDR	**P**ublic **P**rotection and **D**isaster **R**elief
PPP	**P**oint **P**oisson **P**rocess
PV	**P**hoto **V**oltaic
QoE	**Q**uality of **E**xperience

QoS	**Q**uality of **S**ervice
RB	**R**esource **B**lock
RES	**R**enewable **E**nergy **S**ource
RL	**R**enforcement **L**earning
RRH	**R**emote **R**adio **H**ead
RRM	**R**adio **R**esource **M**anagement
SBS	**S**mall **B**ase **S**ation
SDN	**S**oftware **D**efined **N**etworking
SINR	**S**ignal to **I**nterference plus **N**oise **R**atio
TD	**T**emporal **D**ifference
UE	**U**ser **E**quipment
UDN	**U**tra **D**ense **N**etwork

Dedicated to my parents, Adriana and Aldo.

Chapter 1

Introduction

1.1 Scenario and Motivation

Energy efficiency in cellular networks is becoming a key requirement for network operators to reduce their operative expenditure (OPEX) and to mitigate the footprint of Information and Communication Technologies (ICT) on the environment. Costs and greenhouse gases emissions of ICT grew in the last few years due to the escalation of traffic demand from mobile devices such as smartphones and tablets. The global mobile data traffic grew 63% in 2016 [2], also cloud-based and Internet of Things services are expected to further aggravate this trend. In fact, mobile traffic will increase sevenfold between 2016 and 2021, which correspond to an increase at a compound annual growth rate (CAGR) of 47%, reaching 49.0 exabytes per month by 2021. Therefore, it is commonly accepted that the fifth generation (5G) of cellular networks will support $1,000$ times more capacity per unit area than 4G.

According to a recent report by Digital Power Group [3], the world's ICT ecosystem already consumes about 1500 TWh of electric energy annually, approaching 10% of the world electricity generation and the $2-4\%$ of carbon footprint by human activity. For example, the energy consumption of ICT represents the 25% of all car emissions in the world and it is equal to all airplane emissions in the world. Telecom operators consume 254 TWh per year (77% of the worldwide electricity consumption of the ICT) with an annual growth rate higher than 10% [4]. Telecom Italia is the second industry in Italy for energy consumption after only the railway industry. Besides, considering the mobile traffic growth rate, it is expected to reach up to the 51% in 2030 [5]. Nowadays the energy bill of mobile network operators (MNO)s has become an important portion of their OPEX, e.g., it already reaches the cost of the personnel required to manage the network for a Western European MNO in 2007 [6]. Consequently, the Average Revenue

Per Unit (ARPU) has been decreasing across the years. A notable example is represented by the case of Vodafone Germany, that experienced an annual shrinking of 6% on average in the period 2000-2009 [6].

Consequently, many major industries have already put environmental sustainability in their roadmap to 5G [7, 8]. This can be translated in a change of the design paradigm of the next generation cellular networks, shifting from coverage and capacity oriented systems, typical of 3G and 4G networks, to energy oriented in 5G. Many standardization bodies already started working on this aspect, e.g., the European Telecommunications Standards Institute (ETSI) [9] and the 3rd Generation Partnership Project (3GPP) [10]. In addition, governmental bodies have introduced policies fostering the usage of sustainable energy for reducing the greenhouse gas emissions due to the human activity. Recently, EU started a plan on energy and climate targets for 2030, which includes the minimum target of 27% for the share of renewable energy consumed in the union [11]. The goal is to arrive with zero carbon emissions in 2060.

In the last decade, the research community has been paying close attention to the *energy efficiency* (EE) of the radio communication networks. The effort concentrated in adjusting the network capacity according to the actual traffic conditions. In fact, up to now, the predominant system design paradigm was to deploy networks able to satisfy the peak of traffic, independently of the time they occur and their duration. However, the most energy hungry component of the cellular network is represented by the access part, which approaches the 80% of the total consumption [12]. In consequence, dynamically switch ON/OFF base stations (BSs) [13] have been identified as one of the most promising EE technique. However, this solution has been received distant from MNOs since it might generate problems of coverage holes and possible failures of network equipment due to the frequent ON/OFF switches.

As a result, the introduction of energy harvesting (EH) capabilities represents an interesting approach to further increase the energy savings allowing simultaneously to mitigate both the costs and the environmental impact of new mobile telecommunication systems. In fact, thanks to the progress in the hardware of the network equipment, the BSs peak power consumption decreased from 3 KW for the 2G BSs to a thousand of W for the 4G ones. In the last years, the idea of using renewable energy sources (RESs) in cellular networks has been already proposed, like in [14] and [15]. However, it has been exploited only in very specific scenarios where the grid connection was not present or extremely unreliable, such as in rural areas. In these cases, solar and wind power has been used in hybrid installation for integrating the diesel generators due the high energy requirements of old BSs. Starting from 2008, the GSM Association (GSMA) has begun the Green Power for Mobile Programme for promoting and investigating the usage of renewable energies for powering the $118,000$ off-grid BSs in developing countries, which would allow the saving of 2.5 billion of liter of diesel per year (0.35% of global diesel consumption of the 700 billion). One of the main challenges for 5G networks for enabling higher energy savings with EH will be its integration with the smart grid technology. In particular, MNOs can adopt the micro-grids architecture, which has been defined by the US Department of Energy as "a group of interconnected loads and distributed energy resources (mainly renewables) within clearly defined electrical boundaries that act as a single controllable entity with respect to the power grid". A micro-grid would enable to connect and disconnect from the grid and to operate in both grid connected and island mode. A further step has been done by the European Union with recently released the EU Winter Package, aimed at providing guidelines for the next generation of power grids. The main idea is to foster cooperation among local energy communities by providing them with the infrastructure to work in island mode and with market-based retail energy prices.

Moreover, 5G will bring ultra-dense networks (UDN) of small BSs (SBSs), especially for satisfying the high traffic demand in urban scenarios [16]. The UDNs consist on a multi-tier network architecture where SBSs with reduced coverage (e.g., picocells, femtocells and microcells) are deployed in massive numbers to provide primarily capacity enhancements, while the traditional pre-planned tier of macro BSs (MBSs) is preserved to provide baseline capacity and coverage. This architecture is also known as HetNet. This paradigm has a twofold motivation: firstly the SBSs resources are shared among a lower number of users due to the smaller coverage area of the SBS and, secondly, by decreasing the distance between the transmitter and the receiver, communications experience better channel conditions which implies the usage of more efficient modulation and coding schemes (MCSs). Moreover, SBSs have the potential of substantially reducing the energy consumption of the network [17], due to the low power dissipation of the transmission components (i.e., power amplifier and its cooling system) combined with the higher spectral efficiency. In fact, the energy consumption of the SBSs is reduced to a hundred of W for the micro cells and tens of W for the pico ones. This implies that applying switch ON/OFF strategies to this new architecture has limited impact on the EE [18] but helps in introducing energy harvesting capabilities. The typical renewable system is composed by a photovoltaic (PV) solar panels and a battery for the energy storage, to allow the accumulation of the exceed energy that cannot be directly used and make it available for the periods when PV source is not generating energy. Therefore, a proper harvesting and storage system design is needed to provide a reliable energy income to the BS. Standard design approaches are usual to model the system for guaranteeing its full self-sustainability. However, in this case the obtained PV sizes result in impractical deployments, especially in urban scenarios (e.g., in street furniture) [19].

Therefore, an optimization of the energy utilization is needed. The SBSs together with the distributed energy harvesters and storage systems can be coordinated by dynamic renewable energy management, similarly to what done for micro-grids [20].

However, by reducing the capacity of the harvesting system, the intermittent and erratic nature of the renewable energies has to be considered in order to be able to manage the high variations in the incoming energy. In fact, even in summer and in good weather conditions areas like Los Angeles, the harvested energy in the peak irradiation hour can vary up to the 85%, as showed in [21]. Similarly, also seasons have a strong impact in the energy income and have to be considered when optimizing for having a solution working for the whole year.

Self-Organized Network (SON) paradigm is expected to be a key enabler in 5G to provide intelligence and autonomous adaptability to network elements for improving the system efficiency and simplifying the management of such a complex architecture. In particular, softwarization and Artificial Intelligence (AI) have been identified as the main technologies for implementing the SON paradigm and providing a flexible and dynamic Radio Resource Management (RRM). On the one hand, Software Defined Networking (SDN) [22] and Network Function Virtualization (NFV) [23] provide a flexible infrastructure for collecting the necessary system information and reconfiguring the network elements [24]. SDN separates control and data planes and, by centralizing the control, enables many advantages such as programmability and automation. NFV enables softwarized implementation of network functions on a general purpose hardware, improving scalability and flexibility. On the other hand, AI gives the tools for automatic and intelligent system (re-)configuration [25]. Machine learning (ML) contributes with valuable solutions to extract models that reflect the user and network behaviors. Reinforcement Learning (RL) can be used for more dynamic decision making problem working in real-time and at short time scales.

SBSs powered by renewable energies can help in reducing the impact of ICT in the carbon emissions by saving energy in the SBS tier and allowing the adoption of energy efficiency mechanisms in the macro BS. Like in a symbiotic process, SBSs can in parallel move toward a more energy efficient network paradigm and, at the same time, help in solving the problem of the huge demand. As presented in [26], the use of small-cell networks represents a challenging solution for targeting the future traffic demand in a cost and energy efficient way even without the usage of renewable energies. However, according to the expected performance of Long Term Evolution (LTE) UDNs, cellular networks can move to a more sustainable paradigm cutting down their energy grid dependency in a seamless way with respect to the QoS provided becoming a reference architecture for 5G solutions.

1.2 Problem Statement

The introduction of RES in HetNet is not only an integration engineering problem, since it has to deal with the characterization of intermittent and/or erratic energy sources, and the design, optimization and implementation of core network, BS and mobile elements especially considering the need of massive deployment for targeting the high demand. In detail, the following issues need to be solved:

1. *Characterization of the RESs:* In order to optimize the behavior of the network, a detailed characterization of the energy income has to be performed since, considering the intrinsic nature of the RES, their availability is not deterministic. For instance, solar harvested energy is ruled by atmospheric conditions (i.e., seasons, weather, geographic location, etc.) and can be also affected by specific installation phenomena (e.g., partial shadowing by trees or buildings). On this matter, a statistical behavior can help in accurately include the RES behavior in the design of network.

2. *Characterization of the network usage patterns:* Similarly to RES, there are crucial elements of the network that have to been characterized in order to correctly model it. The energy drained by the BSs represents one of the most important one, since it is one of the variables that enables the energy efficient optimization toward a sustainable network. In turn, as presented in [17], the energy needed by a BS is related to the amount of traffic it is has to serve; therefore, spatial-temporal traffic models have to be take into account, too.

3. *Self-organization:* Considering that the SBSs will be massively deployed, self-organization is essential for efficiently managing radio resources of SBSs, due to their huge number and unknown position. It is expected that SBSs need to have the capability of autonomously making RRM decisions without compromising the macro cell performances. For instance, SBSs can share their traffic with the macro layer when they experience low battery or low traffic. Load balancing becomes of crucial importance for the operators and has to consider a new variable, the energy reserves of the SBSs. However, SBSs will be massively deployed, possibly some of them in a dynamic fashion (e.g., for capacity extension during high traffic spot-like events like concerts, football matches, etc.), their number and position will be unknown to the network operator, so that the load balancing cannot be handled only by means of centralized static solutions.

4. *QoS:* SBSs dimensioning and corresponding resource allocation is an important aspect of HetNet design, since they are expected to be deployed at massive scale

and in an uncoordinated fashion. Towards this objective, an efficient joint management of the traffic demand and the energy reserves in the SBSs is also a challenge. The design of online RRM solutions for cellular networks with energy constrained elements is an open issue and is a novel topic in literature.

5. *Low power consumption:* Despite of the already low power consumption of the SBSs, energy saving mechanisms for reducing the power consumption of the SBSs by improving PHY related technologies and layer 2 algorithms will help in scale down the equipment needed by RES and in, more in general, in their management. Recently, the softwarization of the radio access part started attracting interest due to the high flexibility it enables.

6. *Energy market trends:* The trend in energy market is that the energy price in future power grids will change hourly. However, standard networks are not optimized to this respect, since in general the network energy consumption directly depends on the requested capacity. Using RES, the network will have now an energy reserve which enables the possibility to trade some of the energy that they harvest.

In this Ph.D. dissertation we focus on a subset of the open issues of the energy sustainability of self-organized HetNet partially powered by RES from an online RRM perspective. In particular, we will pay special attention to the open issues described in points 1, 3, 4 and 6.

1.3 Objectives and Methodology

The goal of this thesis is to investigate on scenarios where harvested ambient energy is employed to steer LTE HetNets toward a more sustainable paradigm, reducing the energy consumption from the grid and, more than that, where communication networks blend with future electricity grids, as the one depicted in Fig. 1.1. The usage of RES can be distinguished in two different operative cases: i) energy self-sustainable network elements and ii) grid energy saving thanks to the efficient use of the network elements powered with RES. In the first paradigm, the problem is to guarantee network reliability by managing the limited available energy resources since there is no connection to the electric grid. While, in the second vision, RESs are used as an alternative green solution for powering part of the network in order to reduce its carbon footprint and represents the core of the contribution. It is to be noted that, the second paradigm can, in turns, have a further extension which comprises the possibility that future network elements may trade some of the energy that they harvest to make profit and provide ancillary services to the power grid. In pico deployments, for instance, it may occur in the form of

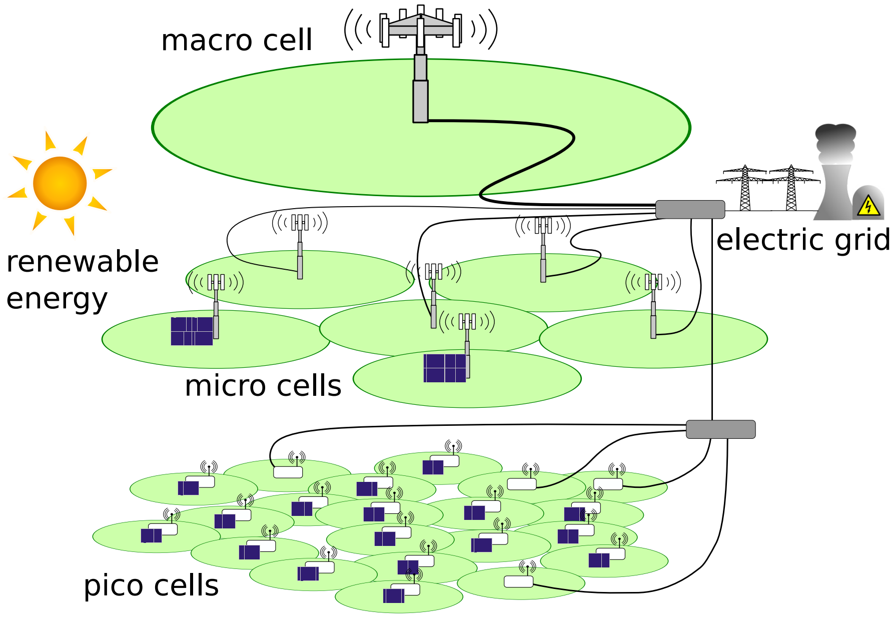

FIGURE 1.1: HetNet powered with RES reference architecture.

supporting connected loads, such as street lighting or weather stations. Instead, selling energy to the grid operator may make sense for micro and macro cells where the amount of energy harvested easily matches or surpasses that of residential users.

Solar energy has been chosen as reference RES due to its widespread adoption and its high efficiency in terms of energy produced compared to its costs. To this end, an harvested solar energy model has been implemented through a simple but yet accurate stochastic Markov processes for the description of the energy scavenged by outdoor solar sources. The Markov models that we derived are obtained from extensive solar radiation databases. The basic idea is to derive the corresponding amount of energy from hourly radiance patterns that is accumulated over time in order to represent it in terms of its relevant statistics. We tested Markov models with different number of states and data clusterization models for having both simple solutions and accurate ones.

We characterized the problem of distributed energy aware SBS control by considering the aforementioned Markov processes for modeling the solar energy harvested. The high dynamism typical of the HetNet scenarios jointly with the complexity of the system suggest the usage of distributed control systems rather than centralized, where the scalability and the flexibility can become rapidly a bottleneck. We focus on the energy aware online control for improving the energy-efficiency of the system by optimizing the usage of the renewable energy reserves in the SBS tier. We propose to model the SBS tier as a multi-agent system [27], where each SBS is an intelligent and autonomous agent, which learns by directly interacting with the environment and by properly utilizing the past experience. The novel solution will make able the SBS tier to work without the knowledge of the traffic demand and the expected solar harvested energy income. Due to the complexity and the dynamism of the scenario, which does not allow to define an integrated probabilistic model, we propose to solve the RRM with a reinforcement learning solution [28].

Multi-agent RL (MRL) systems are an effective way to treat complex, large and unpredictable problems since they offer modularity in distributing the implementation of the solution across different agents. However, such distribution might suffer the problem of finding simultaneously a solution among all the agents that is good for the whole system. Therefore, the Layered Learning (LL) [29] and heuristically accelerated MRL (HAMRL) [30] paradigms are adopted to simplify the problem by decompose it in subtasks. The global solution is then obtained in a hierarchical fashion: the learning process of a subtask is aimed at facilitating the learning of the next higher subtask layer. We adopted the logical layers classification intrinsic in the nature of the HetNet. The first layer implements an MRL approach and is in charge of the local online optimization at SBS level as function of the traffic demand and the energy incomes. The second layer is in charge of the network-wide optimization and is based on Artificial Neural Networks (ANNs) aimed at estimating the model of the overall network. The architecture for implementing the two levels and enable their interaction is based on a SDN paradigm. According to the review of the literature, this is the first work in the literature that has proposed online solutions with realistic environmental conditions and considering the optimization across different energy harvesting conditions, as will be also discussed in Chapter 2.

1.4 Outline of the thesis

This section gives a brief overview of the contents of the following chapters, which are summarized in Fig. 1.2.

Chapter 2

This chapter provides the necessary background information concerning the description of network design and switching ON/OFF approaches presented in the literature. It starts with the required background knowledge, including a description of the reference scenarios and architectures. In continuation, a survey of the state-of-the-art and current trends is given. The chapter examines the energy efficient solutions that are applied in two different network architectures: single-tier and HetNet. In this chapter some preliminary work devoted to evaluate the feasibility of the solutions investigated are also presented for introducing the reference solutions for HetHet with EH capabilities.

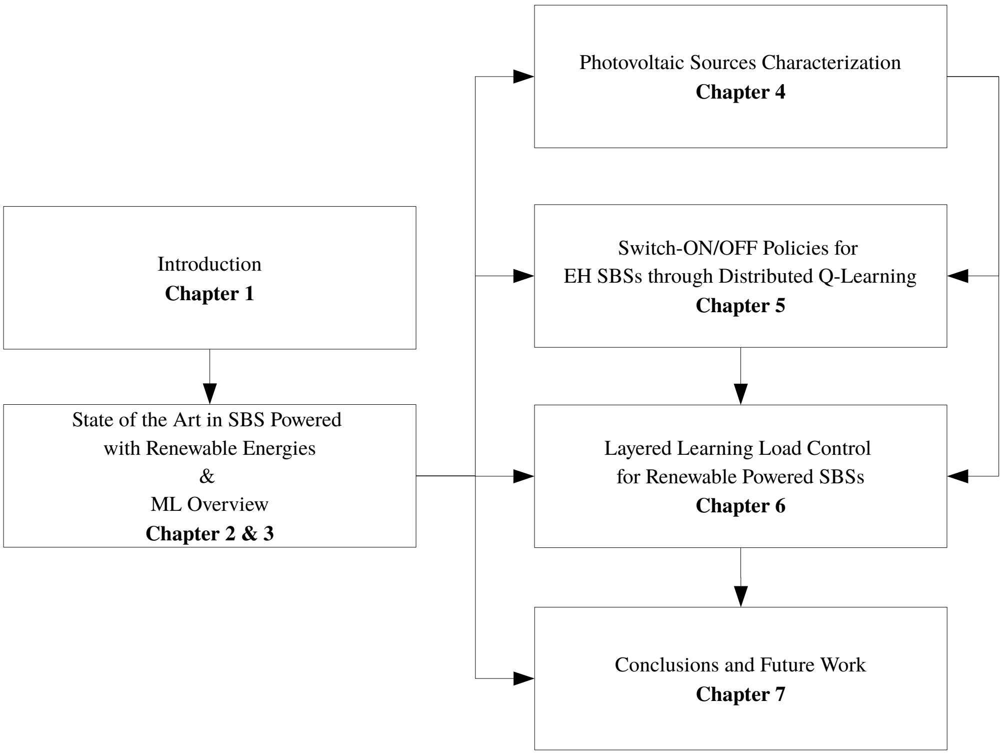
Photovoltaic Sources Characterization
Chapter 4
Introduction
Chapter 1
Switch-ON/OFF Policies for
EH SBSs through Distributed Q-Learning
Chapter 5
State of the Art in SBS Powered
with Renewable Energies
&
ML Overview
Chapter 2 & 3
Layered Learning Load Control
for Renewable Powered SBSs
Chapter 6
Conclusions and Future Work
Chapter 7

FIGURE 1.2: Outline of the dissertation.

The work presented in this chapter has been published in the following papers:

- G. Piro, M. Miozzo, G. Forte, N. Baldo, L.A. Griego, G. Boggia, P. Dini, "HetNets Powered by Renewable Energy Sources: Sustainable Next-Generation Cellular Networks", in *IEEE Internet Computing*, vol. 17, no. 1, pp. 32-39, Jan.-Feb. 2013.

- D. Zordan, M. Miozzo, P. Dini, M. Rossi, "When telecommunications networks meet energy grids: cellular networks with energy harvesting and trading capabilities", in *IEEE Communications Magazine*, vol. 53, no. 6, pp. 117-123, June 2015.

- N. Piovesan, A. Fernandez Gambin, M. Miozzo, M. Rossi, P. Dini, "Energy sustainable paradigms and methods for future mobile networks: A survey", *Computer Communications*,Volume 119,2018,Pages 101-117.

- P. Dini, M. Miozzo, N. Bui, N. Baldo, "A Model to Analyze the Energy Savings of Base Station Sleep Mode in LTE HetNets", *in Proceedings of IEEE GreenCom 2013*, 20-23 August 2013, Beijing (China).

- N. Baldo, P. Dini, J. Mangues, M. Miozzo, J. Núñez-Martínez, "Small cells, wireless backhaul and renewable energy: a solution for disaster aftermath communications", *in Proceedings of 4th International Conference on Cognitive Radio and Advanced Spectrum Management (COGART 2011) - Cognitive and Self-Organizing Networks for Disasters Aftermath Assistance*, 26-29 October 2011, Barcelona (Spain).
- M. Miozzo and N. Bartzoudis and M. Requena and O. Font-Bach and P. Harbanau and D. López-Bueno and M. Payaró and J. Mangues, "SDR and NFV extensions in the ns-3 LTE module for 5G rapid prototyping", *in Proceedings of 2018 IEEE Wireless Communications and Networking Conference (WCNC)*, April 2018, Barcelona (Spain).

Chapter 3

The main principles of the theory behind the ML methods used in this thesis are presented in chapter 3. The overview of reinforcement learning algorithms is discussed for both the single-agent and multi-agent case, introducing the algorithms used and their main challenges in the application in the considered scenario. Finally, an introduction on neural networks and on their training solutions is presented.

Chapter 4

Chapter 4 provides a novel model for the energy harvesting process, describing the methodology to model the energy inflow as a function of time through stochastic Markov processes. The proposed approach has been validated against real energy traces, showing good accuracy in their statistical description in terms of first and second order statistics. This model will be used for generating the solar harvested energy profile in the evaluation of the HetNet control solutions proposed in this thesis.

The work presented in this chapter has been published in this paper:

- M. Miozzo, D. Zordan, P. Dini, M. Rossi, " SolarStat: Modeling Photovoltaic Sources through Stochastic Markov Processes", *in Proceedings of IEEE Energy Conference*, 13-16 May 2014, Dubrovnik (Croatia).

Chapter 5 In this chapter we present the innovative contribution of this thesis on the online control of HetNet with EH capabilities. Different distributed Q-learning solutions are investigated both analyzing their temporal behavior and their network performance. The results presented, despite of being encouraging, show that scalability of the solution might be a problem in case of dense SBSs networks.

The work presented in this chapter has been published in the following papers:

- M. Miozzo and L. Giupponi and M. Rossi and P. Dini, "Distributed Q-learning for Energy Harvesting Heterogeneous Networks", *in Proceedings of 2015 IEEE International Conference on Communication Workshop (ICCW)*, June 2015, London (UK).
- M. Miozzo and L. Giupponi and M. Rossi and P. Dini, "Switch-On/Off Policies for Energy Harvesting Small Cells through Distributed Q-Learning", *in Proceedings of 2017 IEEE Wireless Communications and Networking Conference Workshops (WCNCW)*, March 2017, San Francisco (USA).

Chapter 6

In Chapter 6, the Layered Learning solution for HetNet powered with solar energy is presented. In particular, a hierarchical framework based on a two-layered optimization has been adopted: where the bottom layer implementing multi-agent RL is enhanced by the above layer through its network-wide view through a control based on neural networks. The goal is to improve the coordination of the agent issues of distributed Q-learning solutions for guaranteeing high EE in systems with dense deployment of SBSs. Simulation results prove that the proposed layered framework outperforms both a greedy and a completely distributed solution both in terms of throughput and energy efficiency.

The work presented in this chapter has been published in the following papers:

- M. Miozzo and P. Dini, "Layered Learning Radio Resource Management for Energy Harvesting Small Base Stations", *in Proceedings of 2018 IEEE Vehicular Technology Conference (VTC Spring)*, June 2018, Port (Portugal).
- M. Miozzo and N. Piovesan and P. Dini, "Layered Learning Load Control for Renewable Powered Small Base Stations", *submitted to IEEE Transactions on Green Communications and Networking.*

Chapter 7

The document is closed with Chapter 7, where the high level assessment of the achievements accomplished through the research presented herein, the conclusions and perspectives for future works are presented.

Chapter 2

State of the Art and Beyond

2.1 Introduction

In the last decade several solutions have been proposed for reducing the energy consumption of the radio communication networks, as testified by the vivid literature on this topic [31]. In general, this family of solutions has been named as *green communication and networking* and it includes models to characterize the energy consumption of the network elements and strategies for energy optimization for all the layers of the protocol stack, such as: power amplifiers, radio transmission techniques, media access control (MAC) algorithms, networking solutions and architectures.

In terms of energy consumption, the most important element of the network is represented by the BS, according to it impact of 80% in the energy budget of the overall radio access network [12]. Consequently, the main effort concentrated in optimizing the network from BS usage perspective. To this end, two main approaches have been adopted so far: *offline* and *online* optimization. The formers are usually based on stochastic geometric and are devoted to draw the general trends and guidelines for deploying optimal energy architectures without considering specific details of the scenario. The latter are usually sub-optimal solutions which however can consider more realistic models of the system components and allows a closer approximation to realistic scenarios. To this end, learning solutions represent a valuable way to implement a self-organization approach that enables to deploy cellular network in a flexible way able to adapt to the most important environmental variables. This background information is important, since it facilitates the understanding of the motivations behind the contributions of this thesis.

This chapter is structured as follows: Section 2.2 introduces the energy consumption model of the different types of BSs, which allows to better understand the principles behind the energy efficiency solutions. Section 2.3 presents the review of the existing literature with the more consolidated energy efficiency techniques for both standard cellular network and for the ones with EH capabilities. After presenting the most common methods and widely used solutions found in the literature, a description of the research challenges and open issues is given in Section 2.4, introducing the main contributions of this thesis. Finally, Section 2.5 concludes the chapter.

2.2 BS Energy Model

Before delving into the description of the techniques to make the network energy efficient and self-sufficient, next we review the main achievements in power consumption measurement and models for base stations. One of the most detailed BS energy models adopted in literature has been developed in the framework of the Energy Aware Radio and neTwork tecHnologies (EARTH) EU founded project [32]. By taking in consideration the principal elements that drain energy in a LTE BS (i.e., power amplifiers, baseband unit, radio frequency module, AC-DC converters, the main supply unit and the cooling system), in [17] an accurate model has been derived. As depicted in Fig. 2.1, the power amplifier (PA) is one of the main power draining component in all type of the BSs. Moreover, PA generates a dependency on the load of the BS both in macro and micro BS. In the former, the power consumption can change up to the 44%, while in the latter 27%. Reducing the form factor and the PA needs, the cooling system (CO) part disappears but the one of the baseband processor (BB) increases its contribution. However, it is to be noted that, for very small BSs like pico and femto, the load of the BS marginally affects the power consumption.

The BS power consumption model presented in Fig. 2.1 can be approximated with a linear function, defined as follows:

$$P = P_0 + \beta\rho \tag{2.1}$$

where $\rho \in [0, 1]$ is the traffic load of the BS normalized to its maximum capacity, and P_0 is the power consumption when $\rho = 0$. The values of P_0 and β for each type of BS are reported in table 2.1.

Remarkably, P_0 represents a significant part of the total energy consumed by any BS and, due to this, researchers have investigated the use of sleep modes during low traffic periods. Moreover, it is expected that P_0 of new sites will be reduced by about 8% on average thanks to recent technological advances [33], thus further decreasing the BS energy cost during low traffic periods.

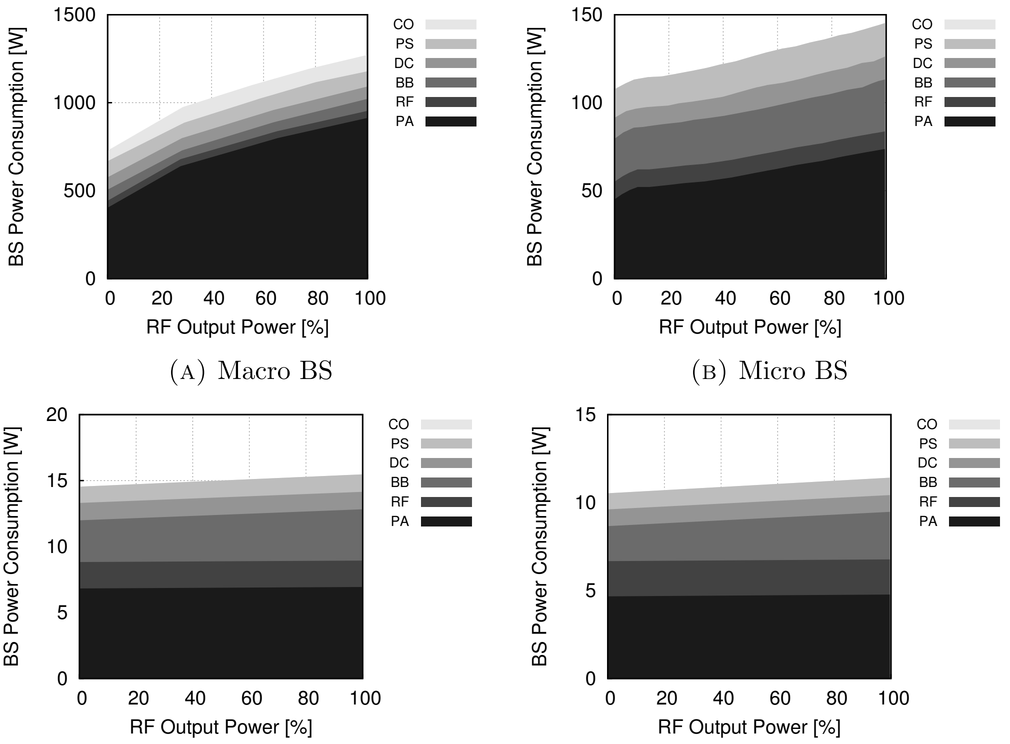

(A) Macro BS

(B) Micro BS

(C) Pico BS

(D) Femto BS

Figure 2.1: Power consumption dependency on relative linear output power in all BS types for a 10MHz bandwidth, 2x2 MIMO configurations and 3 sectors (only Macro) scenario based on the 2010 State-of-the-Art estimation. Legend: PA=Power Amplifier, RF=small signal RF transceiver, BB=Baseband processor, DC: DC-DC converters, CO: Cooling, PS: AC/DC Power Supply [1].

Table 2.1: Power model parameters for various types of BS.

BS Type	P_0 [W]	β
Macro	750.0	600
Micro	105.6	39
Pico	11.6	1.1
Femto	10.4	0.9

In the next future, the introduction of SDR and SDN-NFV solutions enabled a further degree of flexibility in the architecture of the network by allowing to split network functionalities in different network elements. This process started a few years ago with the Cloud Radio Access Network (CRAN) solutions [34], in which only some physical layer processing is left next to the antenna, called the remote radio head (RRH), while the baseband processing is carried out in data centers, namely base band unit (BBU). More recently, Heterogeneous Cloud Radio Access Network (HCRAN) architecture [35] introduced new type of virtualizations by decoupling transmissions functions from proprietary hardware-dependent implementations, enabling their execution in different hardware resource of the network. Various splits at PHY, MAC, RLC and PDCP layers are considered for relaxing the stringent requirements of CRAN while maintaining its centralized processing benefits [36]. The energy model of such novel architectures has not been yet proposed in literature. However, it can be estimated based on the model introduced in [37], which is a general flexible power model of LTE base stations and provides the power consumption in Giga Operation Per Second (GOPS). To this respect, in [38] and [39] we provided a preliminary assessment on the energy consumption figures of different HCRAN configurations through an emulation platform based on the LTE module of the popular ns-3 Network simulator [40] and a real-time implementation of the physical layer functionalities based on field-programmable gate array (FPGA). From this analysis, we showed that important energy savings can be obtained at RRH when moving part of the lower layer network functionalities to the BBU. Moreover, we highlighted also that the bandwidth of the system is the most important parameter for what concern the energy consumption of the RRH since it can affect up to 50% on the overall energy budget of the RRH.

2.3 Techniques for Energy Efficiency

2.3.1 Single Tier Networks

In standard 3G architectures, where the type of BSs is reduced to macro and micro and they are treated as a single tier, the most promising solution to optimize the BS energy consumption is by putting them in *sleep mode* (or OFF mode). In this case, in order to sleep a BS and guarantee the coverage, the BSs in the set of the ones that remain awake (ON mode) have usual to re-adjust their transmission power and, possibly, the tilt of the antenna, enabling the communications also the users that was previously served by the BS slept, technique called *cell zooming* or *cell breathing.*

Sleep Mode

The cellular networks have been dimensioned to support traffic peaks, i.e., the number of BSs deployed in a given area should be able to provide the required Quality of Service (QoS) to the mobile subscribers during the highest load conditions. However, during off-peak periods the network may be underutilized, which leads to an inefficient use of spectrum resources and to an excessive energy consumption (note that the energy drained during low traffic periods is non-negligible due to the high values of P_0 in Eq. (2.1)). For these reasons, sleep modes have been proposed to dynamically turn OFF some of the BSs when the traffic load is low. This has been extensively studied in the literature, considering different problem formulations [13]. However, since BSs cannot serve any traffic when asleep, it is important to properly tune the enter/exit time of sleep modes to avoid service outage.

The authors of [41] propose centralized and distributed clustering algorithms to cluster those BSs exhibiting similar traffic profiles over time. Upon forming the clusters, an optimization problem is formulated to minimize their power consumption. Optimal strategies are found by brute force, since the solution space is rather small and its complete exploration is still doable. A similar approach is presented in [42] where a dynamic switching ON/OFF mechanism locally groups BSs into clusters based on location and traffic load. The optimization problem is formulated as a non-cooperative game aiming at minimizing the BS energy consumption and the time required to serve their traffic load. Simulation results show energy costs and load reductions while also provide insights of when and how the cluster-based coordination is beneficial.

User QoS is added to the optimization problem in [43]. In this case, as the problem to solve is NP-hard, the authors propose a suboptimal, iterative and low-complexity solution. The same approach is used in [44–47], playing with the trade-off between energy consumption and QoS. The Quality of Experience (QoE) is included in [48], where a dynamic programming (DP) switching algorithm is put forward. The user QoE is utilized in place of standard network measures such as delay and throughput. Other parameters that have been considered are the channel outage probability (also referred to as coverage probability), i.e., the probability of guaranteeing the service to the users located in the worst positions (e.g., at the cell edge) and the BS state stability parameter, i.e., the number of ON/OFF state transitions. For instance, a set of BS switching patterns engineered to provide full network coverage at all times, while avoiding channel outage, is presented in [49]. The coverage probability, along with power consumption and energy efficiency metrics, are derived using stochastic geometry in [50–52]. The QoE is also affected by the user equipment (UE) positions according to the channel propagation phenomena. To this respect, in [53] the selection of the BSs to be switched OFF is taken in order to provoke less impact to the UEs' QoE according to their distance to the handed off BSs.

In order to support sleep modes, neighboring cells must be capable of serving the traffic in OFF areas. To achieve this, proper *user association* strategies are required. In a scenario where sleeping techniques are not applied, each user is associated with the BS that provides the best Signal to Interference plus Noise Ratio (SINR). However, when BSs can go to sleep, user association is more complex and requires traffic prediction as well as very fast decision-making. Otherwise, users may suffer a deterioration of their QoS. A framework to characterize the performance (outage probability and spectral efficiency) of cellular systems with sleeping techniques and user association rules is proposed in [54]. In this paper, the authors devise a user association scheme where a user selects its serving BS considering the maximum expected channel access probability. This strategy is compared against the traditional maximum SINR-based user association approach and is found superior in terms of spectral efficiency when the traffic load is inhomogeneous. According to the BS state stability concept, a bi-objective optimization problem is attained in [55] and solved with two algorithms: (i) near optimal but not scalable, and (ii) with low complexity, based on particle swarm optimization.

The authors in [56, 57] propose solutions based on stochastic analysis for designing the deployment of macro BSs able to guarantee the QoS requirements and save energy by switching OFF subsets of BSs.

In [58] the notion of energy partition, an association of powered-ON and powered-OFF BSs, is used to enable network-level energy saving. It then elaborates how such concept is applied to perform energy re-configuration to flexibly re-act to load variations encouraging none or minimal extra energy consumption. Similarly, in [59] the authors introduce the notion of network-impact, which takes into account the additional load increments brought to its neighboring BSs, for detecting which BS to turn OFF as the one that will minimally affect the network.

Finally, RL techniques are investigated in [60] to solve the energy saving problem in order to make the system able to automatically reconfigure itself. In particular, the BS switching operation problem has been modeled according to the actor-critic method. The simulation results reported show the effectiveness of presented energy saving scheme under various practical configurations.

Cell Zooming

This family of methods is complementary to the sleep techniques and has been introduced to avoid the coverage gaps that may occur as BSs go to sleep. It amounts to adjusting the cell size according to traffic conditions, leading to several benefits: (i) load balancing is achieved by transferring traffic from highly to lightly congested BSs, (ii) energy saving through sleeping strategies, (iii) user battery life and throughput enhancements [61]. To compute the right cell size, cell zooming adaptively adjust the transmit powers, antenna tilt angles, or height of active BSs. Centralized and distributed cell zooming algorithms are proposed in [62], where a cell zooming server, which can be either implemented in a centralized or distributed fashion, controls the zooming procedure by setting its parameters based on traffic load distribution, user requirements, and

Channel State Information (CSI). A different approach is proposed in [63], where the authors design a BS switching mechanism based on a power control algorithm that is built upon non-cooperative game theory. A closed-form expression cell zooming factor is defined in [64], where an adaptive cell zooming scheme is devised to achieve the optimal user association. Then, a cell sleeping strategy is further applied to turn OFF light traffic load cells for energy saving. In general, most zooming scenarios entail a computationally intractable formulation, so affordable solutions based on iterative algorithms or heuristics abound in the literature, see, e.g., [65, 66].

Remarkably, cell zooming entails an increase in the transmit power of the active BSs, which leads to a higher energy expenditure for the BSs that are on. However, when used in combination with sleeping strategies, this leads to additional energy savings. Some researchers are oriented towards the study of sleeping schemes in conjunction with cooperative communication strategies for distributed antennas, also referred to as *Coordinated Multi Point* (CoMP). This technique increases spectral efficiency and cell coverage without entailing a higher BS transmit power and reducing the co-channel interference. The authors of [67] prove the effectiveness of this approach in terms of energy and capacity efficiency when sleep modes are combined with downlink CoMP. Despite these advantages, their results also reveal that imperfect downlink channel estimations and an incorrect CoMP setup can lead to energy inefficiency.

An online algorithm is proposed in [68] for a cell-breathing solution based on a clustered architecture. Since it a distributed solution, it allows to improve the scalability constraints given by a centralized approach and the risk of having one-point failure in network coordination. Moreover, it dynamically adjusts the traffic thresholds to define the BS behavior in order to be able to follow traffic fluctuations.

2.3.2 HetNets

Considering HetNet, the problem has been concentrated in defining strategies for sleeping the SBSs rather than the macro BSs. Similarly to the macro BS case, stochastic analysis has been used for defining the trends and the optimum deployment principles of HetNet [69–71]. In [72] a distributed online scheduling algorithm for SON HetNets is proposed which optimizes jointly the resource allocation, the transmission power and the UE attachment in terms of call admission control. In [73] the authors propose a noncooperative game among the BSs that seeks to minimize the trade-off between energy expenditure and load requirements when putting in sleep mode the SBSs. All the techniques in the above do not consider the traffic demand in the optimization problem.

In [74], closed-form expressions of coverage probability and average user load are formulated through stochastic geometry. Optimal resource allocation schemes are proposed to minimize power consumption and maximize coverage probability in a HetNet, and are validated numerically. User association mechanisms that maximize energy efficiency in the presence of sleep modes are addressed in [75], where the energy efficiency is defined as the ratio between the network throughput and the total energy consumption. Since this leads to a highly complex integer optimization problem, the authors propose a Quantum particle swarm optimization algorithm to obtain a suboptimal solution.

In [76] an offline algorithm that defines the timing for putting the SBSs in sleep mode as function of the system load has been presented. However, in [18] we showed that, when considering the energy model profiles in [17], the amount of energy saved is reduced due to the fact that the macro BS has to manage the traffic of the users previously attached to the SBS switched OFF. In fact, as highlighted in Fig. 2.1, when the macro BS is loaded with more traffic, its power consumption might considerably increase affecting the one of the whole network. This is coherent with HetNets paradigm, where the spectrum efficiency of the SBSs is greater with respect to the one of the MBS.

2.3.3 HetNet with Energy Harvesting Capabilities

The increasing interest in energy harvesting (EH) application in cellular networks from the research community is testified by the rich literature [77] on this relative new topic. On this matter, the contributions can be divided, in turns, in two problems: communication cooperation and energy trading [78]. In communication cooperation scenarios the solutions have to enable mechanisms to deal with the energy as a hard constraint, since the system cannot work when the energy is finished. While in energy trading problem, the energy derived by RES has to be optimized to increase the energy efficiency of the whole system or, in case of considering the energy market, to increase the benefits generated thanks to the energy trading.

On this matter, we performed two feasibility studies on HetNet with EH capabilities for assessing the actual challenges of such problems that will be detailed in what follows. Then, a review of the main techniques proposed for the problem of energy cooperation is discussed.

Feasibility Studies

In the context of communication cooperation solutions, we proposed a feasibility study for LTE-like cellular network deployments with photovoltaic panels [79]. The system

Table 2.2: PV and storage ratings and installation costs for both grid-powered and energy-sustainable base stations.

		LTE BS		
		Macro	Micro	Pico
PV ratings	[kW]	8.45	0.9	0.09
Storage ratings	[Ah]	1250	104.2	20.8
PV system land occupation	[m^2]	61.43	6.43	0.46
CAPEX for the grid connection	[€]	16450	13650	12750
CAPEX for the PV+storage plant	[€]	240100	11900	1190

design took in consideration all the principal elements of the access network, among them:

1. The OPEX due to the electricity consumption according to the model presented in Section 2.2.
2. The capital expenditure (CAPEX) of the grid-connected nodes has been modeled as the cost of the infrastructure for providing grid electricity.
3. The CAPEX of the off-grid nodes includes both the cost of the photovoltaic solar panel and of the batteries, both of them dimensioned for the worst case scenario where solar panels do not generate energy during 7 contiguous days.

In Tab. 2.2 the installation costs for grid-powered nodes are reported for the worst case scenario when the BS are always at full load. Looking at the PV system land occupation, we noticed that RES can be a viable cost-effective solution for SBSs, while it is still not possible to exploit it for MBS. However, it is to be noted that, with these simple dimensioning solutions the solar panel dimensions are still rather large for considering their deployment in street furniture (i.e., a micro BS would need a PV module of 6.43m^2).

In [80], we advanced this study by considering a more realistic scenario with real energy harvesting traces and traffic demand profiles. Moreover, we introduced the design concept of *outage probability*, defined as the fraction of time during which the BS is unable to serve the users' demand due to an insufficient energy reserve. In that case, the BS has to be momentarily switched OFF or put into a power saving mode. The size of harvesters and batteries has been evaluated as a function of the outage probability for different geographical locations. In detail, hourly energy generation traces from a solar source have been obtained for the cities of Los Angeles (CA) and Chicago (IL), US. For the solar modules, the commercially available Panasonic N235B photovoltaic technology has been considered. These panels have single cell efficiencies as high as 21.1%, delivering

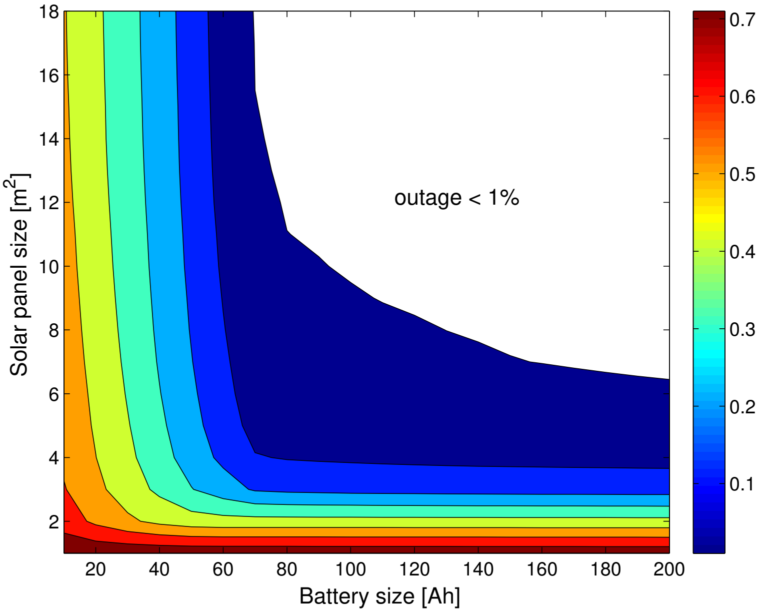

Figure 2.2: Contour plot of the outage probability for a micro cell operated off-grid (battery voltage is 24V). Different colors indicate outage probability regions, whose maximum outage is specified in the color map in the right hand side of the plot. The white filled region indicates an outage probability smaller than 1%.

about 186W/m^2. The raw irradiance data were collected from the National Renewable Energy Laboratory [81] and converted, accounting for this solar power technology, into harvested energy traces using the SolarStat tool of [21], that will be presented in detail in Chapter 3. For the demand profile, it is commonly accepted and confirmed by measurements that the energy use of base stations is time-correlated and daily periodic. In this article, we use the load profiles obtained within the EARTH project and reported in [1]. The BS operates off-grid and the above models are accounted for the energy harvested and the cell load. Therefore, we are concerned with the right sizing of solar panel and battery, so that the BS can be perpetually operated.

The contour plot for the outage probability for micro BSs is shown in Fig. 2.2 considering solar traces from Los Angeles. Different colors are used to indicate outage probability regions (maximum outages are specified in the associated color map). The white filled area indicates the parameter region where the outage probability is smaller than 1%. The outage probability graphs for pico and macro BSs show a similar trend, rescaled to higher (macro) or smaller (pico) values along both axes. From Fig. 2.2, we see that panels of size smaller than 15 square meters and battery capacities of at most 150Ah at 24V suffice for micro BSs, which is in line with the results in Table 2.2. For pico and macro deployments, solar panels range in size from 0.7 to 1.4 square meters (pico) and from 40 to 80 square meters (macro) and battery capacities form 20 to 90Ah at 12V (pico) and from 300 to 1500Ah at 48V (macro). Taking an outage of 1% as our design parameter, all the points on the boundary of the white-filled region are equally good. The results for the city of Los Angeles are rather good, indicating that the nearly-zero energy is indeed a feasible goal. In fact, both battery and panel sizes are acceptable given the dimensions of typical installation sites for the considered BSs. Instead, for the city of Chicago the energy inflow is less abundant, and this is especially so during the winter months. In that case, reasonable panel and battery sizes (even slightly higher than those discussed for Los Angeles) lead to outages of 10% or higher. Due to this, grid-connected operation is required for locations where the energy inflow is moderate (especially during the winter).

Now, we consider the energy trading problem where a grid-connected BS that can sell or buy energy from the grid. Most likely, the energy price in future power grids will change hourly. This practice is not yet adopted worldwide but there are relevant programs that already use it. A relevant example can be found in Illinois, US, where electrical companies are offering new hourly electricity pricing programs where energy prices are set a day-ahead by the hourly wholesale electricity market run by the Midcontinent Independent System Operator (MISO). In this way, customers can optimize their usage patterns, saving money in their energy bills. In this work, we use publicly available historical energy price data from these programs to discuss suitable energy management policies. From telecommunication perspective, energy harvesting and future market policies will permit at least two additional optimization strategies. First, the system could adapt its behavior to the energy price, i.e., it could be energy frugal when the energy cost is high, whilst adopting more aggressive policies when the cost drops. Second, part of the energy that is accumulated could be sold or re-distributed among other network elements.

To this end, an energy manager intelligently chooses in which amounts and when energy e_t (the decision variable) has to be purchased or sold so that the system maximizes its profit. In detail, we considered a system that evolves in slotted time t, where the slot duration is one hour. At any given time t, the BS may sell or buy a certain amount of energy e_t, which is positive when energy is sold and negative when purchased. When energy $e_t < 0$ is purchased from the grid operator, a monetary cost $C(e_t)$ is incurred, which corresponds to the price of energy in slot t. Instead, when energy $e_t > 0$ is sold, a reward $R(e_t) = rC(-e_t)$ is accrued, with $r \leq 1$ being a discount factor. This means that the energy sold is paid less than that purchased, as this is usually the case in current energy markets and is expected to remain so for future ones. Also, we use $C(e_t) = 0$ for $e_t \geq 0$ and $R(e_t) = 0$ for $e_t \leq 0$, meaning that no cost is incurred when selling and no reward is accrued when buying. At each time t, the demand d_t has to be fully served and the energy required to do so is harvested, taken from the battery or bought from the grid. This corresponds to maximizing the total monetary reward, expressed as $f(T) = \sum_{t=0}^{T}[R(e_t) - C(e_t)]$, over the time horizon of interest $t \in \mathcal{T}$ (with $\mathcal{T} = \{0, 1, \ldots, T\}$). The solution to this problem amounts to finding the optimal allocation $\{e_t^*\}_{t\in\mathcal{T}}$ for all time slots $t \in \mathcal{T}$. Here, we do so through dynamic programming considering the actual traces for hourly energy prices, user demand and harvested energy. Based on the optimization performed by the energy manager, we studied how to dimension the solar add-on in order to maximize the net profit, considering an amortization period T of ten years and given that the optimal policy e_t^* is used throughout. The net profit over this period is obtained summing the revenue $f(T)$ to the cost incurred when the BS is powered in full by the energy grid, and subtracting the CAPEX associated with the resulting harvesting hardware.

For the following example results, we have accounted for the current price of solar panels, which is about 0.5\$/kWh and a battery cost of 300\$/kWh. Table 2.3 and Table 2.4 show the 10-year net income for pico, micro and macro cells that can be achieved in the cities of Chicago and Los Angeles, respectively. For the net income the notation we used "X\$ (Y, Z)", where X is the net income in US dollars, Y is the solar panel size (square meters) and Z is the battery size (Ah). According to the considered CAPEX cost, optimal designs tend to pick smaller battery capacities and invest more on solar modules. In the tables, two designs D1 and D2 are shown for each type of BS, where D2 returns the maximum net profit within the considered parameter range. Notably, a positive income is accrued in almost all cases. As expected, Los Angeles allows for higher revenues due to the more abundant energy inflow that is experienced at that location. D1 was added to show that even a suboptimal design, which may be required due to space limitations, still provides positive incomes and is a sensible alternative. The only case returning a negative net profit is Chicago for Macro BSs, where an additional year (eleven years) would be required to amortize the CAPEX.

Table 2.3: Net income and annual revenue for the city of Chicago.

BS type	D1 (net income)	D2 (net income)	D2 (annual revenue)
Pico	19\$ $(1, 20)$	58\$ $(2, 20)$	71\$
Micro	232\$ $(10, 80)$	607\$ $(20, 80)$	709\$
Macro	-1566\$ $(60, 500)$	-695\$ $(80, 500)$	1395\$

As one may expect, the actual sizing for the solar add-on depends on the energy selling price as well as on the location. Nevertheless, the rather good results that we have shown here are encouraging. These, are due to the modest cost of PV technology, that has been plummeting over the last decade (10-fold reduction). In addition, we observe that while commercial panels at the time of writing have maximum efficiencies of about 21%, new

Table 2.4: Net income and annual revenue for the city of Los Angeles.

BS type	D1 (net income)	D2 (net income)	D2 (annual revenue)
Pico	51$ $(1, 20)$	117$ $(2, 20)$	130$
Micro	544$ $(10, 80)$	1193$ $(20, 80)$	1295$
Macro	446$ $(60, 500)$	1813$ $(80, 500)$	2568$

developments with efficiencies as high as 44% are on the way [82]. The battery cost is still rather high, but trends are encouraging for it as well. As an example, since 2008, the cost reduction has been of about one third for lithium ion cells, which is the technology of choice at the time of writing. These facts can be found in numerous reports, see, e.g., [83] and allow us to assert that the scenarios envisioned here are already feasible and are expected to become even more appealing in the near future, as the harvesting CAPEX will further drop and PV efficiencies will improve.

The main outcome of these studies is that the system may be feasible and cost-effective in locations with relatively high solar irradiation, considering the cost and dimension of the energy harvesting hardware and of the grid energy. However, as discussed in [21], that there may be a high variability in the energy harvested during the day and this also holds for the summer months. This means that, although the energy inflow pattern can be known to a certain extent, intelligent and adaptive algorithms that control the BSs based on current and past inflow patterns as well as predictions of future energy arrivals have to be designed. Moreover, the design of energy efficient sleeping modes is expected to be a very effective means to further reduce the energy consumption figure. For these reasons, we have been motivated to concentrate our effort in the study of energy efficient solutions for HetNet with EH capabilities, that constitutes the core of the contribution of this thesis. The reference solutions of this scenario are presented in the following subsection.

Energy Cooperation Solutions

The usage of RES in HetHets opens the door a new optimization paradigm: the standard problem of energy saving for reducing the RES requirements is enriched by the one of energy constrained wireless networks, that is the optimization of the usage of the available energy reserves. In [84], the authors extended the work on energy saving in k-tier HetNet ([69]) by including the EH variable in order to manage the SBSs powered with RES with sleep mode strategies. In this model, the authors define a metric called *availability* ρ_k which represents the fraction of time a k^{th} tier BS can be kept on since it has enough energy reserve. This work aims at defining the set of K-tuple $(\rho_1, \rho 2, \dots, \rho_k)$, called *availability region* that are achievable with uncorrelated strategies (i.e., the decision of sleeping a BS is taken by each BS independently). The authors proved that there exists a fundamental limit on the availabilities ρ_k which cannot surpassed by uncoordinated strategies. The energy harvested a k^{th} tier BS has been modeled as a Binomial process, as approximation of its Poisson energy arrival process μ_k at each solar cells since they number is usually large. The user allocation scheme considered is orthogonal, which implies that there is no intra-cell interference. The user locations are assumed to be taken from an independent Poisson Point Process (PPP) [85]. The level of energy of a k^{th} tier is modeled as a continuous time Markov chain (CTMC) with birth process as described before and death process with a rate that depends on the number of users served by the BS, that are assumed to require a fix amount of energy per second. The authors present some general results on the battery capacity and the dimensioning of the energy harvesting system for having the same performance of a similar network with reliable energy sources. The method is flexible and general; therefore, it represents a good solution for providing guidelines in the design of the cellular network. However, it cannot be extended to realistic scenario due to the complex analytical models that are made of, especially for what concern the user traffic model, the BS energy one and the energy harvesting one.

In [86], the authors provided a solution to deal with the uncertainty of the renewable energies for energy self-sustainable cellular networks. In detail, they propose an Intelligent Energy Managed Service to be mounted in each BS that is able to control the power consumption as function of the stored energy in the battery supply, the expected amount of renewable energy to be harvested as function of the weather forecast and historical base station power consumption information. The algorithm proposed adjusts the power consumption as function of the battery level, the prediction of energy wasted and the prediction of the energy incomes as function of the weather conditions. The solution has been tested with field trial experiments carried out during the Mobile World Congress 2010 hold in Barcelona (Spain), where Vodafone deployed a solar based 100% green site (sponsored by Huawei) and supported by simulations on the long term with historical weather data. The results show that with the prediction technique the outage of the system is reduced and, in parallel, the harvesting system can be minimized.

In [87] the authors proposed an algorithm called Intelligent Cell brEathing (ICE) aimed at minimizing the maximal energy depleting rate (EDR) of the low-power base stations powered by renewable energy with cell breathing techniques. In this case the authors considered two types of base stations: high-power BSs (HBSs) and low-power BSs (LBSs). The LBS are powered by RES while HBS are powered by the electric grid. The authors proposed to dynamically change the transmission power of the LBSs in order to minimize the maximum ratio between the total consumed power and the energy income. The BS energy model is different from the one in [17] and is based on a fixed power consumption component plus a variable one determined by the transmission power level. They demonstrated that this problem in NP-hard. They solved it iteratively by introducing the energy dependent set (EDS) composed by LBSs with similar EDR and decrementing the power level of the LBSs to allow users switching from LBSs in a specific EDS to those outside it in order to find the optimal users allocation and power level configuration. The results show that ICE balances the energy consumption among the LBSs, augment the number of user served and decrease the outage.

In [88], the authors considered a different scenario, where BSs are connected by resistive power lines and can cooperate by sharing the energy reserves. The authors demonstrate that, with deterministic energy consumption and traffic profiles at all the BSs, the optimal energy distribution can be found by solving a linear program optimization problem. Alternatively, when the energy income is stochastic an online algorithm is presented based on a greedy heuristic.

In [89], the authors introduced the concept of *Zero grid Energy Networking* (ZEN) which consists of mesh network of BSs powered only with RES. The scenario considered is the one of rural coverage where there is no connection to the electric grid and therefore the BS need to energy self-sufficient. They firstly solved the problems of dimensioning the renewable energy system by considering the daily typical traffic and energy harvested profile for the cities of Aswan, Palermo and Torino generated with a simulator called PVWatts [90]. With the PV system dimensioning of before, they also evaluated the storage system capacity and the impact of introducing wind turbine. Finally, they relaxed the assumption of energy self-sustainability and they optimized the RES equipment requirements with an offline algorithm by introducing SBSs sleep mode strategies in a two tier network extending what done in [76].

In [91] the ski rental problem has been proposed to optimize the switch ON/OFF problem for ultra-dense EH SBS networks. Each agent operates autonomously at each small cell and without having any a priori information about future energy arrivals. The algorithm is compared against a greedy scheme that uses sleep modes when the battery level is below a fixed threshold. The analysis is carried out considering Poisson arrivals for energy and traffic, which may provide a non-realistic approximation to these processes.

Reinforcement Learning has been used in [92] for optimizing the control of a single EH SBS as a function of the local harvesting process and storage conditions. However, the effect of the simultaneous switching OFFs by multiple SBSs on the overall network performance is not studied. This effect has been analyzed in [93], where a two-tier urban cellular network composed by macro BSs powered by the power grid and energy harvesting SBSs is considered. The authors evaluated the bounds of a centralized optimal direct load control of the SBS using an offline dynamic programming method that has all the knowledge on the system variables a-priori. The optimization problem is represented using Graph Theory and the problem is stated as a Shortest Path search. The results show that an encouraging energy efficiency improvement can be theoretically achieved.

The authors in [94] provide useful insight on the impact of the parameters quantization in networks of BS powered with solar energy. They discuss the choice of parameter quantization for time, weather, and energy storage and provide guidelines for the development of accurate and credible models that can support the power system design to achieve a correct dimensioning. The main findings are that a credible and accurate model requires: i) a time granularity equal to 1 hour that allows capturing the energy production and consumption fluctuations during the day; ii) the discretization of the weather conditions according to 5 or 7 levels of average daily solar irradiance; iii) a storage energy quantum of the order of 1/5 of the minimum energy consumption per time slot.

Finally, an interesting application of HetNet powered by RES is represented by the so called public protection and disaster relief communications (PPDR), where the lack of electrical grid is often impossible as a consequence of an emergency situation. As we highlighted in [95], in such scenarios a flexible architecture like HetNet allows to rapidly provide communication services to both emergency responders and civilians. The proposed infrastructure is a network of energy self-sufficient LTE SBSs powered by RES that features an all-wireless multi-hop backhaul network together with self-organization capabilities which can replace the standard cellular network even when its radio access part is totally compromised.

2.4 Beyond the State of the Art

The main goal of this thesis is to get closer to a real scenario with respect to the work presented before on EH by investigating online solutions. In detail, considering [84] we envisage that by taking into account the traffic profile, the system can work in a more efficient way even when outside the availability region, allowing to reduce the capacity of the RES system. Moreover, RL can optimize the system even without historical data of the energy consumption and the users demand as in [86].

Similarly to [87], the target is to minimize the energy used by the part of the network connected to the grid, the macro BS. However, we considered that SBSs can be put in sleep mode in case of low traffic in order to save energy for the peaks, where it would be more problematic to be managed by the network.

Therefore, the scenario in [89], well fit with our vision, except from the fact that we concentrate on general HetNet scenarios, where SBSs are supporting the MBSs especially for capacity extension rather than coverage extension. However, we coincide in the final example scenario where they evaluate the sleep mode solutions apart from the fact that the algorithm is based on the knowledge of traffic and harvested energy profiles.

To this end, learning solutions are adopted for avoiding the usage of deterministic o statistical data in the design of the network in order to implement a self-organization approach that enables to deploy SBSs in a flexible way independently from the most important environmental variables (e.g., weather conditions, traffic profiles and BSs location). Self-organization is defined as the ability of entities to spontaneously arrange given parameters following some constraints and without any human intervention. To do this, entities have to somehow represent the environment where they perform and the gathered information has to be interpreted for them to correctly react. Consequently, learning solutions represent a viable tool for self-organization since they allow to translate the environmental sensed information into actions. Considering the specific problem of this work, network of SBSs can be interpreted as multi-agent systems.

In the following chapter, the main ML principles used in this thesis are introduced.

2.5 Concluding Remarks

This chapter has provided some background information that is relevant to the contributions of this thesis, which will be thoroughly presented in the following chapters. Initially, the reference energy model for different type of BS has presented. The state-of-the-art works concerning the energy efficiency algorithms have been discussed next. In continuation, an overview of the schemes available in the literature when introducing EH capabilities to HetNets highlighting the principles, the contributions, but also the limitations of proposed solutions. Thus, after presenting open issues and challenges, the main novel contributions of this thesis has been detailed with respect to the literature.

The remaining of this thesis is organized in four parts. The first part provides the necessary principles of ML methods, presenting the Q-learning and the prediction solutions that constitutes the main building blocks of the framework presented in this Ph.D. dissertation. The second part (Chapter 4) is focused on proposing an accurate energy model based on stochastic Markov processes for the description of the energy scavenged by outdoor solar sources. The third part of the thesis (Chapter 5) is devoted to propose a novel solution based on distributed Q-learning algorithm for improving the EE of the system by switching ON/OFF SBSs powered with solar panels. Finally, in the fourth part (Chapter 6), an enhanced switching OFF solution adopting Layered Learning is given for solving the problem of conflicts among the agents.

Chapter 3

Machine Learning Background

3.1 Introduction

Machine Learning has recently attracted a remarkable attention from the research community for its flexibility in solving complex problems. ML-based tools are expected to be the main enablers for providing the required flexibility to 5G system and implement the SON functionalities. Machine Learning can contribute both for extracting models that reflect the user and network behaviors and for more dynamic decision making problem working in real-time. The former is commonly used in data analysis problem for evaluating the behavior of specific parameters of the system to drive the decisions made by 5G SON functionalities. Typically, this is performed through learning-based classification, prediction and clustering models. The latter are more adequate when independent and dynamic problems are considered, as in the case of SBS with EH capabilities systems. To this end, RL is the concept adopted in ML for implementing reactive agents, since it works by learning from interactions with the environment, and observing the consequences when a given action is executed. Therefore, multi-agent systems represent a logical method to treat these types of problem, considering the intrinsic nature of the scenario, which is composed of various SBSs that have to be controlled simultaneously.

For these reasons, we considered to adopt both solutions based on RL and prediction. RL is used to provide the incremental learning behavior to the solution for obtaining online algorithms that are able to adapt to the environment. These solutions typically keep memory of the interactions by means of some representation mechanism, e.g., look-up tables. Therefore, the complexity of RL methods is exponential in the number of agents, because each agent has to store its own variables. To this end, we used prediction-based tools for guiding the RL techniques in finding a solution. In detail we adopted the Multi-layer FeedForward Neural Networks (MFNN) for being able to estimate the effect of the RL decision making process of each agent on the overall system before it takes place. This estimation is then used as a feedback for the RL solution thanks to the heuristically accelerated RL paradigm. Finally, the overall architecture has been organized in a hierarchical fashion for clearly divide the problem in subtasks.

In wireless communications, RL solutions has been already used in literature [60, 96] both for reconfiguring the network elements to improve the energy efficiency according to the actual traffic and to study which sleep policies, respectively. In [97, 98] it has been used for the problem of interference coordination.

In this chapter, we present the main principle of the ML tools used in this thesis. In Section 3.2 we introduce the ML philosophy. In Section 3.3, we present the main principle of the neural networks. Finally, in Section 3.4 we conclude the chapter.

3.2 Machine Learning

Machine Learning methods can be classified in three main categories as function on the type of feedback used for learning: unsupervised learning, supervised learning and reinforcement learning.

In *supervised learning* the task of the learner is to predict the value of the outcome for any valid input after having seen a number of training examples. The training examples are pairs of input objects and desired outputs, usually represented in form of vectors. When the outputs are continuous, the learning problem is called regression. Alternatively, the problem is referred as classification when the outputs are discrete values. After the end of the training phase, the learning solution predicts the value for any new valid input object [99]. This method is called “supervised” learning since the learning process is driven by the desired output variable.

In *unsupervised learning* the objective is to learn underlying statistical structure or distribution of unlabeled input patterns with unknown probability distribution. The trained system is able to reconstruct pattern from noisy input data though the learned statistical structure. This type of learning is referred as “unsupervised” because of the absence of explicit desired output, as in supervised learning, or any reward from the environment, as in RL, in the evaluation of the solution [100].

Reinforcement learning is the family of learning solutions that has the ability of learning behaviors online and automatically adapting to the temporal dynamics of the system [101]. At each time step, the agent senses the state of the environment and take an action to transit in a new state. The environment returns a scalar reward (or cost), which evaluates the impact of the selected action. Consequently, RL is applied for creating autonomous system that improve themselves iteratively with the accumulated experience at each cycle.

According to the specific problem to solve, the above methods can be more or less suitable. For instance, supervised and unsupervised learning methods are not appropriate for interactive problems where the agents have to learn from their past experience and be able to adapt to unpredictable environment characteristics, which is the scenario of the problem we want to solve. However, they can help in understanding the behavior of specific part of the environment, e.g., they can predict the value or classify some specific sensible parameters. In literature RL solutions are typically formulated in a centralized fashion, where a central entity takes decisions, e.g., a BS in an LTE system. However, when considering network of SBSs, the process has to be distributed in order to better fit the deployment model and be able to deal with the scalability of the system. Therefore, we focus on decentralized learning processes based on RL.

The first studies in the field of distributed learning come from the game theory when Brown proposed the fictitious play algorithm in 1951 [102]. The literature of single agent learning in ML is extremely rich, while only recently the attention has been focused on distributed learning aspects, in the context of multi-agent learning. Rapidly, it became an interesting interdisciplinary area and the most significant interaction point between computer science and game theory communities. The theoretical framework can be found in Markov decision process (MDP) for the single agent system, and in stochastic games, for a multi-agent system. In what follows, we give a brief introduction of learning in single and multi-agent systems. In Section 3.2.1, we analyze RL for the case of the single-agent, while in Section 3.2.2 the one of the multi-agent. Section 3.2.3 provides the definition of TD algorithms, while Section 3.2.4 details on the Q-learning. Section 3.2.5 provides some open issues and challenges in the MRL.

3.2.1 Learning in single agent systems

A MDP provides a mathematical framework for modeling decision-making processes in situations where outcomes are partly random and partly under the control of the decision maker. MDP are valuable tool for describing a wide range of optimization problems. A MDP is a discrete time stochastic optimal control problem. Here, operators take the form of actions, i.e., inputs to a dynamic system, which probabilistically determine successor states. A MDP is defined in terms of a discrete-time stochastic dynamic system with finite state set $\mathcal{S} = \{s_1, \ldots, s_n\}$ that evolves in time according to a sequence of time steps, $t = 0, 1, \ldots, \infty$. At each time step, a controller selects an action a_k from a

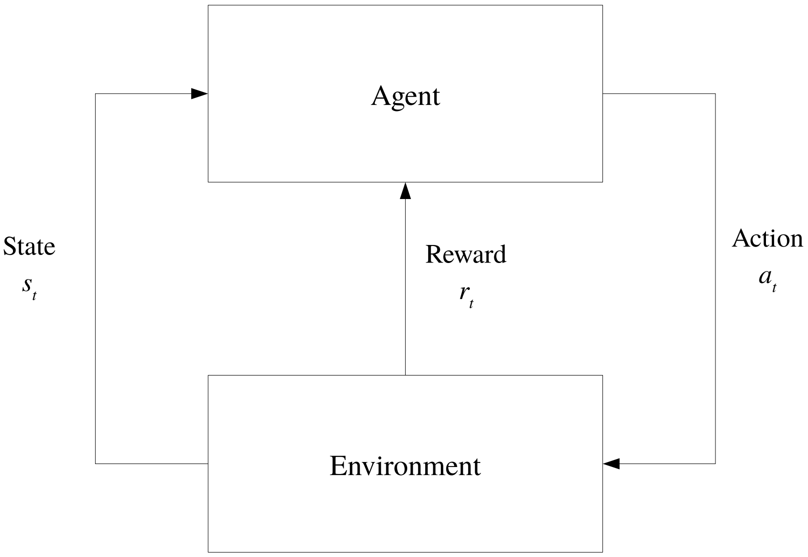

Figure 3.1: Learner-environment interaction.

finite set of admissible actions $\mathcal{A} = \{a_1, \dots, a_l\}$ based on the perceived system current state s_i. The action is then executed by being applied as input to the system, which consequently evolves from state s_i to s_j, with a state transition probability $P_{i,j}$. As a result of the execution of the action a_k in state s_i, the environment return an immediate reward $r(s_i, a_k)$. In what following, we refer to states, actions, and immediate reward by the time steps at which they occur, by using s_t, a_t and r_t, where $a_t \in \mathcal{A}$, $s_t \in \mathcal{S}$ and $r_t = r(s_t, a_t)$ are, respectively, the state, action and reward at time step t. A graphic representation is shown in Fig. 3.1. Summarizing, a MDP consists of:

- a set of states $\mathcal{S}$.
- a set of actions $\mathcal{A}$.
- a reward function $R : \mathcal{S} \times \mathcal{A} \rightarrow \Re$.
- a state transition function $P : \mathcal{S} \times \mathcal{A} \rightarrow \Pi(\mathcal{S})$, where a member of $\Pi(\mathcal{S})$ is a probability distribution over the set $\mathcal{S}$ (i.e., it maps states to probabilities).

The state transition function probabilistically defines the next state of the environment as a function of its current state and the agent's action. The reward function specifies expected instantaneous reward as a function of current state and action. In order to be a *Markov* model, the state transitions have to be independent of any previous environment states or agent actions. The goal of a MDP problem is to find the policy that maximizes the reward of each state s_t. Therefore, the objective is to find an optimal policy for the infinite-horizon discounted model, relying on the result that, in this case, there exists an optimal deterministic stationary policy [101].

To solve RL problems there are three fundamental classes of methods, i.e., dynamic programming, Monte Carlo and temporal difference (TD) learning. The first one rely of the knowledge of the state transition probability function from state s to state v, $P_{s,v}(a)$. On the other hand, the second and the third solve the RL problems without any knowledge of the transition probability function. When a sample transition model of states, actions and rewards can be built, Monte Carlo method can be applied. Alternatively, if the only way to collect information about the environment is to interact with it, TD methods have to be applied. In doing this, TD methods combine elements of DP and Monte Carlos: they learn directly from experience, as in Monte Carlo methods, and they gradually update prior estimates values, as in DP.

The core of RL algorithms is represented by the computation of the *value functions*. The state-value function $V(s)$ measures how good, based on the future expected reward, is for an agent to be in a given state, while the state-action value function $Q(s, a)$ measures how good is to execute an action based on the future expected reward. The expected rewards for the agent in the future are given by the action it will take, thus the value functions depend on the policies being followed. The state-value of state s is defined as the expected infinite discounted sum of the rewards that the agent gains starting from state s and executing the complete decision policy π

$$V^{\pi}(s) = \mathbb{E}_{\pi}\left\{\sum_{t=0}^{\infty} \gamma^t r_t | s_t = s\right\} \tag{3.1}$$

where $0 \leq \gamma < 1$ is a discount factor which determines how much expected future rewards affect decisions made now. Analogously, the Q-value $Q(s, a)$ is the expected decreased reward for executing action a at state s and then following policy π, in detail:

$$Q^{\pi}(s, a) = \mathbb{E}_{\pi}\left\{\sum_{t=0}^{\infty} \gamma^t r_t | s_t = s, a_t = a\right\} \tag{3.2}$$

Therefore, in order to solve a RL problem the best return in the long term has to be found. This is referred as finding an optimal policy, which will be the one that is giving the maximum expected return. We define the optimal value of state s as:

$$V^{*}(s) = \max_{\pi} V^{\pi}(s) \tag{3.3}$$

This optimal value function is unique according to the principle of Bellman's optimality [101], and can be defined as the solution to the equation:

$$V^*(s) = \max_a \left(R(s,a) + \gamma \sum_{v \in \mathcal{S}} P_{s,v}(a) V^*(v) \right) \tag{3.4}$$

which means that the value of state s is the expected reward $R(s,a) = \mathbb{E}\{r(s,a)\}$, plus the expected discounted value of the next state, v, when taking the best available action. Given the optimal value function, we can specify the optimal policy as:

$$\pi^*(s) = \arg\max_a \left(R(s,a) + \gamma \sum_{v \in \mathcal{S}} P_{s,v}(a) V^*(v) \right) \tag{3.5}$$

Now we define an intermediate maximum of $Q(s,a)$, denoted $Q^*(s,a)$, applying the Bellman's criterion in the action-value function, where the intermediate evaluation function for every possible next state-action pair (v, a') is maximized, and the optimal actions is performed with respect to each next state v. Therefore, $Q^*(s,a)$ is:

$$Q^*(s,a) = R(s,a) + \gamma \sum_{v \in \mathcal{S}} P_{s,v}(a) \max_{a' \in \mathcal{A}} Q^*(v,a') \tag{3.6}$$

Finally, we can determine the optimal action a^* with respect to the current state s, which represents π^*. Thus, $Q^*(s,a^*)$ is maximum, and can be expressed as:

$$Q^*(s,a^*) = \max_{a' \in \mathcal{A}} Q^*(s,a') \tag{3.7}$$

3.2.2 Learning in multi-agent systems

The characteristics of the distributed learning systems are as follows: i) the intelligent decisions are made by multiple intelligent and uncoordinated nodes; ii) the nodes partially observes the overall scenario; and iii) their inputs to the intelligent decision process are different from node to node since they come from spatially distributed sources of information. Multi-agent system perfectly matches these characteristics, considering each node as an independent intelligent agent. The theoretical framework is based on stochastic games [103] and described by the five-tuple $\{\mathcal{N}; \mathcal{S}; \mathcal{A}; P; \mathcal{R}\}$. In detail

- $|\mathcal{N}| = N$ is the set of agents, ranging from $1, \ldots N$;

- $\mathcal{S} = \{s_1, s_2, \ldots, s_n\}$ is the set of possible states, or equivalently, a set of N-agent stage games;
- $\mathcal{A}$ is the joint action space defined by the product set $\mathcal{A}^1 \times \mathcal{A}^2 \times \ldots \times \mathcal{A}^N$, where $\mathcal{A}^i = \{a_1^i, a_2^i, \ldots, a_l^i\}$ is the set of actions available to the ith agent;
- P is a probabilistic transition function defining the probability of going from one state to another provided the execution of a certain joint action;
- $\mathcal{R} = \{r^1 \times r^2 \times \ldots \times r^N\}$, where r^i is the reward of the ith agent in a certain stage of the game, which is a function of the joint actions of all N nodes.

In fully cooperative stochastic games, the reward functions coincide for all the agents: $r_1 = \cdots = r_N$. In this case the agents have the same goal: to maximize the common return. If $N = 2$ and $r_1 = -r_2$, the two agents have opposite rewards and the game is called fully competitive. Finally, mixed games are the ones that cannot be defined neither as fully cooperative or competitive.

The typical problems in multi-agent systems are usually modeled as non-cooperative games, since the distributed decisions made by the multiple nodes strongly affect the one made by the others. Stochastic games form a natural model for such interactions. A stochastic game is played over a state space, and is played in rounds. In each round, each player chooses an available action simultaneously with and independently from all other players, and the game moves to a new state under a possible probabilistic transition relation based on the current state and the joint actions. We can distinguish in this context two different forms of learning: i) the agent can learn the strategies of the opponents in order to formulate the best response accordingly, and ii) the agent can learn his own strategy that perform well against the opponents, independently from learning the strategies of the opponents. The former is defined as model-based learning, and it requires some partial information of the strategies of the other players. The second approach is referred to as model-free learning, and it does not necessarily require to learn a model of the strategies played by the other players. To facilitate distributed and autonomous functioning of wireless networks, model-based learning approaches are considered not to be appropriate since they require each node/agent to acquire knowledge on the actions played by the other agents which might yield to high overheads. In fact, this approach, generally adopted in game theory literature, is based on building some model of other agents' strategies, following which, the node can compute and play the best response strategy. This model is then updated based on the observations of their actions. On the other hand, model-free approaches, also known as TD learning, are adequate since they avoid building explicit models of other agents' strategies and learn over time how properly the various available actions perform in the different states.

3.2.3 TD Learning

TD learning is a prediction method based on the future values of a given signal. The name TD comes from the use of the differences in predictions over successive time steps to drive the learning process [28]. Agents implementing TD methods are implemented in an online fashion, thus learning from every transition without considering the subsequent actions. Consequently, after the training phase, the agents can improve their behavior, improvements that continue over time. The algorithms in this category typically keep memory of the appropriateness of playing each action in a given state by means of some representation mechanism, e.g., look-up tables, neural networks, etc. This approach follows the general framework of RL and has its roots in the Bellman equations [101].

One of the main dilemma of RL algorithms is the trade-off between exploration and exploitation. Exploration is the phase in which the agent learns across all available actions in order to determine the best one to be used at the end of the learning process. Alternatively, in the exploitation phase the agent uses the knowledge already acquired to obtain the maximum reward.

A policy π maps state to actions, i.e., it defines the actions the agent has to follow to maximize the reward. TD methods ca be classified in two groups with respect to the policies, 1) the behavior policy, which learns the comportment of the agent in term of the actual action to be selected by the agent, and 2) the estimation policy, which determines the policy evaluated, or the action in the next state used for the evaluation of behavior policy. In RL there are two methods to implement the exploration, the on-policy and off-policy. They differ in the form the select the estimation policy. The on-policy methods evaluate or improve the policy used to perform the decision, i.e., they estimate the value of a policy while using it for control. This implies that, the policy adopted by an agent is a given state, the behavior policy, is the same used to select the action (estimation policy) based on which it evaluates the behavior followed. On the contrary, off-policy methods distinguish between behavior and estimation policies. In fact, the policy to generate the behavior is unrelated to the policy evaluated. In this case, the policy evaluated is the one corresponding to the best action in the next state, π^*, given the current agent experience.

The goal of the agents in TD learning is to select actions that maximize the discounted reward they receive over the future. This is the role of the discount rate γ in the state value function, Eq. 3.1 and in the state-action value function, Eq. 3.2. While, α represents the weight of the new information in the state and state-action value update. The action selection policy plays also a crucial role in RL, by defining the criterion the agent have to follow in the selection of the action. The criterion can be either to perform exploration or to exploit the acquired knowledge. As introduced before, exploration has to be included in the action selection policies in order to achieve good behaviors based on explicit trial-and-error processes.

Among the TD methods, we adopted the off-policy Q-learning algorithm, since it has more efficient learning properties, as detailed in what following. Q-learning is proven to converge to an optimal policy in a single agent system, as long as the learning period is enough long, and can be extended to the multi-agent stochastic game by having each agent ignore the other agents and pretend that the environment is stationary. Even if this approach has been shown to correctly behave in many applications, it is not characterized by a strict proof of convergence, since it ignores the multi-agent nature of the environment and the Q-values are updated without regard for the actions selected by the other agents. Therefore, the convergence of multi-agent Q-learning is an open issue, as detailed in Section 3.2.5, and have to be evaluated on a case-by-case basis.

3.2.4 Q-learning algorithm

Q-learning algorithm has been proposed in 1989 by Watkins in his Ph.D. thesis [104] and the proof of convergence of this algorithm was presented in 1992 by Watkins and Dayan in [105]. The goal of Q-learning is to find $Q^*(s,a)$ in a recursive manner using available information (s,a,v,r), where s and v are the states at time t and $t+1$, respectively, a is the action taken at time t and r is the reward of executing a in s. Q-learning estimates π^* while following π, as it is a off-policy algorithm. This means that the behavior of the agent is determined by the action selection policy followed by it, which is the policy π, while the Q-value updating process is performed based on the minimum Q-value in the next state, independently of the policy being followed [28]. The Q-value is computed according to the rule:

$$Q(s,a) \leftarrow Q(s,a) + \Delta Q(s,a) \tag{3.8}$$

where $\Delta Q(s,a)$ is defined as:

$$\Delta Q(s,a) = \alpha[r + \gamma \max_a Q(v,a) - Q(s,a)] \tag{3.9}$$

where α is the learning rate, which weights the importance given to the information observed after executing action a, and γ is the discount factor which determines the importance of future rewards. When γ is equal to 0 will make the agent short-sighted by only considering current rewards, while using values approaching to 1 will make it strive for a long-term high reward. Algorithm 1 presents the Q-learning procedure.

The main advantage of Q-learning is that it does not include the cost of exploration in the Q-value update. This characteristic makes Q-learning consistent with the principle of knowledge exploitation. This implies that the policy found by the algorithm is applied without including the exploration after the end of the learning process. Thus, the off-policy learning solutions allow the agents to exploit the acquired knowledge in a very effective way since the beginning of the learning process.

Algorithm 1 Q-learning

```
for each $s \in \mathcal{S}, a \in \mathcal{A}$ do
    Initialize $Q(s, a)$ arbitrarily
end for
for each step do
    Choose $a$ from $s$ following the action selection policy
    Execute $a$
    Collect $r$
    Observe $v$
    $Q(s, a) \leftarrow Q(s, a) + \alpha[r + \gamma \max_a Q(v, a) - Q(s, a)]$
    $s \leftarrow v$
end for
```

3.2.5 Challenges in MRL: Agents Coordination

The definition of a good MRL goal is a difficult challenge, since the agents' environment are correlated and cannot be maximized independently. Non-stationarity arises in MRL because all the agents in the system are learning simultaneously. Each agent is therefore faced with a moving-target learning problem: the best policy changes as the other agents' policies changes [106]. In fact, the exploration phase is further complicated in MRL since agents explore to obtain information not only about their local environment, but also about the other agents in order to adapt to their behavior. Therefore, any agent's action on the environment depends also on the action taken by the other agents, which introduces the need of coordination. In fully cooperative stochastic games, the common return can be jointly maximized. In other cases, as the one investigated in this work, the agents' returns are typically different and correlated, and they cannot be maximized independently. Therefore, specifying a good general MRL goal is a difficult problem. The goal has to incorporate the stability of the learning dynamics of the agent on the one hand, and the adaptation to the changing behavior of the other agents on the other hand. Stability means the convergence to a stationary policy, whereas adaptation ensures that performance is maintained or improved as the other agents are changing their policies.

Convergence to equilibria is a basic stability requirement [107], since agent's strategies should eventually converge to a coordinated equilibrium, like the Nash equilibria. However, it is unclear the connection between the Nash equilibria and the performance in the dynamic stochastic game [108]. In [109] rationality is added as an adaptation criterion upon the required convergence. Rationality is defined as the requirement that the agents converges to a best-response when the other agents remain stationary. An alternative to rationality is presented in [110] with the concept of no-regret, which is defined as the requirement that the agent achieves a return that is at least as good as the return of a any stationary strategy.

Another family of solutions is represented by the ones that define an empirical coordination among the agents. In [30], the authors suggest to increase the convergence rate or RL algorithms by using a heuristic function for selecting actions in order to guide the exploration of the stat-action space in a more efficient way. Heuristically accelerated MRL approach, that has been originally proposed to improve the training phase of a single-agent RL problem, has been be extended to the multi-agent scenario in [111]. The idea is to use case-based reasoning for heuristic acceleration to exploit similarities between states of the environment already experienced in the past to make a guess on which action has to be taken. HAMRL has been already successfully applied in the wireless communication domain in the field of inter-cell interference coordination (ICIC) problem in [112]. In this work HAMRL has been applied to distributed Q-learning for implementing a decentralized ICIC controller aimed at reducing the interference in the LTE downlink channel of a network of macro BSs.

The introduction of an external heuristic suggests the construction of a hierarchical solution, which is able to coordinate the agents by having a centralized view of the effect of the agent's action on the overall environment. This type of ML paradigm is called Layered Learning [113]. It has been originally designed for solving the robotic soccer problem, and is intended in general for domains that are too complex for learning a mapping directly from an agent's sensory inputs to its actuator outputs. In fact, robotic soccer has to deal with limited communication, real-time, noisy environments with both team-mates and adversaries, which is too complex for agents to learn direct mappings from their sensors to actuators. The appropriate behavior granularity for the decomposition and the aspects of the behaviors to be learned are determined by the specific domain. Therefore, the definition of the subtask in layered learning is not automated. In fact, it is the domain that defines the layers. ML is used as a central part of layered learning to exploit data in order to train and adapt the overall system. Like the task decomposition itself, the choice of machine learning method depends on the subtask. The main characteristic of layered learning is that each learned layer directly affects the learning at the next layer. A learned subtask can affect the sub-sequent layer either (i) by providing a portion of the behavior used during training or (ii) by creating the input representation of the learning algorithm.

HAMRL and LL will be presented more in detail in Chapter 5, where have been used to mitigate the coordination problem of distributed Q-learning when solving the problem of SBSs powered with renewable energies.

3.3 Neural Networks

An artificial neural network (ANN), often called simply neural network (NN), is a model of computation inspired by the neurons of the human brain. In simplified models, the human brain consists of a large number of basic computing devices, the neurons, that are connected to each other through synapses in a complex communication network. The resulting network is the actual engine of the brain that allows to perform complex computations. Artificial neural networks adopt the same principles of the brain for solving problems through computational tools.

A neural network is implemented as a directed graph whose nodes correspond to neurons and edges correspond to links between them [114]. Each neuron receives as input a weighted sum of the outputs of the neurons connected to its incoming edges. In what following we focus on feed-forward NN, which means that the correspondent graphs does not contain cycles.

The neuron has two operative modes: training and using. The former mode corresponds to the phase where data are supplied to a neuron along with the instruction to activate or not, depending on the received input. In the latter, new data is presented and the neuron is activated or not activated based on the similarity of the input pattern to those for which the neuron was trained. In case the type of data presented during the training is labeled, the training method belong to the supervised learning. Alternatively, for unlabeled data the training method falls in the unsupervised learning category.

3.3.1 Feed-forward Neural Networks

The basic element of an ANN is represented by the neuron (also called perceptron), which consists of a linear combination of fixed non-linear functions $\theta_j(x)$. In detail, for a vector of input $x_i, i = 1 \ldots, N$, it takes the form:

$$y(\boldsymbol{x}, \boldsymbol{w}) = \sigma \left(\sum_{j=1}^{N} w_j \theta_j(\boldsymbol{x}) \right) \tag{3.10}$$

where w_i are the weights associated to each input and $\sigma(\cdot)$ is a non-linear activation function, typically the sigmoid function $f(x) = 1/((1 + e^{-x}))$.

A feedforward neural network is described as a directed acyclic graph G of vertexes V and edges D, $G = (V, D)$, and a weight function over the edges, $w : D \to \mathbb{R}$. Each single neuron is modeled as a simple scalar function, $f : \mathbb{R} \to \mathbb{R}$. The basic neural network model is composed by a series of neurons organized in L layers in a way that the input information moves only in one direction (i.e., there are no cycle in the networks like in a recurrent neural network). Let define I as the number of neurons in layer l. The bottom layer, L_0, is the input layer and it contains $N + 1$ neurons, which are the inputs plus the "constant" neuron always at 1. The last layer is composed by only one neuron and represents the output of the neural network. Each neuron in a layer $l = 2, \ldots, L$ has $I_l = I_{l-1}$ inputs, each of which is connected to the output of a neuron in the previous layer. Layers $2, \ldots, L - 1$ are called hidden layers. We denote by $v_{t,i}$, the ith neuron of the tth layer and by $o_{t,i}(\boldsymbol{x})$ the output of $v_{t,i}$ when the network is fed with the input vector $\boldsymbol{x}$. For every $i \in [n]$, the output of neuron i in L_0 is simply x_i, where n is dimensionality of the input space. The last neuron in L_0 is the constant neuron, which always outputs 1. Therefore, for $i \in [n]$ we have $o_{0,i}(\boldsymbol{x}) = x_i$ and for $i = n + 1$ we have $o_{0,i}(\boldsymbol{x}) = 1$. The other outputs can be calculated iteratively, in a layer by layer manner. Considering we have already calculated the output of a specific layer t, we can calculate the output of layer $t + 1$ as follows. Fix some $v_{t+1,j} \in L_{t+1}$. Let $a_{t+1,j}(\boldsymbol{x})$ denote the input to $v_{t+1,j}$ when the network is fed with the input vector $\boldsymbol{x}$, then:

$$a_{t+1,j}(\boldsymbol{x}) = \sum_{r:(v_{t,r},v_{t+1,j})\in E} w\left((v_{t,r}, v_{t+1,j})\right) o_{t,r}(\boldsymbol{x}) \tag{3.11}$$

and

$$o_{t+1,j}(\boldsymbol{x}) = \sigma\left(a_{t+1,j}(\boldsymbol{x})\right) \tag{3.12}$$

That is, the input of $v_{t+1,j}$ is a weighted sum of the outputs of the neurons in L_t that are connected to $v_{t+1,j}$, where weighting is according to w, and the output of $v_{t+1,j}$ is simply the application of the activation function σ on its inputs. An example diagram of a network with one hidden layer is provided in Fig. 3.2.

3.3.2 Neural Network Training

A MFNN can approximate arbitrary continuous functions defined over compact subsets of R^N by using a sufficient number of neurons at the hidden layers. In order to achieve

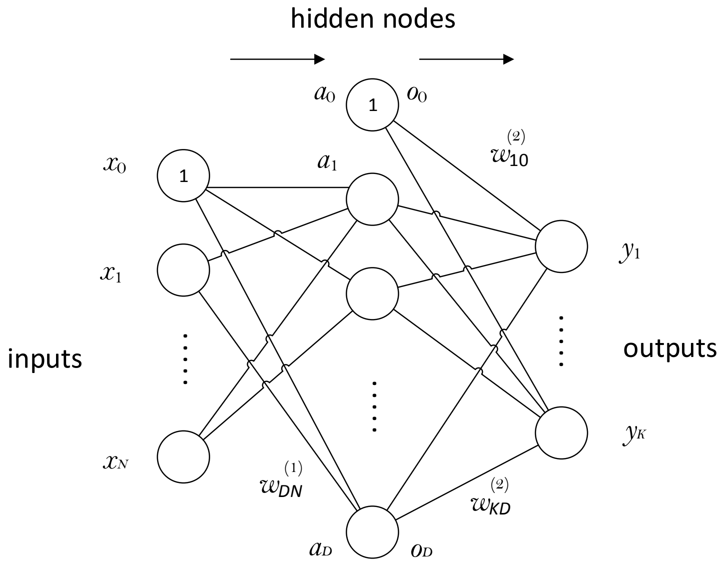

Figure 3.2: Network diagram for a MFNN with one hidden layer.

this, it is necessary to determine the values of the weights correspondent to the function to be approximated, the so called network training. Given a training set of input vectors $\boldsymbol{x}_n$, where $n = 1, \ldots, N$, together with a corresponding set of target vectors $\boldsymbol{t}_n$, the training objective is to minimize the function

$$E(\boldsymbol{w}) = \frac{1}{2} \sum_{n=1}^{N} \parallel \boldsymbol{y}(\boldsymbol{x}_n, \boldsymbol{w}) - \boldsymbol{t}_m \parallel^2 \tag{3.13}$$

which implies to find the weight vector $\boldsymbol{w}$ so that

$$\nabla E(\boldsymbol{w}) = 0. \tag{3.14}$$

However, the error function typically has a high nonlinear dependence on the weights and bias parameters, and so there will be many points in weight space at which the gradient is very small. Because it is very difficult to find an analytical solution to Eq. (3.14), it is common practice to rely on iterative numerical procedures. Most common techniques involve choosing some initial value $\boldsymbol{w}^{(0)}$ for the weight vector and then moving through weight space in a succession of steps of the form

$$\boldsymbol{w}^{(\tau+1)} = \boldsymbol{w}^{(\tau)} + \Delta \boldsymbol{w}^{(\tau)} \tag{3.15}$$

The simplest approach to comprise a small step in the correct direction is to choose the weight update in Eq. (3.15) in the direction of the negative gradient, so that

$$\boldsymbol{w}^{(\tau+1)} = \boldsymbol{w}^{(\tau)} - \eta \nabla E\left(\boldsymbol{w}^{(\tau)}\right) \tag{3.16}$$

where the parameter $\eta > 0$ is known as the learning rate. The error is defined with respect to a training set, so the entire training set has to be processed at each step in order to evaluate ∇E. Techniques that use the whole data set are called *batch* methods. When the weight vector is moved toward the direction of the greatest rate of decrease of the error function, the optimization is called *gradient descent*. This approach has been demonstrated to be a poor algorithm in [99], despite of being intuitively reasonable. In order to find a good minimum, it may be necessary to run a gradient-based algorithm multiple times using different randomly chosen starting point, and comparing the resulting performance on an independent validation set. However, there is an online version that has proved useful in practice for training neural networks [115]. In this case, the error function is considered as a sum of terms defined per each data point:

$$E(\boldsymbol{w}) = \sum_{n=1}^{N} E_n(\boldsymbol{w}) \tag{3.17}$$

This variation, also known as *sequential gradient descent*, is based on updating the weight vector one data point at a time, in detail

$$\boldsymbol{w}^{(\tau+1)} = \boldsymbol{w}^{(\tau)} - \eta \nabla E_n\left(\boldsymbol{w}^{(\tau)}\right) \tag{3.18}$$

This method allows to easily escape from local minima, since a stationary point with respect to the error function for the whole dataset is difficult to be a stationary point also for each data point individually.

Therefore, the problem to solve now is to find an efficient technique for evaluating the gradient of an error function $E(\boldsymbol{w})$ for a feed-forward neural network. The most widespread solution is called *error backpropagation* or simply *backpropagation* and is based on a local message passing scheme in which the information is sent forwards and backwards through the network [99]. For explaining the backpropagation, we start considering the evaluation of the derivative of E_n with respect to a weight w_{ij}, where the outputs of the units depend on the specific input pattern n. In order to keep the notation uncluttered, we will omit the subscript n from the network variables. Applying the chain rule for partial derivative we have

$$\frac{\partial E_n}{\partial w_{ij}} = \frac{\partial E_n}{\partial a_j}\frac{\partial a_j}{\partial w_{ij}} \tag{3.19}$$

exploiting the fact that E_n depends on the weights w_{ij} via summed input a_j to unit j. Thanks to Eq. (3.19), we can introduce the *errors*, defined as

$$\delta_j \equiv \frac{\partial E_n}{\partial a_j} \tag{3.20}$$

Considering Eq. (3.11), we can rewrite Eq. (3.19) as

$$\frac{\partial E_n}{\partial w_{ij}} = \delta_j o_i \tag{3.21}$$

since $o_i = \frac{\partial a_j}{\partial w_{ij}}$. Therefore, the derivative can be obtained by simply multiplying the value of δ for the unit at the output end of the weight by the value of o for the unit at the input end of the weight. Thus, the derivative can be calculated only evaluating the values of δ_j for each hidden and output unit in the network, and then apply Eq. (3.21). Using the chain rule for partial derivatives, we can rewrite Eq. (3.20) as

$$\delta_j \equiv \frac{\partial E_n}{\partial a_j} = \sum_k \frac{\partial E_n}{\partial a_k}\frac{\partial a_k}{\partial a_j} \tag{3.22}$$

where the sum is over all nodes k to which node j sends connections. Substituting Eq. (3.11) and Eq. (3.12) in Eq. (3.22), we can obtain the backpropagation formula

$$\delta_j = \sigma'(a_j) \sum_k w_{kj}\delta_k \tag{3.23}$$

From Eq. (3.23), we can see how the value of δ for a particular hidden node can be obtained by propagating the δs backward from nodes in the higher layers of the network. Thanks to the values of δs from the output unit that we already know, we can evaluate the δs for all the hidden nodes by recursively applying Eq. (3.23).

3.4 Concluding Remarks

This chapter has provided some background information of ML methods that constitute the main building block of the solutions presented in this Ph.D. dissertation. In detail, the TD learning methods has been presented for the multi-agent problem, focusing on the Q-learning algorithm. Moreover, the NNs have been introduced as they will be used in the layered learning framework.

Chapter 4

Photovoltaic Sources Characterization

4.1 Introduction

The standard approaches for the integration of a solar panel into existing electrical apparatuses are often not sufficient as keeping these devices fully operational at all times would demand for unrealistically large solar modules, even for SBSs [79]. To overcome this, the energy coming from the renewable sources should be wisely used, predicting future energy arrival and the energy consumption that is needed by the system to remain operational when needed. This calls for complex optimization approaches that will adapt the behavior of modern systems to the current application needs as well as to their energy reserves and the (estimated) future energy inflow [116].

A large body of work has been published so far to mathematically analyze these facts, especially in the field of wireless sensor networks. However, often researchers have tested their ideas considering deterministic [117, 118], independent and identically distributed across time slots [119] or time-correlated Markov models [120]. While these contributions are valuable for the establishment of the theory of energetically self-sufficient networks; seldom, the actual energy production process in these papers has been linked to that of real solar sources, to estimate the effectiveness of the proposed strategies in realistic scenarios.

The work in this chapter aims at filling this gap, by providing a methodology and a tool to obtain simple and yet accurate stochastic Markov processes for the description of the energy scavenged by outdoor solar sources. In this study, we focus on solar modules as those that are installed in wireless sensor networks or LTE SBSs, by devising suitable

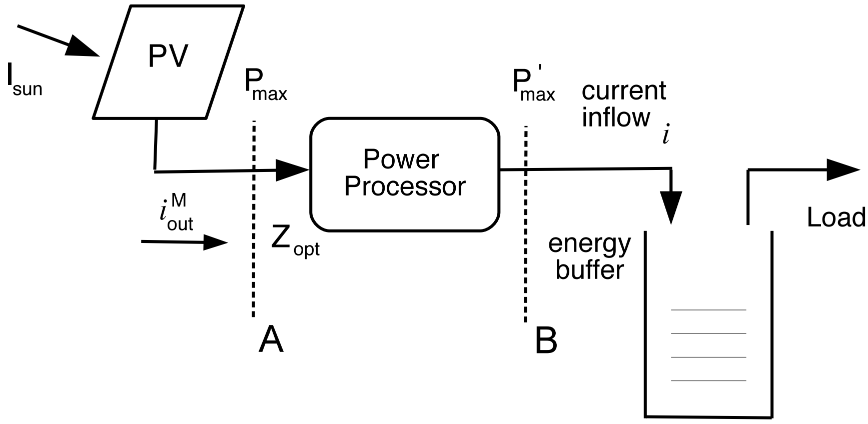

FIGURE 4.1: Diagram of a solar powered BS.

Markov processes with first- and second-order statistics that closely match that of real data traces. Our Markov models allow the statistical characterization of solar sources in simulation and theoretical developments, leading to a higher degree of realism.

This chapter is organized as follows. In Section 4.2 we detail the system model and, in particular, how the raw radiance data are processed to estimate the corresponding instantaneous harvested power. This requires the combination of several building blocks, including an astronomical model (Section 4.2.1) to estimate the actual irradiance that hits the solar module, given the inclination of the sun during the day and the module placement, an electrical model of photovoltaic cells (Section 4.2.2) and a model for the DC/DC power processor (Section 4.2.3), which is utilized to maximize the amount of power that is collected. Hence, in Section 4.2.4 we describe the Markov model that we use to statistically describe the energy inflow, according to two clustering approaches for the raw data. The results from this Markov model are shown in Section 4.3, whereas our conclusions are presented in Section 4.4.

4.2 System Model

The system model adopted in this work is depicted in the diagram of Fig. 4.1 where we identify the key building blocks for our study: the solar source (indicated as I_{sun}), the PV panel, the DC/DC power processor and the energy buffer (i.e., a rechargeable battery). In following subsections we start with the characterization of the effective solar irradiance, I_{eff}, that in general depends on the geographical coordinates of the installation site, the season of the year and the hour of the day. Hence, I_{eff} is translated by the PV module into some electrical power and a DC/DC power processor is used to ensure that the maximum power is extracted from it.

4.2.1 Astronomical Model

The effective solar radiance that hits a photovoltaic module, I_{eff}, depends on physical factors such as its location, the inclination of the solar module, the time of the year and the hour of the day. Solar radiation databases are available for nearly all locations around the Earth and their data can be used to obtain the statistics of interest. An astronomical model is typically utilized to translate the instantaneous solar radiance I_{sun} (expressed in W/m^2) into the effective sunlight that shines on the solar module. According to [121], the effective solar radiance that hits the solar module, I_{eff}, is $I_{\text{eff}} \propto I_{\text{sun}} \cos\Theta$, where $\Theta \in [-90^\circ, 90^\circ]$ is the angle between the sunlight and the normal to the solar module surface[1]. Astronomical models can be found in, e.g., [121] and Chapter 8 of [122].

In short, I_{eff} depends on many factors such as the elliptic orbit of the Earth around the sun (which causes a variation of the distance between Earth and sun across different seasons), the fact that the Earth is itself tilted on its axis at an angle of 23.45°. This gives rise to a *declination* angle ν, which is the angular distance North or South of the Earth's equator, which is obtained as:

$$\nu(N) \simeq \sin^{-1}\left[\sin(23.45^\circ)\sin\left(D(N)\right)\right] , \tag{4.1}$$

where $D(N) = 360(N-81)/365^\circ$ and N is the day number in a year with first of January being day 1. Other key parameters are the *latitude* $La \in [0, 90^\circ]$ (positive in either hemisphere), the *longitude* Lo, the *hour angle* $\zeta(t,N) \in [0, 360^\circ]$, that corresponds to the azimuth's angle of the sun's rays due to the Earth's rotation, the inclination ξ of the solar panel toward the sun on the horizon and the azimuthal displacement ψ, which is different from zero if the normal to the plane of the solar module is not aligned with the plane of the corresponding meridian, that is, the solar panel faces West or East.[2] $\zeta(t,N)$ is given by $\zeta(t,N) = 15(AST(t,N) - 12)^\circ$, where $AST(t,N) \in [0,24]$ hours, is the apparent solar time, which is the time based on the rotation of the Earth with respect to the sun and is obtained as a scaled version of the local standard time t (we refer to t' as t adjusted accounting for the daylight savings time) for the time zone where the solar module is installed. $AST(t,N)$ is computed as follows. Briefly, we obtain the Greenwich meridian angle, $GMA = UTC_{\text{off}} \times 15^\circ$, which corresponds to the angle between the Greenwich meridian and the meridian of the selected time zone: UTC_{off} is the time offset between Greenwich and the time zone and 15 is the rotation angle of the Earth per hour. Thus, we compute $\Delta t = (Lo - GMA)/15^\circ$, i.e., the time displacement between the selected time zone and the time at the reference Greenwich meridian. At this point, $AST(t,N)$ is obtained as $AST(t,N) = t' + \Delta t + ET(N)$

[1] $\Theta = 0$ ($\Theta = \pm 90^\circ$) if the sunlight arrives perpendicular (parallel) to the module.

[2] $\psi > 0$ if the panel faces West and $\psi < 0$ if it faces East.

(expressed in hours), where $ET(N)$ is known as the *equation of time*, with $ET(N) \simeq [9.87\sin(2D(N)) - 7.53\cos(D(N)) - 1.5\sin(D(N))]/60$.

Finally, the power incident on the PV module depends on the angle Θ, for which we have:

$$\begin{aligned}\cos\Theta(t,N) &= \sin\nu(N)\sin La\cos\xi - \\ &- \sin\nu(N)\cos La\sin\xi\cos\psi + \\ &+ \cos\nu(N)\cos La\cos\xi\cos\zeta(t,N) + \\ &+ \cos\nu(N)\sin La\sin\xi\cos\psi\cos\zeta(t,N) \\ &+ \cos\nu(N)\sin\xi\sin\psi\sin\zeta(t,N)\,. \end{aligned} \tag{4.2}$$

Once an astronomical model is used to track Θ, the effective solar radiance as a function of time t is given by: $I_{\text{eff}}(t,N) = I_{\text{sun}}(t,N)\max(0,\cos\Theta(t,N))$, where the $\max(\cdot)$ accounts for the cases where the solar radiation is above or below the horizon, as in these cases the sunlight arrives from below the solar module and is therefore blocked by the Earth. The sun radiance, $I_{\text{sun}}(t,N)$, for a given location, time t and day N, has been obtained from the database at [81].

4.2.2 PV Module

A PV module is composed of a number n_{sc} of *solar cells* that are electrically connected according to a certain configuration, whereby a number n_{p} of them are connected in parallel and n_{s} in series, with $n_{\text{sc}} = n_{\text{p}}n_{\text{s}}$. A given PV module is characterized by its I-V curve, which emerges from the composition of the I-V curves of the constituting cells. Specifically, the I-V curve of the single solar cell is given by the superposition of the current generated by the solar cell diode in the dark with the so called *light-generated* current i_ℓ [123], where the latter is the photogenerated current, due to the sunlight hitting the cell. The I-V curve of a solar cell can be approximated as:

$$i_{\text{out}} \simeq i_\ell - i_{\text{o}}\left[\exp\left(\frac{qv}{n\kappa T}\right) - 1\right]\,, \tag{4.3}$$

where $q \approx 1.6\cdot10^{-19}$ C is the elementary charge, v is the cell voltage, $\kappa \approx 1.380\cdot10^{-23}$ J/K is the Boltzmann's constant, T is the temperature in degree Kelvin[3], $n \geq 1$ is the diode ideality factor and i_{o} is the *dark saturation current.* i_{o} corresponds to the solar cell diode leakage current in the absence of light and depends on the area of the cell as well as on the photovoltaic technology. The open circuit voltage v_{oc} and the short circuit current

[3] T is given by the sum of the ambient temperature, which can be obtained from the dew point and relative humidity, and of a further factor due to the solar power hitting the panel.

i_{sc} are two fundamental parameters for a solar cell. The former is the maximum voltage for the cell and occurs when the net current through the device is zero. i_{sc} is instead the maximum current and occurs when the voltage across the cell is zero (i.e., when the solar cell is short circuited). If $v_{\mathrm{oc}}^{\mathrm{M}}$ and $i_{\mathrm{sc}}^{\mathrm{M}}$ are the open circuit voltage and short circuit current for the solar module M, the single solar cell parameters are obtained as: $i_{\mathrm{sc}} = i_{\mathrm{sc}}^{\mathrm{M}}/n_{\mathrm{p}}$ and $v_{\mathrm{oc}} = v_{\mathrm{oc}}^{\mathrm{M}}/n_{\mathrm{s}}$ (considering a module composed of homogeneous cells).

The light-generated current for the single solar cell is a time varying quantity, $i_\ell(t,N)$, which depends on the amount of sunlight that hits the solar cell at time t, where N is the day number. Here, we have used the following relation: $i_\ell(t,N) = i_{\mathrm{sc}}F(t,N)$, where the *radiation rate* $F(t,N) \in [0,1]$ is obtained as $F(t,N) = 0.001 I_{\mathrm{eff}}(t,N)$, i.e., normalizing the effective irradiance hitting the solar cell with respect to the maximum radiation of 1 kW/m^2 (referred to in the literature as "one sun" [124]). Hence, $i_\ell(t,N)$ is plugged into 4.3 to obtain $i_{\mathrm{out}}(t,N)$ for a single solar cell as a function of the time t for day N. The total current that is extracted from the solar module is: $i_{\mathrm{out}}^{\mathrm{M}}(t,N) = n_{\mathrm{p}} i_{\mathrm{out}}(t,N)$.

4.2.3 Power Processor

Generally speaking, every voltage or current source has a *maximum power point*, at which the average power delivered to its load is maximized. For example, a Thévenin voltage source delivers its maximum power when operating on a resistive load whose value matches that of its internal impedance. However, in general the load of a generic device does not match the optimal one, which is required to extract the maximum power from the connected solar source. To cope with this, in practice the optimal load is emulated through a suitable *power processor*, whose function is that of "adjusting" the source voltage (section A of Fig. 4.1) until the power extracted from it is maximized,[4] which is also known as maximum power point tracking (MPPT). Ideally, through MPPT, the maximum output power is extracted from the solar panel under any given temperature and irradiance condition, adapting to changes in the light intensity. Commercially available power processors use "hill climbing techniques"; as an example, in [125] the authors propose advanced control schemes based on the downhill simplex algorithm, where the voltage and the switching frequency are jointly adapted for fast convergence to the maximum power point. See also [126] for further information on MPPT algorithms and their comparative evaluation and [127] for a low-power design targeted to wireless sensor nodes. In the present work, we have taken into account the DC/DC power processor by computing the operating point $(i_{\mathrm{out}}^{\mathrm{M}}, v^{\mathrm{M}})$ (see Eq. 4.3) for which the extracted power in section A, $P = i_{\mathrm{out}}^{\mathrm{M}} v^{\mathrm{M}}$, is maximized. Note that, if i_{out} and v are the output current

[4] This corresponds to adapting the input impedance of the power processor to $Z_{\mathrm{opt}} = Z_{\mathrm{source}}^{*}$, where * indicates the complex conjugate.

and the voltage of the single solar cell, we have $i^{\mathrm{M}}_{\mathrm{out}} = n_{\mathrm{p}} i_{\mathrm{out}}$ and $v^{\mathrm{M}} = n_{\mathrm{s}} v$. For this procedure, we have considered the parameters presented before (solar irradiance, rotation of the Earth, etc.) and also the fact that i_{sc} and v_{oc} change as a function of the environmental temperature, which affects the shape of the I-V curve in Eq. 4.3 (see, e.g., the dependence of i_ℓ on i_{sc}). Hence, we have computed the extracted power in two steps: step 1) we have obtained the (ideal) maximum power P_{MPP} that would be extracted by the panel at the MPP by an ideal tracking system:

$$P_{\mathrm{MPP}} = \max_{v}\{i^{\mathrm{M}}_{\mathrm{out}} v^{\mathrm{M}}\} = n_{\mathrm{p}} n_{\mathrm{s}} \max_{v}\{i_{\mathrm{out}} v\}\,, \tag{4.4}$$

where $i_{\mathrm{out}} = i_{\mathrm{out}}(t, N)$ is given by Eq. 4.3. Step 2) the power available after the power processor (section B in Fig. 4.1) is estimated as $P'_{\max} = \eta P_{\mathrm{MPP}}$, where $\eta \in (0, 1)$ is the power processor conversion efficiency, which is defined as the ratio $\eta = P'_{\max}/P_{\mathrm{MPP}}$ and can be experimentally characterized for a given MPP tracking circuitry [127]. $P'_{\max}$ is the power that is finally transferred to the energy buffer.

4.2.4 Semi-Markov Model for Stochastic Energy Harvesting

The dynamics of the energy harvested from the environment is captured by a continuous time Markov chain with $N_{\mathrm{s}} \geq 2$ states. This model is general enough to accommodate different clustering approaches for the empirical data, as we detail shortly.

Formally, we consider an energy source that, at any given time, can be in any of the states $x_s \in \mathcal{S} = \{0, 1, \dots, N_{\mathrm{s}} - 1\}$. We refer to t_k, with $k \geq 0$, as the time instants where the source transitions between states, and we define $\tau_k = t_{k+1} - t_k$ as the time elapsed between two subsequent transitions. In what follows, we say that the system between t_k and t_{k+1} is in *cycle k*.

Right after the k-th transition to state $x_s(k)$, occurring at time t_k, the source remains in this state for τ_k seconds, where τ_k is governed by the probability density function (pdf) $f(\tau|x_s)$, with $\tau \in [\tau_{\min}(x_s), \tau_{\max}(x_s)]$. At the next transition instant, t_{k+1}, the source moves to state $x_s(k+1) \in \mathcal{S}$ according to the probabilities $p_{uv} = \mathrm{Prob}\{x_s(k+1) = v|x_s(k) = u\}$, with $u, v \in \mathcal{S}$. When the source is in state $x_s(k)$, an input current i_k is fed to the rechargeable battery, where i_k is drawn from the pdf $g(i|x_s)$, with $i \geq 0$. That is, when a state is entered, the input current i and the permanence time τ are respectively drawn from $g(i|x_s)$ and $f(\tau|x_s)$. Then, the input current remains constant until the next transition, that occurs after τ seconds. In this work, we assume that the voltage at the energy buffer (section B of Fig. 4.1) is constant, as typically considered when a rechargeable battery is used. Given that, there is a one-to-one mapping between instantaneous harvested power and harvested current.

4.2.5 Estimation of Energy Harvesting Statistics

Based on the aforementioned models, we have mapped the hourly irradiance patterns obtained from [81] into the corresponding operating point, in terms of power $P'_{\rm max}$ and current i after the power processor (section B of Fig. 4.1). Thus, we have computed the statistics $f(\tau|x_s)$ and $g(i|x_s)$ from these data according to the two approaches that we describe next. These differ in the adopted clustering algorithm, in the number of states $N_{\rm s}$ and in the structure of the transition probabilities p_{uv}, $u, v \in \mathcal{S}$.

Night-day clustering: we have collected all the data points in [81] from 1991 to 2010, grouping them by month. Thus, for each day in a given month we have classified the corresponding points into two states $x_s \in \{0, 1\}$, i.e., a low- ($x_s = 1$) and a high-energy state ($x_s = 0$). To do this, we have used a current threshold $i_{\rm th}$, which is a parameter set by the user, corresponding to a small fraction of the maximum current in the dataset. According to $i_{\rm th}$, we have classified all the points that fall below that threshold as belonging to state 0 (i.e., night) and those points above the threshold as belonging to state 1 (day). After doing this for all the days in the dataset, we have estimated the probability density function of the duration τ, $f(\tau|x_s)$, and that of the input current i (after the power processor), $g(i|x_s)$, for each state and for all months of the year. For the estimation of the pdfs we have used the kernel smoothing technique see, e.g., [128]. The transition probabilities of the resulting semi-Markov chain are $p_{10} = p_{01} = 1$ and $p_{00} = p_{11} = 0$ as a night is always followed by a day and vice versa.

Slot-based clustering: as above, we have collected and classified the irradiance data by month. Then, we subdivided the 24 hours in each day into a number $N_{\rm s} \geq 2$ of time slots of constant duration, equal to T_i hours, $i = 1, \ldots, N_{\rm s}$. Each slot is a state x_s of our Markov model. Hence, for each state x_s we computed the pdf $g(i|x_s)$ for each month of the year, considering the empirical data that has been measured in slot x_s for all days in the dataset for the month under consideration. Again, the kernel smoothing technique has been utilized to estimate the pdf. For the statistics $f(\tau|x_s)$, being the slot duration constant by construction, we have that: $f(\tau|x_s) = \delta(\tau - T_{x_s})$, for all states $x_s \in \mathcal{S}$, where $\delta(\cdot)$ is the Dirac's delta. The transition probabilities of the resulting Markov chain are $p_{uv} = 1$, when $u \in \mathcal{S}$ and $v = (u + 1) \mod N_{\rm s}$, and $p_{uv} = 0$ otherwise. This reflects the temporal arrangement of the states.

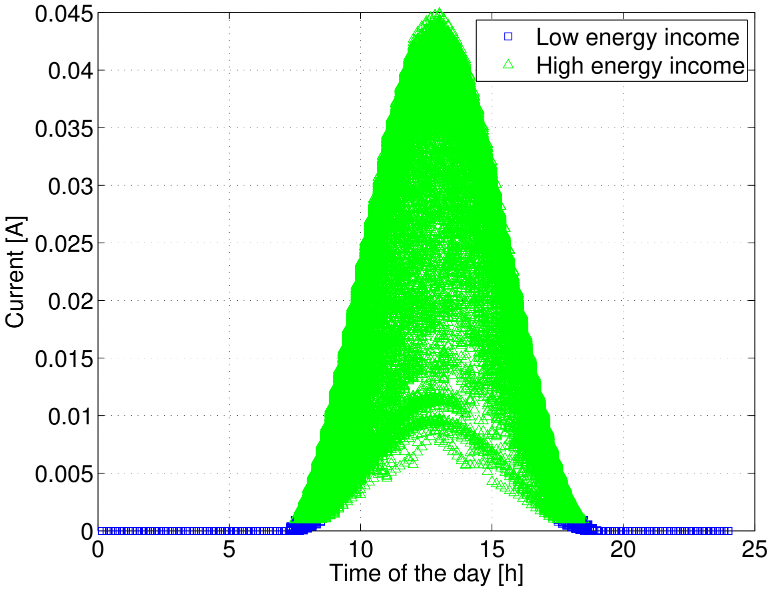

FIGURE 4.2: Result of the night-day clustering approach for the month of July considering the radiance data from years 1999 − 2010.

4.3 Numerical Results

For the results in this section, we have used as reference the commercially available micro-solar panels from Solarbotics, selecting the Solarbotics's SCC-3733 Monocrystalline solar technology [129]. It is to be noted that, the conclusions drawn in this subsection for this type of panel are general and valid also for panel of bigger size, such as the one used for SBSs since the harvested current is only scaled. For this product, the single cell area is about 1 square centimeter, the solar cells have an efficiency of 21.1%, $i_{\rm sc} = 5$ mA and $v_{\rm oc} = 1.8$ V. Next, we show some results on the stochastic model for the solar energy source obtained considering a solar module with $n_{\rm p} = 6$ and $n_{\rm s} = 6$ cells in parallel and in series, respectively. We have selected Los Angeles as the installation site, considering $\xi = 45°$, $\psi = 30°$ and processing the data from [81] as described in the previous section with a cluster threshold equal to $1/50-$th of the maximum current in the dataset.

4.3.1 Night-day clustering

A first example for the night-day clustering approach is provided in Fig. 4.2, which shows the result of the clustering process for the month of July. Two macro states are evident: a low energy state (night), during which the power inflow is close to zero, and a high energy state (day). As this figure shows, the harvested current during the day follows a bell-shaped curve. However, contrarily to what one would expect, even for the

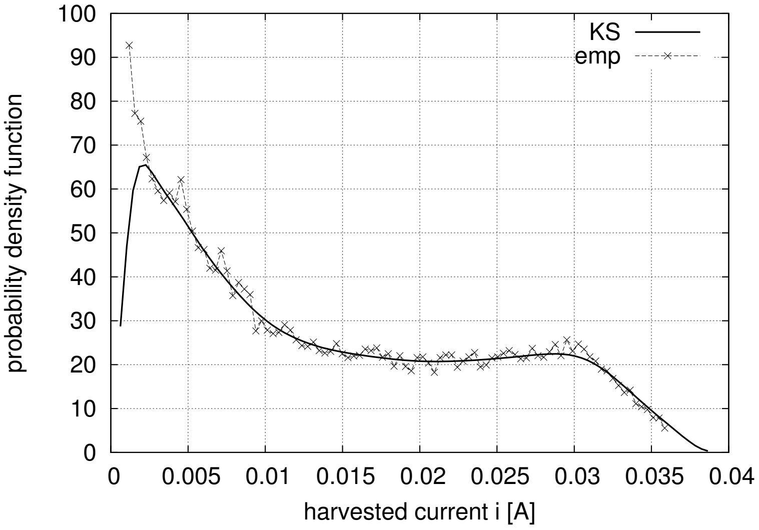

FIGURE 4.3: $g(i|x_s)$ (solid line, $x_s = 0$) obtained through the Kernel Smoothing (KS) technique for the month of February, for the night-day clustering method (2-state semi-Markov model), using radiance data from years $1999 - 2010$. The empirical pdf (emp) is also shown for comparison.

month of July the high-energy state shows a high degree of variability from day-to-day, as is testified by the considerable dispersion of points across the y-axis. This reflects the variation in the harvested current due to diverse weather conditions. In general we have a twofold effect: 1) for different months the peak and width of the bell vary substantially, e.g., from winter to summer and 2) for all months we observe some variability across the y-axis among different days. These facts justify the use of stochastic modeling, as we do in this work, to capture such variability in a statistical sense.

Another example, regarding the accuracy of the Kernel Smoothing (KS) technique to fit the empirical pdfs, is provided in Fig. 4.3, where we show the fitting result for the month of February.

In Figs. 4.4 and 4.5 we show some example statistics for the months of February, July and December. In Fig. 4.4, we plot the pdf $g(i|x_s)$, which has been obtained through KS for the high-energy state $x_s = 0$. As expected, the pdf for the month of July has a larger support and has a peak around $i = 0.04$ A, which means that is likely to get a high amount of input current during that month. For the months of February and December, we note that their supports shrink and the peaks move to the left to about 0.03 A and 0.022 A, respectively, meaning that during these months the energy scavenged is lower and is it more likely to get a small amount of harvested current during the day. Fig. 4.5 shows the cumulative distribution functions (cdf) obtained integrating $g(i|x_s)$ and also the corresponding empirical cdfs. From this graph we see that the cdfs obtained through KS closely match the empirical ones. In particular, all the cdfs that we

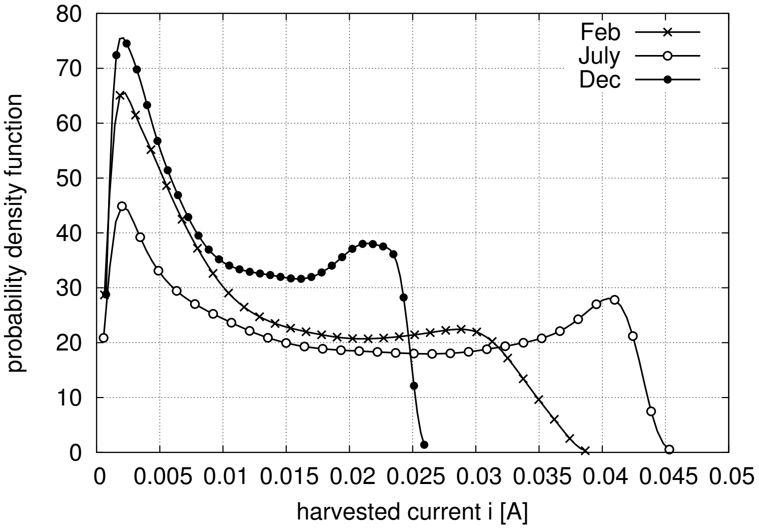

FIGURE 4.4: Pdf $g(i|x_s)$, for $x_s = 1$, obtained through Kernel Smoothing for the night-day clustering method (2-state Markov model).

have obtained through KS have passed the Kolmogorov-Smirnov test when compared against the empirical ones, for a confidence of 1%, which confirms that the obtained distributions represent a good model for the statistical characterization of the empirical data. The pdf for state $x_s = 1$ is not shown as it has a very simple shape, presenting a unique peak around $i = 0^+$. In fact, the harvested current is almost always negligible during the night.[5] Figs. 4.6 and 4.7 respectively show the pdf $f(\tau|x_s)$ obtained through KS and the corresponding cdf for the same location and months of above, for $x_s = 0$. Again, Fig. 4.6 is consistent with the fact that in the summer days are longer and Fig. 4.7 confirms the goodness of our KS estimation. Also in this case, the statistics for all months have passed the Kolmogorov-Smirnov test for a confidence of 1%. The pdfs for state $x_s = 1$ are not shown as these are specular to those of Fig. 4.6 and this is also to be expected as the sum of the duration of the two states $x_s = 0$ (daytime) and $x_s = 1$ (night) corresponds to the constant duration of a day. This means that the duration statistics of one state is sufficient to derive that of the other.

4.3.2 Slot-based clustering

The attractive property of the 2-state semi-Markov model obtained from the night-day clustering approach is its simplicity, as two states and four distributions suffice to statistically represent the energy inflow dynamics. Nevertheless, this model leads to

[5] Note that our model does not account for the presence of external light sources such as light poles.

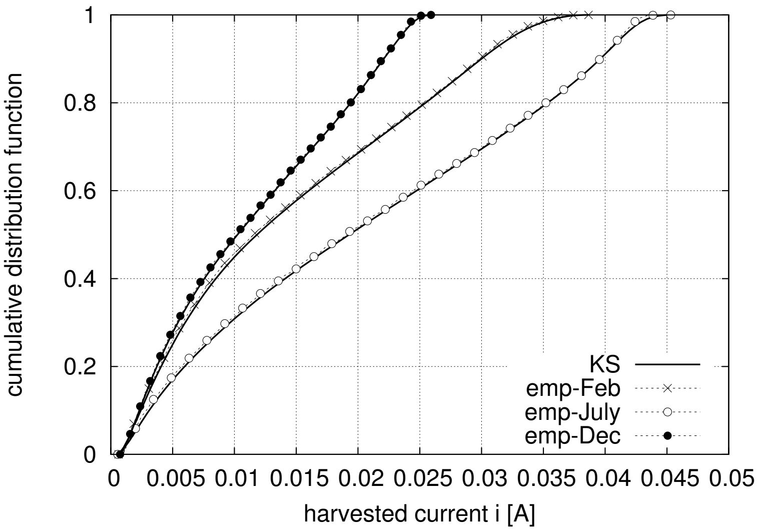

FIGURE 4.5: Cumulative distribution function of the harvested current for $x_s = 1$ (solid lines), obtained through Kernel Smoothing (KS) for the night-day clustering method (2-state Markov model). Empirical cdfs (emp) are also shown for comparison.

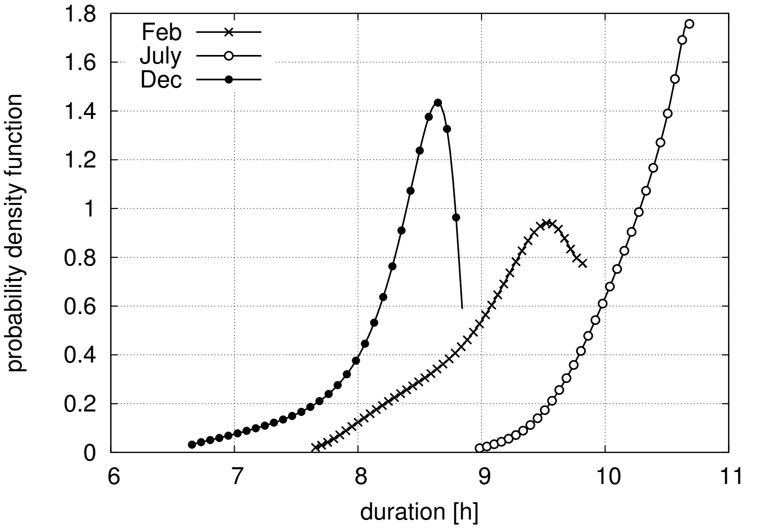

FIGURE 4.6: Pdf $f(\tau|x_s)$, for $x_s = 1$, obtained through Kernel Smoothing for the night-day clustering method (2-state Markov model).

a coarse-grained characterization of the temporal variation of the harvested current, especially in the high-energy state.

Slot-based clustering has been proposed with the aim of capturing finer temporal details. An example of the clustering result for this case is given in Fig. 4.8, for the month of July for $N_s = 12$. All slots in this case have the same duration, which has been fixed a priori and corresponds to $24/N_s$ hours.

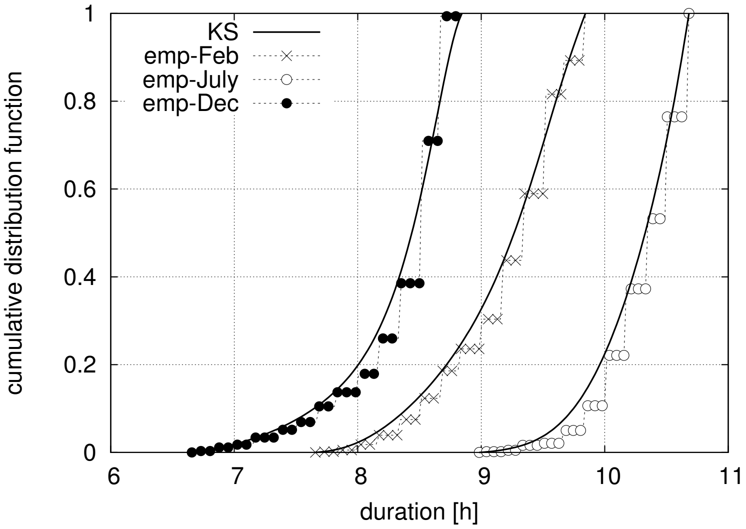

FIGURE 4.7: Cumulative distribution function of the state duration for $x_s = 1$ (solid lines), obtained through Kernel Smoothing (KS) for the night-day clustering method (2-state Markov model). Empirical cdfs (emp) are also shown for comparison.

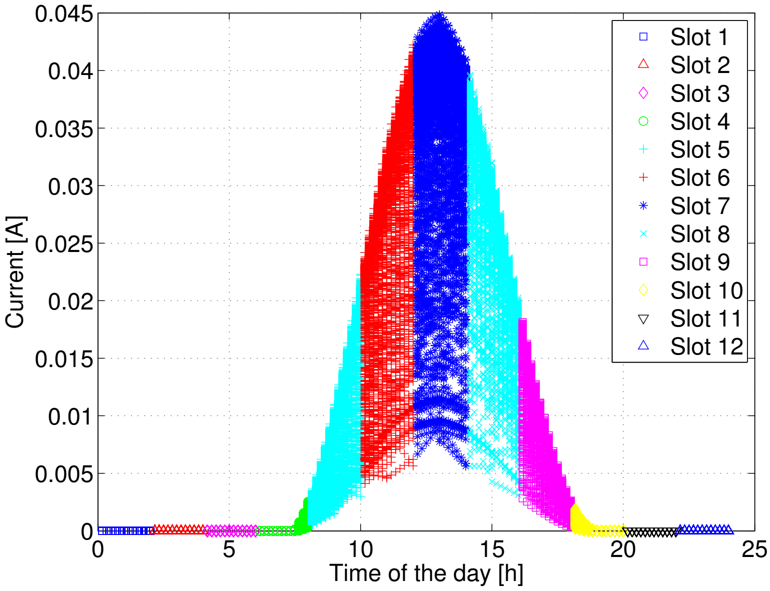

FIGURE 4.8: Result of slot-based clustering considering $N_s = 12$ time slots (states) for the month of July, years 1999 − 2010.

Fig. 4.9 shows the pdf $g(i|x_s)$ for the first three states of the day (slots 5, 6 and 7, see Fig. 4.8) for the month of July, which have been obtained through KS. As expected, the peaks (and the supports) of the pdfs move to higher values, until reaching the maximum of 0.04 A for slot 7, which is around noon. Due to the symmetry in the solar distribution within the day, the results for the other daytime states are similar and therefore have not been reported. In Fig. 4.10 we compare the cdfs obtained through KS against the

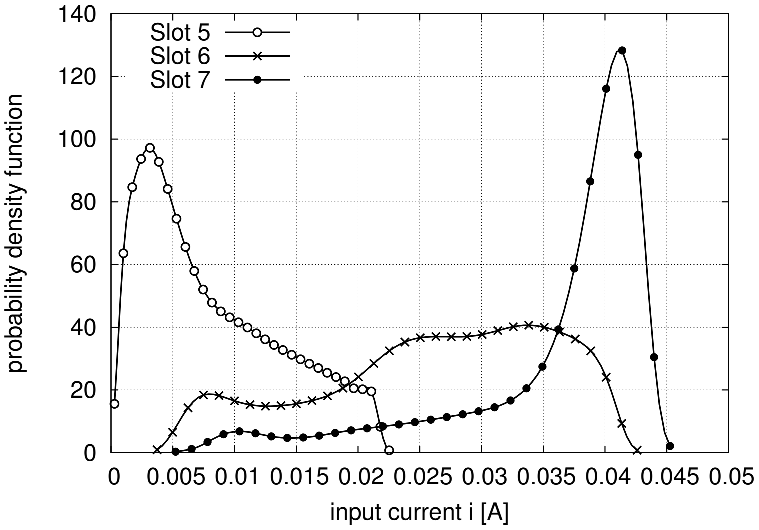

FIGURE 4.9: Pdf $g(i|x_s)$ for $x_s = 5, 6$ and 7 for the slot-based clustering method for the month of July.

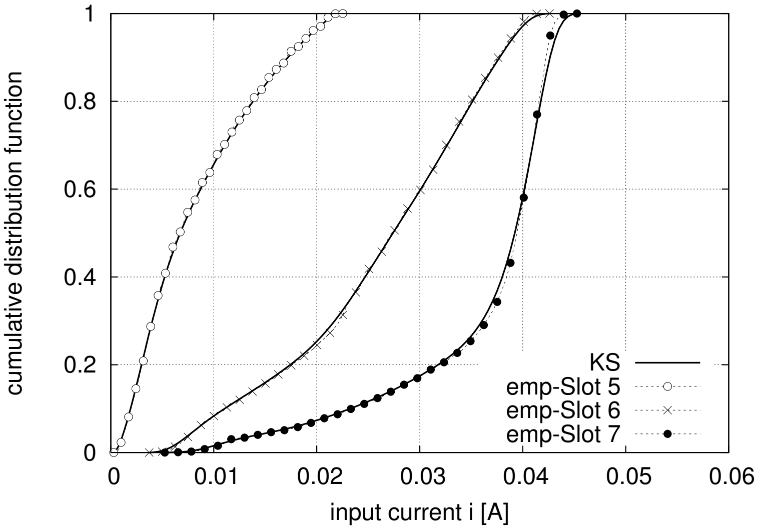

FIGURE 4.10: Comparison between KS and the empirical cdfs (emp) of the scavenged current for $x_s = 5, 6$ and 7 for the slot-based clustering method for the month of July.

empirical ones. Also in this case, all the cdfs have passed the Kolmogorov-Smirnov test for a confidence of 1%.

A last but important results is provided in Fig. 4.11, where we plot the autocorrelation function (ACF) for the empirical data and the Markov processes obtained by slot-based clustering for a number of states N_s ranging from 2 to 24 for the month of January. With the ACF we test how well the Markov generated processes match the empirical data in terms of second-order statistics. As expected, a 2-state Markov model poorly resembles the empirical ACF, whereas a Markov process with $N_\mathrm{s} = 12$ states performs

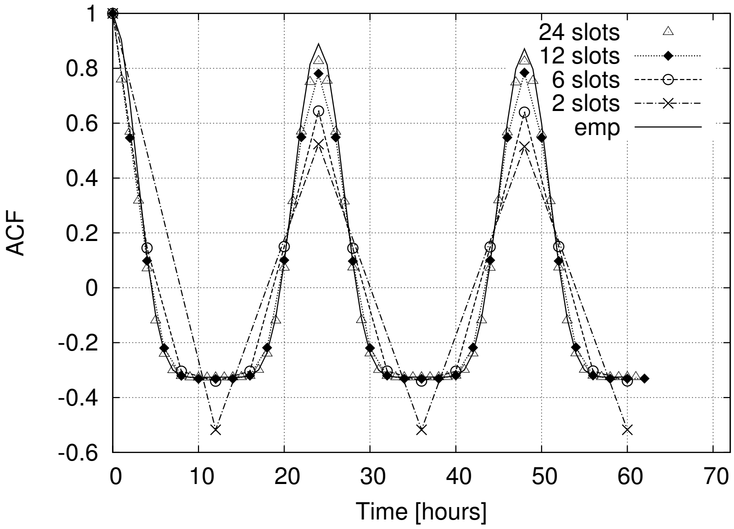

Figure 4.11: Autocorrelation function for empirical data ("emp", solid curve) and for a synthetic Markov process generated through the night-day clustering (2 slots) and the slot-based clustering ($6, 12$ and 24 slots) approaches, obtained for the month of January.

quite satisfactorily. Note also that 5 of these 12 states can be further grouped into a single macro-state, as basically no current is scavenged in any of them (see Fig. 4.8). This leads to an equivalent Markov process with just eight states.

We highlight that our Markov approach keeps track of the temporal correlation of the harvested energy within the same day, though the Markovian energy generation process is independent of the "day type" (e.g., sunny, cloudy, rainy, etc.) and also on the previous day's type. Given this, one may expect a good fit of the ACF within a single day but a poor representation accuracy across multiple days. Instead, Fig. 4.11 reveals that the considered Markov modeling approach is sufficient to accurately represent second-order statistics. This has been observed for all months. Hence, one may be thinking of extending the state space by additionally tracking good (g) and bad (b) days so as to also model the temporal correlation associated with these qualities. This would amount to defining a Markov chain with the two macro-states g and b, where $p_{gb} = \text{Prob}\{\text{day } k \text{ is } g | \text{ day } k-1 \text{ is } b\}$, with $k \geq 1$. Hence, in each state g or b, the energy process could still be tracked according to one of the two clustering approaches of Section 4.2.4, where the involved statistics would be now conditioned on being in the macro-state. The good approximation provided by our model, see Fig. 4.11, show that this further level of sophistication is unnecessary.

Table 4.1: Results for different solar panel configurations with night-day clustering in Los Angeles for the month of August

$n_\mathrm{p} \times n_\mathrm{s}$	Size	$\bar{i}$	max(i)	$\bar{\tau}$	min(τ)	max(τ)
	[cm^2]	[mA]	[mA]	[h]	[h]	[h]
2 x 2	2.99	2.16	4.52	9.73	8.17	10.17
4 x 4	11.98	9.25	19.77	10.18	9.00	10.67
6 x 6	26.96	21.29	45.56	10.26	9.17	10.67
8 x 8	47.92	38.15	82.10	10.32	9.17	10.83
10 x 10	74.88	59.97	129.19	10.34	9.17	10.83
12 x 12	107.83	86.73	186.91	10.35	9.17	10.83

Table 4.2: Results for different solar panel configurations with night-day clustering in Los Angeles for the month of December

$n_\mathrm{p} \times n_\mathrm{s}$	Size	$\bar{i}$	max(i)	$\bar{\tau}$	min(τ)	max(τ)
	[cm^2]	[mA]	[mA]	[h]	[h]	[h]
2 x 2	2.99	1.11	2.48	7.74	5.00	8.33
4 x 4	11.98	4.85	11.03	8.27	6.50	8.67
6 x 6	26.96	11.19	25.67	8.38	6.67	8.83
8 x 8	47.92	20.16	46.01	8.42	6.83	8.83
10 x 10	74.88	31.65	72.44	8.44	6.83	8.83
12 x 12	107.83	45.79	104.83	8.45	6.83	9.00

4.3.3 Panel size and location

To conclude, we show some illustrative results for different solar panel sizes and locations. Table 4.1 and Table 4.2 present the main outcomes for different solar cells configurations for the night-day clustering approach for the months of August and December. Two representative months are considered: the month with the highest energy harvested, August, and the one with the lowest, December. As expected, the current inflow strongly depends on the panel size (linearly). Also, note that the day duration slightly increases for an increasing panel area as this value is obtained by measuring when the energy is above a certain (clustering) threshold. Although we scaled this threshold proportionally with an increasing harvested current, the longer duration of the day is due to the exponential behavior introduced by the scaling factor in Eq. 4.3, see the RHS of this equation.

Finally, in table 4.3 and table 4.4 we show some energy harvesting figures for a solar panel with $n_\mathrm{p} = n_\mathrm{s} = 6$ for some representative cities for the months of August and December, respectively.

Table 4.3: Results for different solar panel locations for $n_\mathrm{p} = n_\mathrm{s} = 6$ for the month of August

Location	$\bar{i}$ [mA]	max(i) [mA]	$\bar{\tau}$ [h]	min(τ) [h]	max(τ) [h]
Chicago, IL	17.03	46.74	10.57	8.50	11.33
Los Angeles, CA	21.29	45.56	10.26	9.17	10.67
New York, NY	17.17	44.62	10.42	8.83	11.00
Reno, NV	22.91	48.52	10.72	9.16	11.00

Table 4.4: Results for different solar panel locations for $n_\mathrm{p} = n_\mathrm{s} = 6$ for the month of December

Location	$\bar{i}$ [mA]	max(i) [mA]	$\bar{\tau}$ [h]	min(τ) [h]	max(τ) [h]
Chicago, IL	5.24	16.08	6.95	4.83	8.00
Los Angeles, CA	11.19	25.67	8.38	6.67	8.83
New York, NY	6.81	18.95	7.57	5.67	8.33
Reno, NV	8.24	21.12	7.85	6.00	8.50

4.4 Conclusions

In this chapter we have considered micro-solar power sources, providing a methodology to model the energy inflow as a function of time through stochastic Markov processes. The latter, find application in energy self-sustainable systems, such as the one considered in this thesis (i.e., the simulation of energy harvesting communication networks) and are as well useful to extend current theoretical work through more realistic energy models. Thus, it allows to accurate model one of the most important environment variable, i.e., the energy. The proposed approach has been validated against real energy traces, showing good accuracy in their statistical description in terms of first and second order statistics. As final remark, it is to be noted that the tool has been developed using Matlab$^{\mathrm{TM}}$and is available under the GPL license at [130].

Chapter 5

Switch-ON/OFF Policies for EH SBSs through Distributed Q-Learning

5.1 Introduction

Massive deployment of SBSs represents the most promising architecture to meet the high capacity demands of mobile networks. Their reduced energy requirements encourage the use of RES as distributed power suppliers. Their adoption is expected to have a twofold positive effect: 1) it will increase the use of renewable sources to provide energy, and consequently to reduce the carbon footprint of ICT, and 2) it will allow savings on power grid bills. Solar energy is probably the most important RES, due to its widespread availability, the good efficiency of photovoltaic technology and its competitive cost [79]. However, the resulting panel sizes may represent an obstacle for urban scenarios, where SBSs are likely to be installed in street furniture (i.e., traffic lamps, street lights, transportation hubs, etc.). Small form-factor solar panels can also be adopted by intelligently allocating energy to the SBSs, putting them in power saving (OFF) mode when necessary, and exploiting the macro BS to compensate for their OFF time. The bottom line is that the panel size can be made small at the cost of some extra processing / optimization, which entails a tight interaction among SBSs and between SBSs and the macro BS.

However, with the introduction of energy harvesting, we also need to consider the erratic and intermittent nature of RES, which further complicates the EE problem and the corresponding ON/OFF strategies. Most of the previous papers published in this area have only provided guidelines for dimensioning the network, while online approaches to control network elements have appeared only recently. In [91], the authors present an algorithm for determining when to switch OFF the SBSs by solving a ski rental problem. The analysis is carried out considering Poisson arrivals for energy and traffic, which may provide a non-realistic approximation to these processes. A solution based on Reinforcement Learning is presented in [92], where the authors concentrate on the performance of a single SBS. However, the impact of multiple SBSs simultaneously switching OFFs within the same area is not considered.

In this chapter, we fill these gaps by proposing a solution considering multiple SBSs in a macro BS area, realistic traffic conditions and solar radiation data from real measurements. SBS network is modeled as a multi-agent system where each agent (SBS) makes autonomous decisions, according to a Decentralized SON paradigm. SBSs supplied by solar energy and batteries (energy storage) are utilized as an overlay layer in a two-tier network with a macro BS powered by the electricity grid. The behavior of small cells can be optimized to offload the traffic from the macro BS according to the energy income and the traffic demand. To this purpose, we designed a distributed online solution based on multi-agent RL, known as *distributed Q-learning*, which allows SBSs to independently learn a RRM policy. This main contribution of this study lies on the following points:

1. proposing a distributed Q-learning solution to control SBSs powered with solar energy
2. extend the standard Q-learning solution with offline trained algorithm
3. investigating the convergence of the algorithms
4. characterizing the ON/OFF switching policies
5. evaluate the network system performance with the proposed solutions compared to a baseline solution
6. calculating the surplus energy that cannot be stored, due to the energy storage capacity constraints

The remainder of the chapter is organized as follows. In Section 5.2 we present the system model. Section 5.3 gives an overview on the distributed Q-learning algorithm, whereas the two proposed algorithms are presented in Section 5.4. In Section 5.5 we discuss some performance results. In Section 5.6 we draw our conclusions and discuss future research directions.

5.2 System Model

We consider a two-tier network composed of clusters of one macro BSs and N SBSs. The macro BSs are connected to the power grid and provide baseline coverage. The SBSs are deployed in a hotspot manner to increase the system capacity, where needed (e.g., shopping hall, city center, etc.). SBSs are solely powered through solar-harvested energy and possess rechargeable batteries to store the harvested energy.

For the BS power consumption model we use the linear model presented in Section 2.2, $P = P_0 + \beta\rho$, where $\rho \in [0, 1]$ is the BS traffic load, normalized with respect to its maximum capacity, and P_0 is its baseline power consumption. We consider medium scale factor "metro cells" as SBSs, featuring a maximum transmission power of 38 dBm. The values of β and P_0 for the macro BS (SBS) are 600 (39)W and 750 (105.6), respectively.

The user equipment resource allocation scheme uses the methodology defined in [131]. This includes a detailed wireless channel model and the dynamic selection of the modulation and coding scheme for each user as function of its channel state.

5.3 Distributed Q-Learning

In this Section we present the distributed Q-learning algorithm already introduced in Chapter 3 and we define the variables used in this work. Distributed Q-learning is an online optimization technique to control multi-agent systems, i.e., a system featuring N distributed agents (the SBSs) which make decisions (switch-ON/OFF) in an uncoordinated fashion. Each agent has to independently learn a policy (switch-ON/OFF) through real-time interactions with the environment. These interactions entail taking actions for the agents and receiving, in return, a reward from the environment. In distributed Q-learning each agent i maintains a local policy and a local Q-function $Q(x_t^i, a_t^i)$ that only depends on its state x_t^i and actions a_t^i, with t being the decision epoch (time). The agents only have a partial view of the overall system and their local states may differ since traffic load and energy income may be unevenly distributed. In particular, the input of the switch-ON/OFF algorithm depends on the SBS location and on the geographical distribution of its users, affecting for instance, the experienced traffic load. The decision making process of each agent is defined according to a MDP with state vector $\boldsymbol{x}_t = (x_t^1, x_t^2, \ldots, x_t^N)$, where x_t^i is the state associated with SBS i at time t. Agent i *independently* chooses an action a_t^i from an action set $\mathcal{A}$ based on its own state x_t^i. At the next decision epoch $t + 1$, the agent receives a reward r_t^i from the environment. The *agent dependent* reward r_t^i is then used to locally update the Q-value, $Q(x_t^i, a_t^i)$, indicating the level of convenience of selecting action a_t^i when in state x_t^i. The Q-value is updated as follows:

$$Q(x_t^i, a_t^i) \leftarrow Q(x_t^i, a_t^i) + \alpha \left[r_t^i + \gamma \max_a Q(x_{t+1}^i, a') - Q(x_t^i, a) \right] \tag{5.1}$$

where α is the learning rate, γ is the discount factor and x_{t+1}^i is the next state for agent i and a' is the associated optimal action, as introduced in Section 3.2.2. This procedure is executed by each agent at each epoch of the system in a synchronized manner. The *asynchronous Q-learning algorithm* proposed in [132], uses a learning rate given by a polynomial function that at time t accounts for the number of visits, up to and including time t, to state-action pair (x, a), termed $n(x, a, t)$. In detail $\alpha^\omega(x, a) = \alpha / n(x, a, t)^\omega$, where $\omega = 1$ leads to a linear learning rate, $\omega \in (1/2, 1)$ to a polynomial one and $\omega = 0$ to a constant learning rate.

To make the best decisions (exploitation) the algorithm must have gathered enough information from the environment (exploration). The exploration phase is commonly controlled by an ε-*greedy* approach, in which random states are visited by the agents with probability ε. Since rigorous convergence results for multi-agent reinforcement learning algorithms are still an open research question, here we refer to the convergence time as the first instant in which the Q-values remain stable within a certain tolerance. In particular, we say that the system has reached convergence when all the SBS batteries are below $B_{\text{th}}^{\text{OFF}}$ for a certain amount of time (e.g., within a window of consecutive days). The rationale behind this definition is to foster the energy sustainability of the SBSs.

5.4 Algorithms

5.4.1 ON/OFF switching through online distributed Q-learning

In this section we provide details on the Q-learning algorithm, by defining state, action set and reward function, for the N agents.

State: The local state x_t^i is defined by:

$$x_t^i = \{S_t^i, B_t^i, L_t^i\}\,, \tag{5.2}$$

where S_t^i is the state of the renewable energy source based on the incoming amount harvested energy (e.g., day and night), B_t^i is the normalized battery energy level, L_t^i is the normalized load for SBS i in slot t, which depends on the number of users served by this SBS. We uniformly quantize S_t^i, B_t^i and L_t^i into 2, 5 and 3 levels, respectively, since we found experimentally that represent a good trade-off between complexity and accuracy.

Action set: The set of possible actions $\mathcal{A}$ consists of the two actions of switching ON and OFF the SBS. We have not considered the option of modulating the load ρ between 0 and 1, due to the energy profile of SBSs. In fact, the β parameter in Table 2.1 for the SBSs is usually small, and therefore the parameter ρ has a marginal impact on their energy consumption. When a SBS is switched OFF, the associated users have to connect to the macro BS. However, in case the macro BS is not able to provide them with service, they will be dropped, until the next time slot, when a variation of system state may lead to different RRM decisions.

Reward function: The reward function has been defined as:

$$r_t^i = \begin{cases} 0 & B_t^i < B_{\text{th}}^{\text{OFF}} \text{ or } D_t > D_{\text{th}} \\ \kappa T_t^i & B_t^i \geq B_{\text{th}}^{\text{OFF}} \text{ and } D_t \leq D_{\text{th}} \text{ and SBS } i \text{ is ON} \\ 1/B_t^i & B_t^i \geq B_{\text{th}}^{\text{OFF}} \text{ and } D_t \leq D_{\text{th}} \text{ and SBS } i \text{ is OFF} \end{cases} \tag{5.3}$$

where T_t^i is the normalized throughput of SBS i in slot t, D_t is the instantaneous *system* drop rate, defined as the ratio between the total amount of traffic dropped and the traffic demand in the entire network (accounting for macro and small BSs). The latter is not available locally at the SBSs but can be easily retrieved from the macro BS, e..g, through the private message mechanism of the X2 interface [133]. D_{th} is the maximum tolerable drop rate. Finally, $B_{\text{th}}^{\text{OFF}}$ is a threshold on the battery level. The rationale behind Eq. 5.3 is the following. The condition in the first line implies a zero reward when the battery level falls below $B_{\text{th}}^{\text{OFF}}$ ($B_t^i < B_{\text{th}}^{\text{OFF}}$) or the system drop rate is below D_{th} ($D_t < D_{\text{th}}$). This incentivizes the SBS to turn itself OFF to save energy, as this implies a higher reward. When $B_t^i < B_{\text{th}}^{\text{OFF}}$, this is necessary to promote the energetic self-sustainability of the SBS, whereas when $D_t > D_{\text{th}}$, the system performance is deemed sufficient. Thus, the SBS can be switched OFF and offload the macro BS at a later time. In the second and third line of Eq. 5.3, the reward is proportional to the throughput when the SBS is turned ON and is instead proportional to the inverse of the energy buffer level when the SBS is OFF. Note that the SBS, after a learning phase, will choose to remain ON (and offload the macro BS) when the reward in the second line is higher, i.e., when $\kappa T_t^i > 1/B_t^i$. Note that $1/B_t^i$ may dominate over κT_t^i in case battery level and throughput are both low. In this case, the SBS switches OFF to save energy. The constant κ is used to balance the impact of the two terms (throughput *vs* energy efficiency).

5.4.2 ON/OFF switching based on trained distributed Q-learning

Online learning algorithms suffer from an initial exploration phase to gather information from the environment and, based on this acquired knowledge, make good decisions. This process produces instability and poor performance potentially for a long time, i.e., until a sufficient amount of knowledge is gathered. We proposed an offline training period for the algorithm to setup initial switch OFF/ON policies. In detail, the TRAINING phase consists of running the agent with the energy statistics of a specific month for generating the Q-tables in an offline fashion. This returns the trained Q-values that can be used for initializing the Q-tables of the SBSs when they are deployed in their ONLINE operative mode. The pseudo-code of this solution is presented in Alg. 2. This initial training helps reduce the initial exploration phase and, in case the algorithm is not able to follow the dynamics of the environment, it also helps improve the system performance, by avoiding slow recalibration phases. We note that, the training phase can be either performed with a simulation approach, as we propose, or obtained by other *expert* SBSs that have been already deployed, as in the *transfer learning* paradigm [98].

Algorithm 2 Trained Distributed Q-learning

```
procedure Training($Q^m_{\text{init}}(x^i, a^i)$)
    $Q^m_{\text{init}}(x^i, a^i) \leftarrow 0$
    for $m \in \mathcal{M}$ do
        Run Q-learning($EH_m$)
        $Q^m_{\text{init}}(x^i, a^i) \leftarrow Q$-table$(x^i, a^i)$
    end for
end procedure

procedure Online
    for $m \in \mathcal{M}$ do
        for $m \in \mathcal{D}^m$ do
            $Q$-table$(x^i, a^i) \leftarrow Q^m_{\text{init}}(x^i, a^i)$
            Run Q-learning($EH_m$)
        end for
    end for
end procedure
```

where
$\mathcal{M}$ is the set on months
EH_m = Energy Traces for month m
$\mathcal{D}^m$ is the set of days in month m

5.5 Performance Evaluation

5.5.1 Simulation Scenario

We consider a deployment of a varying number of SBSs within a square macro cell area with a side of 1 km. The macro BS is placed in the center of it, whereas the SBSs are randomly positioned with the constraint that their cells do not overlap. This translates into a minimum inter-SBS distance of 50 m, which corresponds to the coverage radius of a SBS with transmission power of 38 dBm. The coverage area of each SBS is populated with 120 uniformly placed UEs, which allow congesting the SBS in peak traffic hours. Data load is modeled using an urban profile [89], where traffic is concentrated around working hours and has one peak in the morning and one in the afternoon. According to [1], we considered that 20% of the UEs are "heavy users" with a data volume of 900 MB/h, while the remaining UEs are "ordinary users" (112.5 MB/h). As for the RES system, we consider the Panasonic N235B solar modules, which have single cell efficiencies of about 21%, delivering about 186 W/m^2. Each SBS is equipped with an array of 16×16 solar cells (i.e., 4.48 m^2). The battery size is 2 kWh (panel and battery sizes have been chosen so that SBS batteries can be replenished in a full winter day). Realistic harvested energy traces are obtained using the SolarStat tool [21], considering the city of Los Angeles as the deployment location. Fig. 5.1 shows typical profiles for the traffic demand and the harvested energy across two subsequent days. Interestingly, we see that the maxima in the energy inflow and in the traffic demand are not aligned. This means that some optimization actions that could be taken are e.g., saving energy resources and use them when the next traffic peak occurs.

The analysis is performed as follows. We first elaborate on the convergence of the online algorithm, then we characterize the switch ON/OFF policies in different representative months (i.e., January, April and July) and compare the performance of the *online* distributed Q-learning ("QL" in the figures) against that of a distributed Q-learning algorithm trained in an *offline* fashion ("QLT"). We conclude our investigation with an assessment of the energy efficiency of the considered techniques. The Q-learning based algorithms are independently implemented by each SBS. The learning rate is set to $\alpha = 0.5$ and the discount factor to $\gamma = 0.9$ for all SBS, according to our simulation analysis. The constant κ (see Eq. 5.3) is set to 10 as this provides a good trade-off for the considered system parameters. Both algorithms also implement exploration features [134], i.e., random states are visited by the learning agents with probability $\varepsilon = 0.1$. The threshold on the instantaneous traffic drop rate is set to $D_{\text{th}} = 0.05$. QL and QLT are contrasted with a greedy scheme ("Gr" in the figures) where the $i - th$ SBS is switched OFF at time t when its battery level B_t^i drops below $B_{\text{th}}^{\text{OFF}}$, and is reactivated

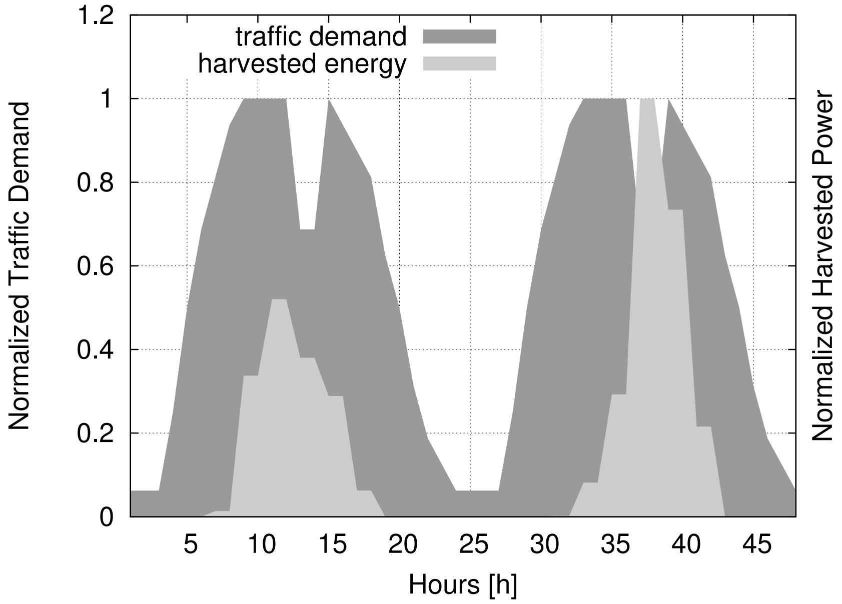

Figure 5.1: Examples of total traffic demand and amount of energy harvested.

at time $t + \Delta$ when it has harvested enough energy for returning above the threshold (i.e., $B^i_{t+\Delta} \geq B^{\text{OFF}}_{\text{th}}$). The battery threshold $B^{\text{OFF}}_{\text{th}}$ is set to 20% of the battery capacity in order to keep the battery within its safe operating regime [135].

5.5.2 Online Algorithm Convergence

At time t, a SBS i is said to be in outage if $B^i_t \leq B^{\text{OFF}}_{\text{th}}$. Then, the total outage time for SBS i over a period of time $T > 0$ is computed as $\int_0^T 1\{B^i_t \leq B^{\text{OFF}}_{\text{th}}\}dt$, where $1\{\cdot\}$ is the indicator function, which is one if the event in its argument is verified and zero otherwise. In a certain day, the system is said to be in outage if the total outage time, obtained summing the outage time of all the SBSs during the day, is higher than 5%. An algorithm is said to have converged when no outage occurs during a window of three consecutive days. An example of the convergence behavior is shown in Fig. 5.2, where the hourly battery level of a SBS is plotted on a per hour basis for the month of January for a network of 3 SBSs. A preliminary phase of instability can be noted until hour 1000 (i.e., lasting about 40 days), where the SBS adopts a greedy-like approach and drops frequently below the threshold since it is using the energy only according to instantaneous availability. After this amount of time, the agent has been able to gather information from the environment in order for its Q functions to stabilize. After that point, the battery level drops below $B^{\text{OFF}}_{\text{th}}$ less often and the density of points starts becoming more prominent above the battery threshold. In proximity of 1300 hours, we can appreciate a temporary instability due to the scarce amount of energy harvested

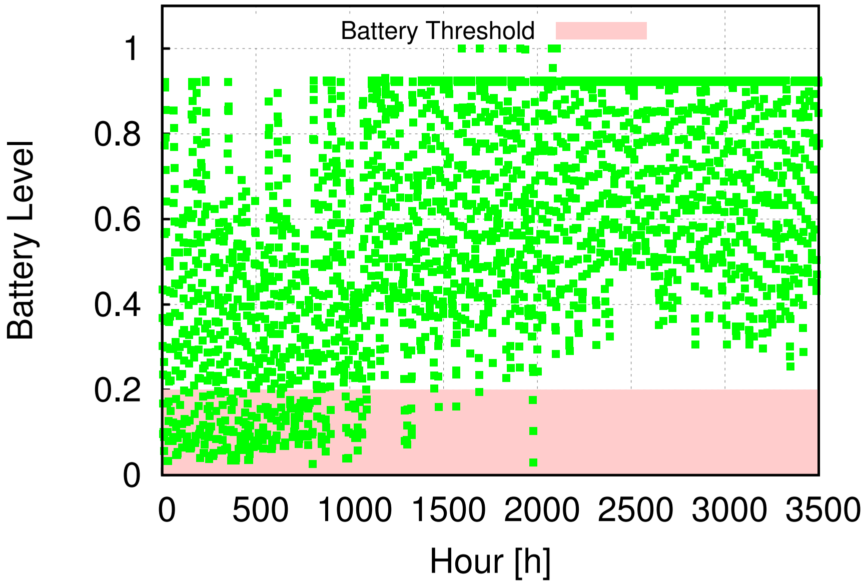

FIGURE 5.2: Battery level for the month of January of a single SBS.

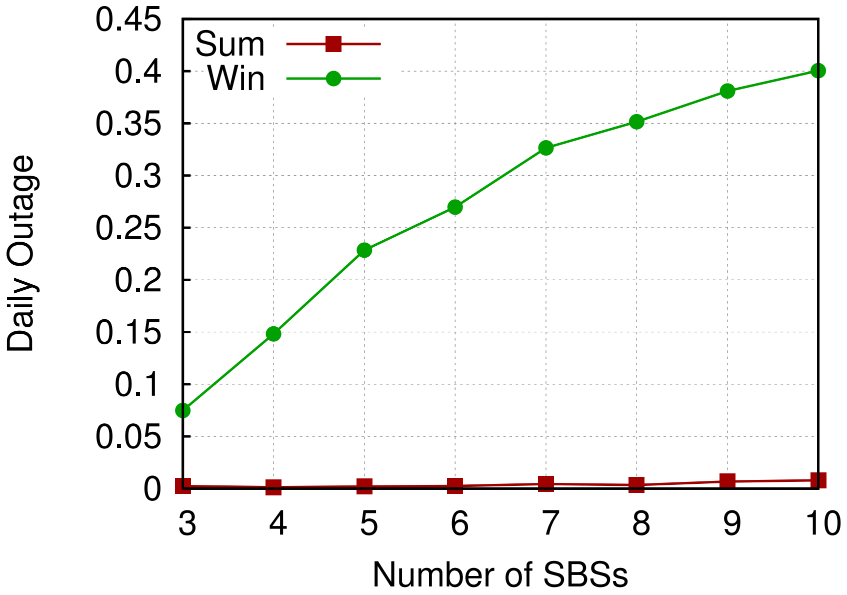

FIGURE 5.3: Average daily outage with multiple SBSs.

during several consecutive days. However, we note that the algorithm promptly reacts and drives the system toward a good (zero-outage) region.

Similar considerations hold for scenarios involving more SBSs. Nonetheless, in such case the instability during the winter can be more frequent, as depicted in Fig. 5.3, which presents the average daily outage rate when varying the number of SBSs. During the summer period, the system is always able to maintain the batteries levels in a safe operative window. On the other hand, in winter periods the daily outage rate is increasing with the number of SBSs, reaching the 40% for 10 SBSs. Multi-agent RL suffers the problem of the coordination among agents, since they may incur in conflicting behaviors, as highlighted in Section 3.2.5. In particular, in this case the SBSs need to find a coordination on when switching OFF for avoiding to overload the macro BS. This task becomes more difficult when the number of SBSs in the network is high, since the SBSs share the macro BSs resources when temporary switching OFF, which implies that they have less opportunities to do this.

5.5.3 Policy Analysis

The switch OFF rate of a single SBS during 24 hours is reported in Fig. 5.4 for polynomial ($\omega = 0.5$) and constant ($\omega = 0$) learning rates for the months of January, April and July. The rate is calculated by simulating 180 days, so as to allow for the completion of the training phase and increase the statistical confidence of the results.

Switch OFFs are more intensive during early morning hours (from 0am to 4am) and in the night (from 9pm to 11pm), due to the scarce harvested energy and the low traffic demand at night-time. When the SBS is turned OFF, the SBS agent chooses to recharge its battery and relies on the macro cell for serving the UEs within its coverage. This behavior is similar for all months. In January, another less intensive switch OFF period can be appreciated from 5am to 9am (switch OFF rate of about 0.3). This is due to a feeble harvesting process during those months. Moreover, it can be noticed that the two values of ω do not significantly affect the shape of the policy. This implies that a constant learning rate ($\omega = 0$) provides the needed flexibility for Q-learning to effectively cope with the system dynamics.

In Fig. 5.5, the switch OFF rate of a SBS in a multi-cell scenario with 10 SBSs is presented. The policies are similar to those in Fig. 5.4 (single cell case). However, we can appreciate a slight reduction in the switch OFF intensity in the early morning. Here, the SBSs switch OFF less often in order not to overload the macro cell and maintain the traffic drop rate below D_{th}. In the months of April and July, the number of switch OFFs is lower than in January, due to an increase in the harvested energy income. According to this, we can appreciate that the algorithm is able both to learn the policy as function of the energy and traffic patterns and to adapt to different scenarios with different number of SBSs.

In Fig. 5.6, we plot an example of the temporal system behavior for a HetNet including 3 SBSs and a macro BS for the last week of December. Here, from top to bottom we show temporal traces concerning traffic demand and instantaneous harvested energy (in the same plot), battery level, policy adopted at the SCs (y-label “Action”) and normalized load at the macro BS (y-label “Macro Load”). From these results various observations

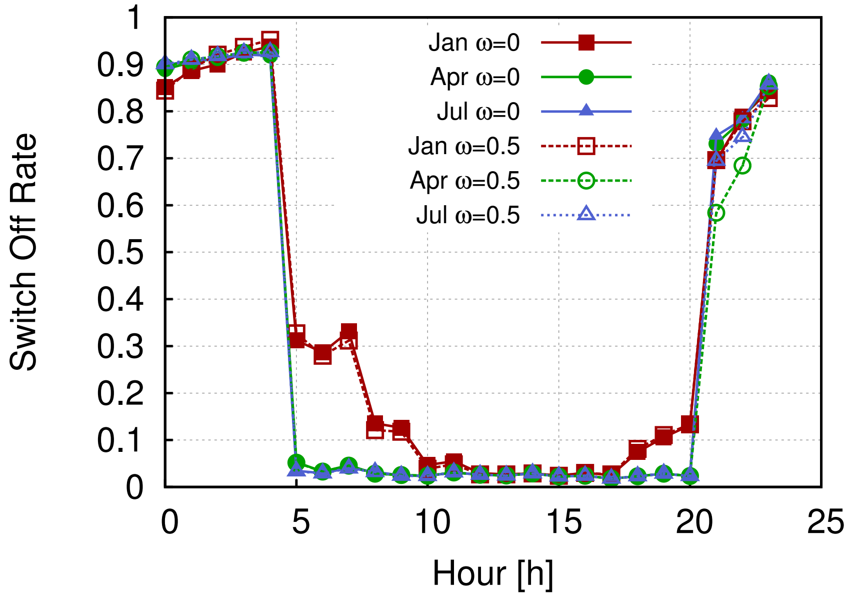

FIGURE 5.4: Switch OFF rate of a SBS during the day with a single SBS.

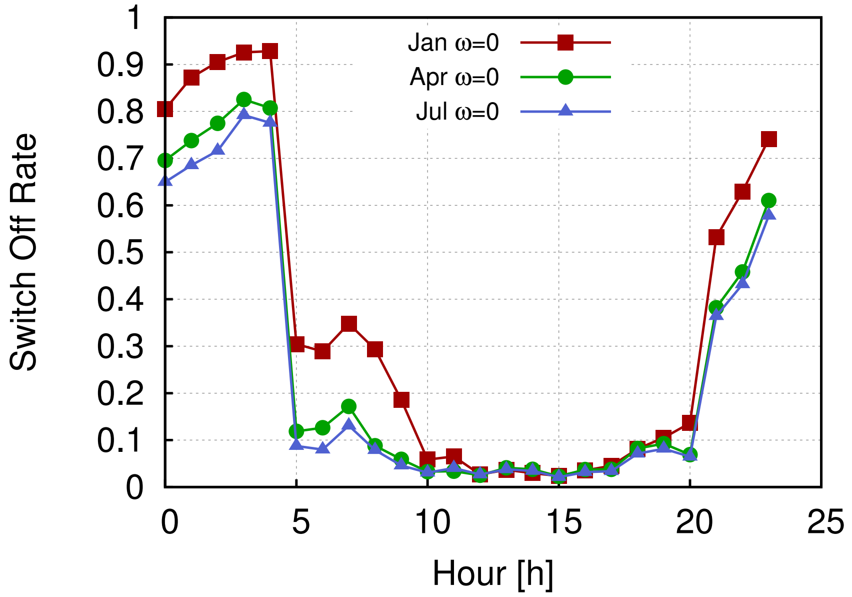

FIGURE 5.5: Switch OFF rate of a SBS during the day with multiple SBSs.

can be made. First, the policy adopted by QL tends to save energy during the night, and this makes it possible to offload more the macro BS during the day, as it can be seen in the bottom plot of Fig. 5.6 in correspondence of the points marked with “(a)”. Also, the impact of our reward function (see Eq. 5.3) can be appreciated in correspondence of label “(b)”. Here, the QL keeps the SBSs ON, as the traffic demand is high, and in this case sleeping would cause congestion at the macro BS. We remark that QL is capable of doing this as it proactively saves some of the harvested energy when the energy inflow is abundant. In contrast, the greedy scheme shows a more aggressive behavior and, as

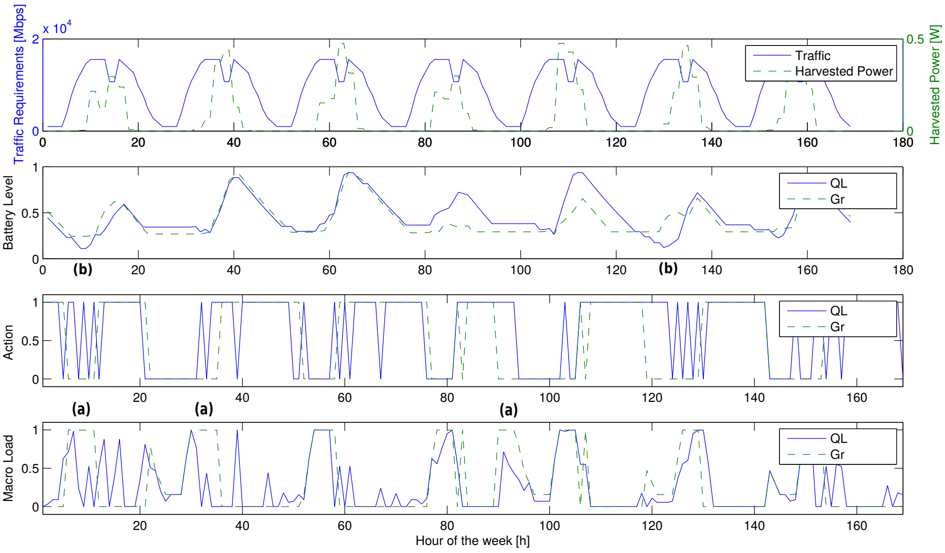

FIGURE 5.6: Example temporal behavior for a HetNet with 3 SBSs and one macro BS. Temporal traces show the status of the SBSs.

a result, it has no residual energy to compensate for an upsurge in the traffic load.

We observe that the energy harvesting traces are the same for all SBSs. We implement this choice since it is expected that the level of solar irradiation will not change much within a macro cell area. In addition, this sort of synchronization with respect to the experienced energy inflow from RESs is enforced by the traffic demand processes, as different SBSs will as well undergo similar traffic profiles. This implies that, in the considered setup, SBSs are often switched ON/OFF simultaneously.

This can be appreciated from Fig. 5.7, where the average load is plotted as a function of the hour of the day for a network with 3 SBSs. The greedy scheme usually leads to a higher load for the macro BS during the morning peak hours, where the batteries are likely to be drained, and therefore most of the SBSs must be turned OFF. On the contrary, QL loads the macro BS slightly more during most of the day in order to put some of the SBSs to sleep (saving energy at these SBSs) and serve more traffic during the morning peak.

5.5.4 Network Performance

In Fig. 5.8 we show the average throughput gain of QL and QLT with respect to the greedy scheme by varying the number of SBSs, whereas in Fig. 5.9 we show the traffic drop rate of QL, QLT and of the greedy algorithm. The results are achieved running simulations across a full year. Statistics are gathered only when the algorithm has

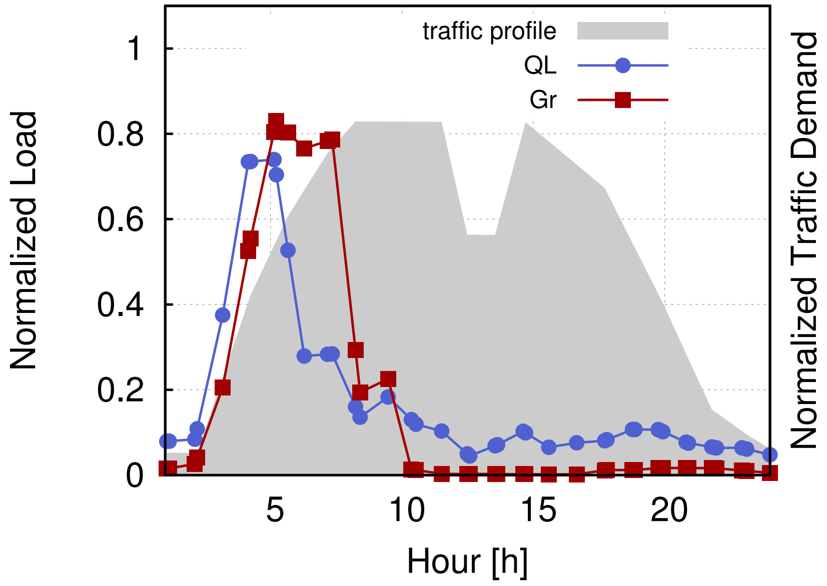

Figure 5.7: Average hourly load for the macro BS in a network with 3 SBSs.

converged and for a duration of 365 days. Since the harvesting process substantially differs for different seasons, we have presented our results separately for the *winter* and the *summer* periods, respectively termed "Win" and "Sum" in the plots. January, February, October, November and December are considered *winter* months.

The effect of ω is not relevant from the throughput and traffic drop perspective. QL and QLT outperform greedy: the throughput gain of Q-learning with respect to greedy is of up to 16% in the winter, which results in a drop rate smaller than 5% for QL and QLT, whereas the drop rate reaches 20% for the greedy scheme. The difference between winter and summer resides in the corresponding switch OFF policies, as discussed in the previous section.

We also note that QL and QLT have similar performance, both in terms of throughput and traffic drop, but they have a different convergence time. In fact, QLT presents 6 times shorter convergence times on average, taking at most 10 days to converge in the worst case scenario of 10 SBSs, with respect to the 40 days needed by QL in the same settings. However, QL can rapidly adapt to the changing dynamics of the harvesting process across the months (as reported in Fig. 5.8 and Fig. 5.9), thus rendering useless the per-month-training of QLT. Therefore, SBS agents shall only be trained to gather the necessary information during their initial exploration phase. Upon that, they can be used in an online fashion and further training is no longer required.

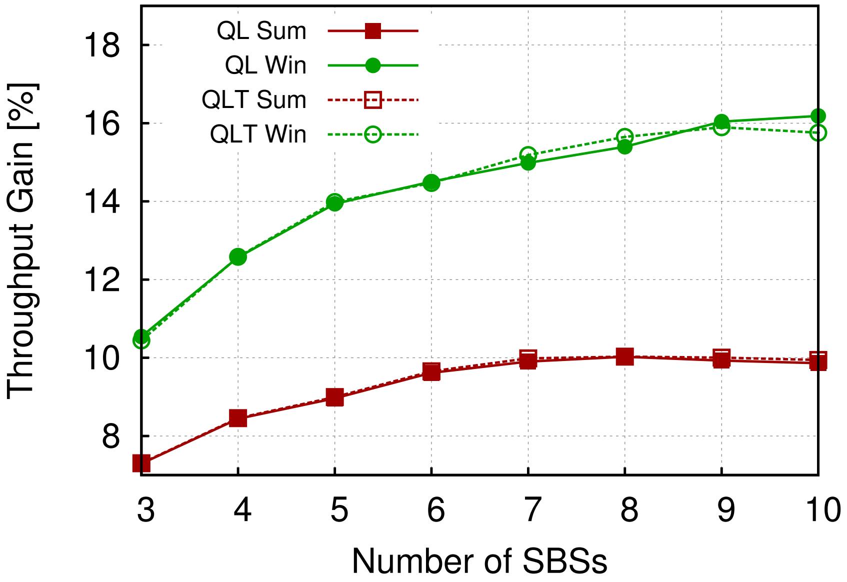

FIGURE 5.8: Average throughput gain [%] of QL and QLT with respect to the Gr scheme.

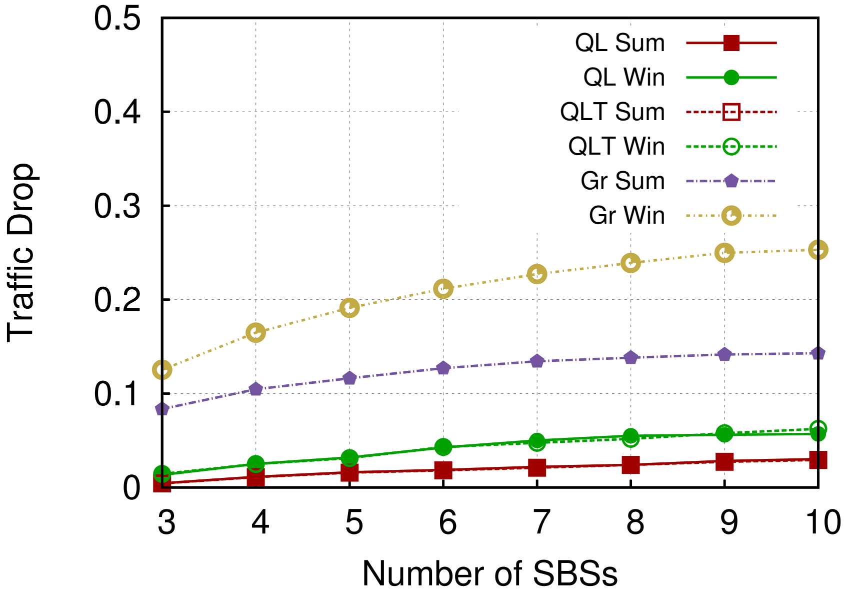

FIGURE 5.9: Traffic drop rate for QL, QLT and Gr.

5.5.5 Energy Efficiency

In this section, the energy performance of QLT is not shown as is the same as that of QL. The energy efficiency is defined as EE $= T_S/E_S$, where T_S is the system throughput and E_S is the total energy drained by the macro BS (from the power grid). The traffic demand profile is also shown.

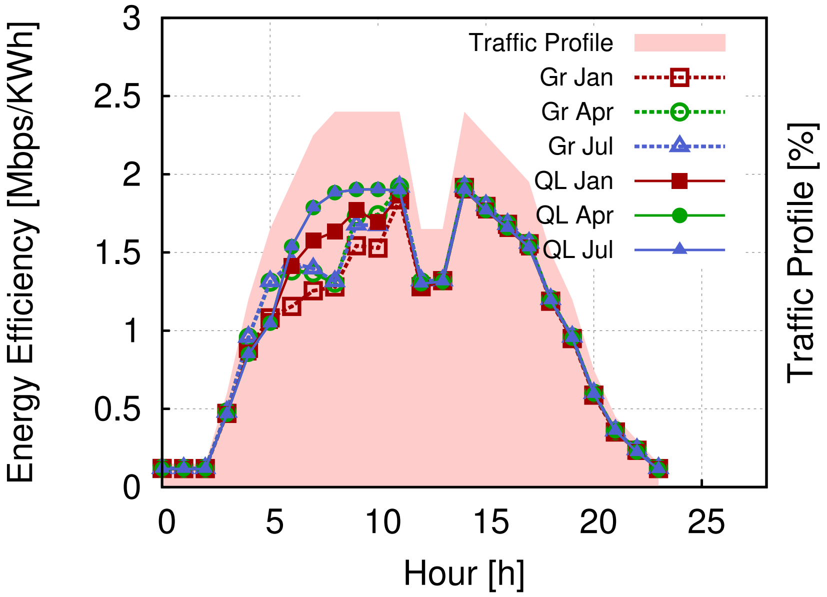

FIGURE 5.10: Average energy efficiency of a SBS during the day with a single SBS.

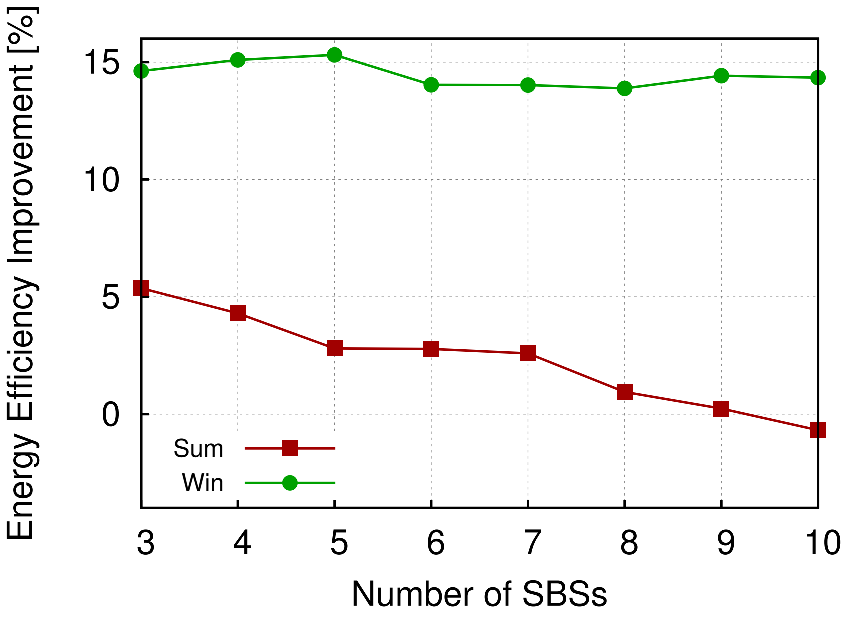

FIGURE 5.11: Energy efficiency improvement [%] of QL with respect to greedy vs number of SBSs.

The energy consumption metric is shown in Fig. 5.10, where the QL energy efficiency is compared with that of the greedy scheme for January, April and July. QL outperforms the greedy scheme during the morning slot (e.g., from 6am to 12pm), since it saves energy during the nocturnal low traffic period in order to have enough energy reserve for the morning peaks of traffic, without compromising the throughput performance.

Fig. 5.11 reports the energy efficiency improvement of QL with respect to greedy, varying the number of SBSs. QL offers a considerable gain, which reaches 15% in the winter

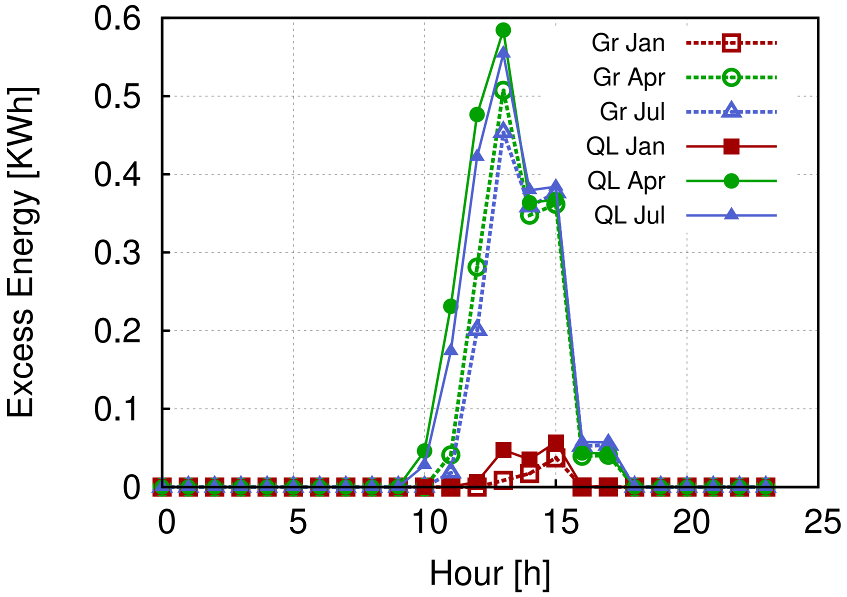

FIGURE 5.12: Average redundant energy during the day for a single SBS.

months. This is due to its higher throughput, which follows from a proper usage of the available energy reserves. The lower gain during the summer months and its decreasing behavior for an increasing number of SBSs are motivated by the fact that the RES system has been dimensioned to provide the necessary energy in the worst case, which is a winter day. This implies that, during the summer, there are days in which the algorithm does not have to smartly save energy, since the harvested energy is enough for the whole day and therefore greedy and QL have similar performance. In this case, the abundant energy has to be discarded by the SBSs, i.e., it can neither be used for transmission nor stored in the battery. This fact is shown in Fig. 5.12 ("excess energy").

With QL, the total amount of grid energy drained by the system spans from 7.3 KWh for a network of 3 SBSs, to 7.9 KWh with 10 SBSs (as compared to 7.5 KWh for the greedy scheme). Note that QL has a worse annual energy consumption performance since it serves more traffic, as we have discussed in Section 5.5.4. QL has a higher energy surplus than greedy. In fact, QL (greedy) reserves 0.124 (0.064) KWh in January, 2.115 (1.619) KWh in April and 2.021 (1.513) KWh in July. This translates into a total amount of energy not used by QL of 400 KWh in the summer (300 for greedy), and of 65 KWh in the winter (36 for the greedy scheme). Considering the higher energy efficiency and the energy surplus of QL, we conclude that QL uses less energy to offload the macro BS. In such a context, SBSs may act as *prosumers* (i.e., an energy consumer and producer) and offer/trade their excess energy to provide ancillary services to the smart grid.

5.6 Conclusions

In this chapter, we have presented a distributed implementation of a switch OFF/ON algorithm aimed at optimizing the energy usage in a dense small cell deployment with solar energy harvesting capability. The solution uses Q-learning techniques to learn the dynamics of energy harvesting and traffic processes and make switch ON/OFF decisions accordingly. Our numerical results demonstrate that distributed learning is a promising approach to make decisions in complex, dense and dynamic scenarios, leading to substantial advantages with respect to greedy schemes, such as higher throughput and energy efficiency. In our future work, we are planning to analyze the behavior of the proposed solution for different types of traffic profiles with different traffic demands for studying the flexibility in adapting to the various 5G operative cases. In addition, we would like to enhance the control performed by the SBSs in order to enable a cooperative optimal computation of the policies that accounts for common (and global) performance objectives. In fact, in the current algorithm, the cooperation is only marginally achieved through the use of the global drop rate in the reward functions that are locally computed by the SBSs.

Chapter 6

Layered Learning Load Control for Renewable Powered SBSs

6.1 Introduction

In this chapter, motivated by the promising results of the distributed MRL solutions presented in Chapter 5, we propose a novel energy efficient framework specifically designed to deal with dense HetNets. In doing this, we will consider the newest techniques that are expected to the be key enabler in 5G of the SON paradigm, i.e., softwarization and AI. On the one hand, SDN and NFV provide a flexible infrastructure for collecting the necessary system information and reconfiguring the network elements. SDN separates control and data planes and, by centralizing the control, enables many advantages such as programmability and automation. NFV enables softwarized implementation of network functions on a general purpose hardware, improving scalability and flexibility. And on the other hand, AI gives the tools for automatic and intelligent system (re-)configuration thanks to ML and RL methods. ML contributes with valuable solutions to extract models that reflect the user and network behaviors, while RL can be used for interactive decision making problem working in real-time and at short time scales.

Recently, the interest in online approaches to control network elements attracted more attention with the goal of optimizing the system by considering its actual instantaneous conditions and introducing more accurate models of harvested energy and traffic demand with respect to the ones used in offline approaches. This type of optimization is based on agents that control each BS, generating a multi-agent optimization problem. Multi-agent systems are an effective way to treat complex, large and unpredictable problems; however, such distribution might suffer the problem of finding simultaneously a solution among all the agents that is good for the whole system, as we introduced in Section 3.2.5 and we will show with numerical results in this chapter.

The main contribution of this chapter is to present an online solution for switching ON/OFF SBS powered by solar PV panels and batteries in an HetNet scenario. The proposed framework is based on a MRL approach for controlling the SBS. The Layered Learning paradigm is adopted to simplify the problem by decompose it in subtasks. Thus, the overall solution for the multi-agent optimization is performed by decomposing the general problem in subtasks. In particular, the global solution is obtained in a hierarchical fashion: the learning process of a subtask is aimed at facilitating the learning of the next higher subtask layer. The first layer implements an MRL approach and it is in charge of the local online optimization at SBS level as function of the traffic demand and the energy incomes. The second layer is in charge of the network-wide optimization and it is based on Artificial Neural Networks (ANNs) aimed at estimating the model of the overall network. The architecture for implementing the two levels and enabling their interaction is based on a SDN paradigm. To the best of the authors' knowledge, this is the first work in the literature that has proposed an online control system for HetNet with EH capabilities based on a learning solution with realistic environmental conditions and considering the optimization across different energy harvesting conditions, as has been discussed in 2.4. Moreover, in this work we compare it against an optimal solution. As a result, the innovative contribution of this chapter can be summarized as follows:

1. Definition of a control framework based on a SDN/NFV paradigm for networks with SBS powered with renewable energies.
2. Design of an online solution based on Layered Learning for the optimization of SBS with energy harvesting capabilities.
3. Characterization of the temporal behavior
4. Characterization of the performance of the whole framework and of the specific algorithms at each layer.
5. Comparison with an optimal solution evaluated offline.

The rest of this chapter is organized as follows. Section 6.2 defines the system model and the architecture of the control framework. Section 6.3 and 6.4 describe the solutions adopted in the two layers with details. Section 6.5 is devoted to the presentation of the simulation scenario where the proposed approach has been evaluated and to describe the correspondent numerical results. Finally, Section 6.6 concludes by summarizing the main results of the work.

6.2 Problem Statement

We consider a two-tier network composed of clusters of one MBS and N SBSs. The MBS provides baseline connectivity and is powered by the electric grid. The SBSs are deployed for increasing the capacity in a hot-spot manner (e.g., shopping hall, city center, etc.). SBSs are solely powered through the energy harvested by a solar panel and are equipped with rechargeable batteries.

The system evolves in cycles, based on the variation of the traffic demand and the energy arrivals in time. The time granularity ΔT is the time difference between two consecutive cycles. The energy harvested by the SBSs at time t is defined by $\boldsymbol{S}_t = [S_1^t, S_2^t, \ldots, S_N^t]$ and the energy stored by each SBS at time t is defined by $\boldsymbol{B}_t = [B_1^t, B_2^t, \ldots, B_N^t]$. The traffic load experienced at time t by each SBS due to the traffic of the UEs is defined as $\boldsymbol{L}_t = [L_1^t, L_2^t, \ldots, L_N^t]$.

At each cycle t, the LL control framework decides the configuration of the cluster of the SBSs in terms of ON/OFF states. When a SBS is switched OFF, the associated users have to connect to the macro BS. However, in case the macro BS is overloaded, it will not able to provide them with service and the users will be dropped, until the next time slot. We define this situation as *system outage.*

The core our proposed solution is based on a multi-agent system, being each agent located at the SBSs. Such a distributed approach is indicated for providing system scalability and allows SON implementation for controlling the different SBSs. Each agent is in charge of defining the ON/OFF policy based on its local environment. In fact, each SBS may experience different traffic and energy harvesting profiles. The agents can be either endowed with an offline behavior or learn new behaviors online, such that the performance of the single agent or of the whole system are improved gradually. The former is usually solved thanks to game theory solution. However, sometimes the complexity of the environment makes difficult or impossible the offline design of the agent behavior. In this case, the latter solution represents a viable approach for optimizing the agent behaviors and it is known as Multi-agent Reinforcement Learning (MRL). A RL agent learns by interacting with its environment. At each time step, the agent takes an *action* according to the state its perceived from the environment. The action causes the environment to transit to a new state and allows the agent to evaluate the benefits incurred in the transition, the so called *reward.* By trying different actions, the agent has to learn the optimal behavior of the system thanks to the cumulative rewards. This phase is called *exploration* and provides the inputs to the stable phase, in which the agents will use the learned policies, called *exploitation.* MRL and Q-learning will be described more in detail in Section 6.3.

The fundamental dilemma in RL is the trade-off between exploration and exploitation. In MRL, this dilemma is even more sensitive, since the exploration phase is further complicated. In fact, agents in MRL explore to obtain information not only about their local environment, but also about the other agents in order to adapt to their behavior. In fact, any agent's action on the environment depends also on the action taken by the other agents. In order to overcome this problem, the agents have to be coordinated for choosing actions that are consistent to achieve their goal. A promising solution to this issue is the heuristically-accelerated MRL [30]. The goal of HAMRL is to guide the exploration using additional heuristic information. A successful application of HAMRL in the telecommunication domain has been presented in [112] for the problem of interference management in LTE networks.

In order to provide a valuable heuristic to the HAMRL control system, the global performance of the system has been considered here. In fact, the agents at each SBS have a local view of the system for maintaining the algorithm complexity at reasonable levels and avoiding to have too large phase of exploration, which is one of main reason of agents conflicts. Therefore, we advocate for a hierarchical management of the system through a Layered Learning solution. The goal of LL is to decompose the problem in subtasks in order to reduce the complexity of the whole optimization problem. The proposed LL solution is based on two-layers in charge of local and network-wide EE control, respectively. The two layers can interact thanks to a SDN framework that provides the infrastructure for collecting the needed parameters and distributing the control policies, as shown in Fig. 6.1. An example of such SDN solution is the EMMA SDN application defined in the H2020 5G Crosshaul project [136]. EMMA is an infrastructure-related application based on the SDN paradigm aimed at monitoring the status of the RAN, fronthaul and backhaul elements and triggering reactions to minimize the energy footprint. The first layer is a set of local agents in the SBSs, each of those in charge of learning switching ON/OFF policies according to the harvested energy arrivals, the available energy budget, the user traffic demand and the energy consumption of the SBSs. To address this objective, agents are implementing a HAMRL algorithm based on our proposal in [137], presented in Chapter 5. Layer 2 is a central manager in charge of collecting local agent state information and assisting Layer 1 in learning intelligent switch ON/OFF policies according to a network global perspective. The second layer implements a MFNN to forecast the MBS load based on the environmental variables of each SBS and a SBSs Centralized Controller (SCC) that decides whether to enforce the local policies of a specific set of SBSs. The algorithm implemented in the two layers will be detailed in Sections 6.3 and 6.4.

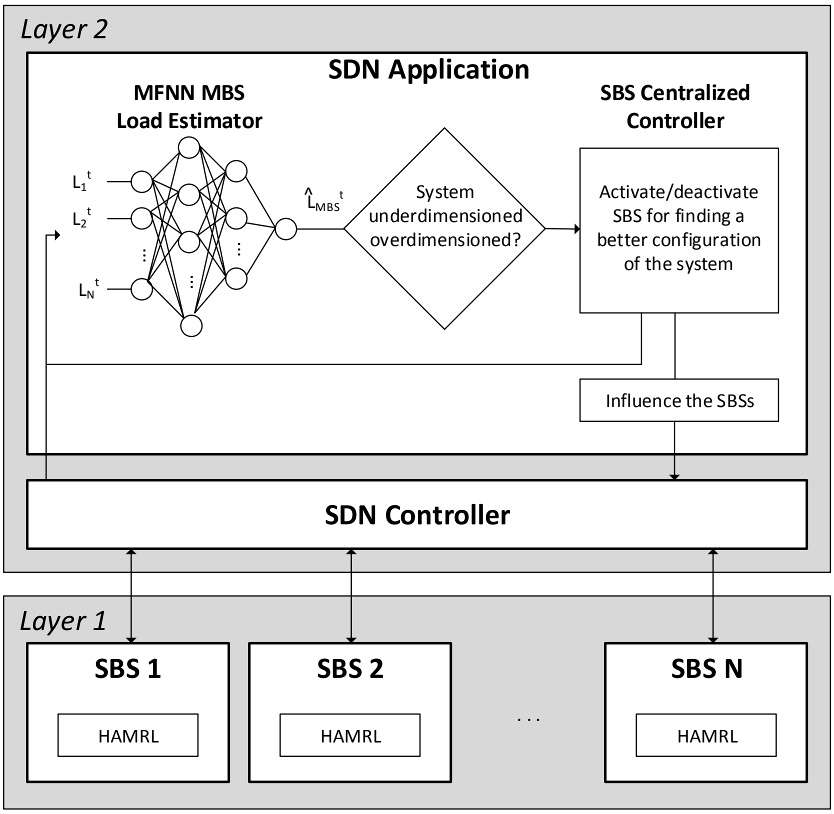

Figure 6.1: Layered Learning control architecture overview.

6.2.1 BS Energy Model

The BS power consumption model adopted is one presented in Section 2.2: $P = P_0 + \beta\rho$, where $\rho \in [0, 1]$ is the BS traffic load, normalized with respect to its maximum capacity, and P_0 is its baseline power consumption. This model is supported by real measurements [1] and closely matches the real power profile of LTE BSs.

6.2.2 Energy Harvesting Model

The energy harvesting process is based on model presented in chapter 4. It consists of a Markov model that provides accurate statistics per month basis by processing the hourly solar energy arrival data over 20 years. In detail, the 24 hours are divided into a number $N_\mathrm{s} \geq 2$ of time slots of constant duration, equal to T_i hours, $i = 1, \ldots, N_\mathrm{s}$. Each slot is a state of the Markov model and the pdf is evaluated through the kernel smoothing technique per month basis, considering the empirical data that has been measured for all days in the dataset for the month under consideration.

6.2.3 Traffic Model

The user equipment (UE) resource allocation scheme uses the methodology defined in [131]. This includes a detailed wireless channel model and the dynamic selection of the modulation and coding scheme (MCS) for each user as function of its SINR, which is given by

$$SINR = \frac{|h_0|^2 P_{t,0}}{\sum_{i=1}^{N_I} |h_i|^2 P_{t,i} + \sigma_0^2}, \tag{6.1}$$

where $P_{t,0}$ and h_0 are the transmission power and the channel gain for the useful transmission respectively, N_I is the number of interferers, whereas $|h_i|^2$ and $P_{t,i}$ represent the channel gain and the transmission power of the i-th interferer. σ_0^2 is the power of the thermal noise. The profile of the traffic of each user is obtained according to the model presented in [138]. The model combines time, location and frequency information for analyzing the traffic patterns of thousands of cellular towers. The analysis demonstrates that the urban mobile traffic usage can be described by only five basic time domain patterns that corresponds to functional regions, i.e., residential, office, transportation, entertainment and comprehensive.

6.3 Layer 1: Local Optimization

6.3.1 Distributed Q-learning and HAMRL

The first layer is composed of a set of distributed agents implementing HAMRL with the goal of dynamically switching ON and OFF the SBSs according to the available harvested energy budget, the user traffic demand and the energy consumption of the SBS. The control decisions are made by multiple intelligent and uncoordinated agents, which can only partially observe the overall scenario. Therefore, the local environment may differ from agent to agent, since they come from spatially distributed sources of information. To this end, the distributed Q-learning technique has been considered [134]. The decision making problem of each agent is defined by an MDP with state vector $\vec{x}_t = \{x_t^1, x_t^2, \dots, x_t^N\}$, where x_t^i is the state associated with SBS i (described in the next Section 6.3.2), at time t. At every MDP state transition, the energy level the batteries $\boldsymbol{B}_{t+1}$ at the beginning of the next slot is evaluated as the sum of the energy already in the battery at the beginning of the current slot $\boldsymbol{B}_t$, plus the energy produced during the time slot $\boldsymbol{S}_t$, minus the energy consumed in the same time slot, that depends on the traffic $\boldsymbol{L}_t$. Each agent i maintains a local policy and a local Q-function $Q(x_i^t, a_i^t)$ representing the level of convenience in taking actions a_i^t in state x_i^t, with t being the decision epoch (time). As a result of the execution of this action, the environment returns an *agent* *dependent* reward r_t^i, which allows the local update of a Q-value, $Q(x_t^i, a_t^i)$. The Q-value is computed according to the rule:

$$Q(x_t^i, a_t^i) \leftarrow Q(x_t^i, a_t^i) + \alpha \left[r_t^i + \gamma \max_a Q(x_{t+1}^i, a') - Q(x_t^i, a) \right] \tag{6.2}$$

where α is the learning rate, γ is the discount factor, x_{t+1}^i is the next state for agent i and a' is the associated optimal action, as introduced in Section 3.2.2. Therefore, thanks to Eq. (6.2) and the reward, the control policy can be learned by exploring the environment. The most common exploration procedure is the ε-greedy, which consists on randomly choosing a sub-optimal action with probability ε, and the one with highest Q-value with probability 1-ε, i.e., $\hat{a} = \arg\max_{a_i}(Q(x_i^t, a_i^t))$. The choice of the maximum Q-value makes Q-learning an off-policy algorithm, since it uses the greedy exploration for estimating the long term reward, while the Q-values are evaluated according to Eq. (6.2).

The idea of HAMRL is to use a heuristic function $H(x_i^t, a_i^t)$ derived from additional knowledge not in its state variables for influencing the action choices of the learning agent in order to modify its current policy $\Pi(x_i^t)$ and guide the exploration. The new combined policy selection formula is:

$$\Pi(x_i^t) = \arg\max_{a_i} \left(Q(x_i^t, a_i^t) + H(x_i^t, a_i^t) \right) \tag{6.3}$$

where $H(x_i^t, a_i^t)$ is a heuristic function derived from additional knowledge not in the state variables. It is used for influencing the action choices and modify the current policy $\Pi(x_i^t)$. Therefore, $H(x_i^t, a_i^t)$ have to be compliant with the Q-table used by the agent (i.e., values and dimensions), in order to be able to properly influence the action to be taken. If $H(x_i^t, a_i^t) = 0$ the algorithm behaves like a regular QL for the i-th SBS.

6.3.2 Our Solution

To represent the environment, we define the local state x_i^t of agent i at time t as $x_i^t = (S_i^t, B_i^t, L_i^t)$, for including the most representative variables, i.e., the instantaneous energy harvested, the battery level and the SBS load. Since these parameters assumes a continuous value, they have been quantized for having a reasonable number of states to be explored. The possible actions are to switching ON and OFF the SBS. The reward of an agent i at time t is defined as follow:

$$r_t^i = \begin{cases} 0 & B_i^t < B_{\text{th}}^{\text{OFF}} \text{ or } D_t > D_{\text{th}} \\ \kappa T_i^t & B_i^t \geq B_{\text{th}}^{\text{OFF}} \text{ and } D_t \leq D_{\text{th}} \text{ and SBS } i \text{ is ON} \\ 1/B_i^t & B_i^t \geq B_{\text{th}}^{\text{OFF}} \text{ and } D_t \leq D_{\text{th}} \text{ and SBS } i \text{ is OFF} \end{cases} \tag{6.4}$$

where D_t is the traffic dropped by the network (i.e., non-served users), T_i^t is the throughput of the SBS. D_{th} is the threshold on system drop-rate (i.e., macro and SBS), whereas $B_{\text{th}}^{\text{OFF}}$ is the security threshold of the battery state of charge (SOC). The constant κ is used to balance the impact of the throughput and energy saving rewards. The reward r_t^i is designed to avoid critical status such as low battery level or too high system drop rates. SBSs are incentivized to save energy in normal load conditions (i.e., $D_t \leq D_{\text{th}}$), by putting a reward proportional to the inverse of the energy buffer level $(1/B_t^i)$ when the SBS is OFF. Alternatively, when the SBS is ON, the reward is proportional to the throughput, as this promotes offloading the macro BS in high traffic situations. The rationale behind this state/action model is borrowed from our previous work [137], presented in Chapter 5. The choice of the $H(x_i^t, a_i^t)$ values is made by Layer 2 and will be detailed in Section 6.4.

6.4 Layer 2: Centralized Optimization

The task of this layer is to guide the agents of the Layer 1 for avoiding conditions of high traffic drop or the wasting of energy. In particular, the second layer is in charge of deciding the local agent(s) to be influenced and returns the most appropriate set of heuristics values $\boldsymbol{H_t} = [H(x_1^t, a_1^t), H(x_2^t, a_2^t), \ldots, H(x_N^t, a_N^t)]$ according to network-wide parameters that are not present in the HAMRL optimization. Layer 2 comprises an MBS load estimator based on a MFNN which provides the input to an SBS Centralized Controller, in charge of evaluating the system load conditions of the whole cluster and selecting the SBSs to be influenced.

6.4.1 MBS Load Estimator

A MFNN estimates the normalized MBS load L_{MBS}^t at the time t as a function of the load of each SBS L_i^t and of their ON/OFF policy Π_i^t. We define the estimated load of the MBS at the time t as $\hat{L}_{\text{MBS}}^t$. A supervised approach has been adopted, i.e., a training set of input-output is used to train the neural network according to the backpropagation algorithm [99].

The basic element of a MFNN is represented by the neuron (also called perceptron), which consists of a linear combination of fixed non-linear functions $\theta_j(x)$. In detail, for a vector of input $x_i, i = 1 \ldots, N$, it takes the form:

$$y(x, w) = f\left(\sum_{j=1}^{N} w_j \theta_j(x)\right) \tag{6.5}$$

where w_i are the weights associated to each input and $f(\cdot)$ is a non-linear activation function, A MFNN is composed by a series of neurons organized in L layers in a way that the input information moves only in one direction (i.e., there are no cycle in the networks like in a recurrent neural network). Let define I as the number of neurons in layer l. The bottom layer, L_0, is the input layer and it contains $N+1$ neurons, which are the inputs plus the "constant" neuron always at 1. The last layer is composed by only one neuron and represents the output of the neural network. Each neuron in a layer $l = 2, \ldots, L$ has $I_l = I_{l-1}$ inputs, each of which is connected to the output of a neuron in the previous layer. Layers $2, \ldots, L-1$ are called hidden layers. A MFNN can approximate arbitrary continuous functions defined over compact subsets of R^N by using a sufficient number of neurons at the hidden layers. In order to achieve this, it is necessary to determine the values of the weights correspondent to the function to be approximated (also known as training phase). More details on the MFFN and its training algorithms has been provided in 3.3.

6.4.2 SBS Centralized Controller

We identify two different operational cases based on the MFNN estimation output $\hat{L}^t_{\text{MBS}}$: i) the system is under-dimensioned, i.e. when $\hat{L}^t_{\text{MBS}}$ is above the threshold $L^{\text{thrHigh}}_{\text{MBS}}$ and ii) the system is over-dimensioned, i.e. when $\hat{L}^t_{\text{MBS}}$ is below the threshold L^{thrLow}_{MBS}. The former can happen when the SBSs have scarce energy reserves and many agents decide to switch OFF simultaneously. In this case, the switching OFF of some SBSs can be delayed, when the battery levels allow such operation. More in detail, the SBS Centralized Controller defines the set of candidate SBSs that can be switched ON (SBS^t_{ON}) among those that are in OFF state and have enough battery reserves. Alternatively, in case ii), the SBSs are providing the overlay capacity just for a few traffic, which can be managed by the macro BS, especially in case some SBSs do not have a huge amount of energy stored. In detail, in this case, the set of candidate SBSs to be switched OFF (SBS^t_{OFF}) is defined among those that are in ON state and have scarce energy reserves (i.e., $B^t_i \leq B^{\text{LOW}}_{\text{th}}$). The number of SBSs in SBS^t_{ON} and SBS^t_{OFF} and their relevant heuristics values $\boldsymbol{H_t}$ are derived based on Algorithm 3. For each SBS i that has been activated or deactivated in this process, the correspondent heuristic value is set to $-Q^{\text{MAX}}_i$ in $\boldsymbol{H_t}$, which was initialized to a vector of 0. In fact, $H(x^t_i, a^t_i)$ must be the lowest value that can influence the choice of action in order to minimize the distortion in the Q-value function due to the use of heuristics [30]. Therefore, for influencing the choice of action of SBS i in state x^t_i, $H(x^t_i, a^t_i)$ should be negative and higher than the maximum Q-value in x^t_i (i.e., Q^{MAX}_i). Alternatively, when $H(x^t_i, a^t_i) = 0$ the correspondent agent will behave like in a regular Q-learning solution.

Algorithm 3 SBS Enforcing

```
procedure EVALUATE $\boldsymbol{H}_t(\boldsymbol{L_t}, \boldsymbol{\Pi_t})$
    $\boldsymbol{H}_t \leftarrow 0$
    Evaluate $\hat{L}^t_{\text{MBS}}$ with $\boldsymbol{L_t}, \boldsymbol{\Pi_t}$
    if $\hat{L}^t_{\text{MBS}} > L^{\text{thrHigh}}_{\text{MBS}}$ then                ▷ Case i)
        $SBS^t_{\text{ON}} \leftarrow$ SBSs in OFF with $B^t_i \geq B^{\text{OFF}}_{\text{th}}$
        Order $SBS^t_{\text{ON}}$ from the lowest $Q^{\text{MAX}}_i$
        while $\hat{L}^t_{\text{MBS}} > L^{\text{thrHigh}}_{\text{MBS}}$ do
            K ← index of the first SBS in $SBS^t_{\text{ON}}$
            $H^t_K \leftarrow -Q^{\text{MAX}}_K$
            Evaluate $\hat{L}^t_{\text{MBS}}$ with $k^{th}$SBS ON
            $SBS^t_{\text{ON}} \leftarrow SBS^t_{\text{ON}} - k^{th}$ SBS
        end while
    else if $\hat{L}^t_{\text{MBS}} < L^{thrLow}_{\text{MBS}}$ then                ▷ Case ii)
        $SBS^t_{\text{OFF}} \leftarrow$ SBSs in ON with $B^t_i \leq B^{\text{LOW}}_{\text{th}}$
        Order $SBS^t_{\text{OFF}}$ from the lowest $Q^{\text{MAX}}_i$
        while $\hat{L}^t_{\text{MBS}} < L^{thrLow}_{\text{MBS}}$ do
            K ← index of the first SBS in $SBS^t_{\text{OFF}}$
            $H^t_K \leftarrow -Q^{\text{MAX}}_K$
            Evaluate $\hat{L}^t_{\text{MBS}}$ with $k^{th}$SBS OFF
            $SBS^t_{\text{OFF}} \leftarrow SBS^t_{\text{OFF}} - k^{th}$ SBS
        end while
    end if
end procedure
```

6.5 Numerical Results and Discussion

6.5.1 Simulation Scenario

The scenario considered in this analysis is composed of a single cluster with 1 MBS placed in the middle of a 1×1 m^2 area and a varying number of SBSs randomly placed and non-overlapping. We consider medium scale factor "metro cells" as SBSs, featuring a maximum transmission power of 38 dBm, which corresponds approximatively to 50 meters of coverage range. The values of β and P_0 of the energy model presented in Section 2.2 for the MBS (SBS) are 600 (39)W and 750 (105.6), respectively.

Each SBS is supplied by an array of 16×16 solar cells of Panasonic N235B solar modules (area 4.48 m^2), that have single cell efficiencies of about 21%, and a lithium ion battery of 1.5 KWh, which has been proven to be the optimal dimensioning for the worst case of winter season [139]. The solar energy arrivals are generated with the SolarStat tool [21] for the city of Los Angeles. The traffic demand is modeled as in [138]. In detail, the office and residential traffic profiles has been considered, respectively termed "Res" and "Off" in the following. Both of them present an intense activity during the day. However, they differ in the profile: the office concentrates the traffic during the daylight hours (e.g., from 10 AM to 6 PM), while the residential has only one peak during the early night hours (e.g., from 6 PM to 12 PM). Users have been classified according to [1], where heavy users request 900 MB/h while ordinary ones need 112.5 MB/h. The main simulation parameters are given in Table 6.1.

Table 6.1: Simulation Parameters.

	Parameter	Value
Scenario	Solar panel size (m^2)	4.48 (16×16)
	Solar panel efficiency (%)	21
	Battery capacity (kWh)	1.5
	MBS transmission power (dBm)	43
	SBS transmission power (dBm)	38
	Bandwidth (MHz)	5
	Epoch duration (h)	1
HAMRL	α	0.5
	γ	0.9
	ε	0.1
	κ	10
	Battery threshold $B_{\mathrm{th}}^{\mathrm{OFF}}$ (%)	20
	System drop-rate threshold D_{th} (%)	3
MFNN	Learning rate (%)	0.1
	First hidden layer nodes no.	$I_1 = \lceil 3/2N \rceil$
	Second hidden layer nodes no.	$I_2 = \lceil 2/3N \rceil$
	Third hidden layer nodes no.	$I_3 = max(\lceil 2/3N \rceil, 2)$
SCC	High congestion threshold $L_{\mathrm{MBS}}^{\mathrm{thrHigh}}$ (%)	85
	Low load threshold $L_{\mathrm{MBS}}^{thrLow}$ (%)	5

6.5.2 MFNN Training Analysis

We start the analysis of the framework presenting the training phase behavior of the MFNN used in Layer 2. Based on simulative analysis, the best number of neurons per layer is $I_1 = \lceil 3/2N \rceil$, $I_2 = \lceil 2/3N \rceil$ and $I_3 = max(\lceil 2/3N \rceil, 2)$. Fig. 6.2 presents the overall mean squared error (mse) of this configuration for a MFNN with two and three hidden layers (respectively "2L" and "3L" in the figures) as a function of the day, which includes 24 system evolution epochs. MFNN with three hidden layers starts with a higher mse; however, it presents lower mse asymptotically (after 500 days). The two MFNNs have a different starting behavior, the one with two hidden layers performs better till 50 days. After that, the errors

As an additional illustrative result, we evaluate two different statistical measures that return the performance of the SBS Centralized Controller decision making process: the sensitivity and the specificity. The sensitivity is defined as the proportion of positive

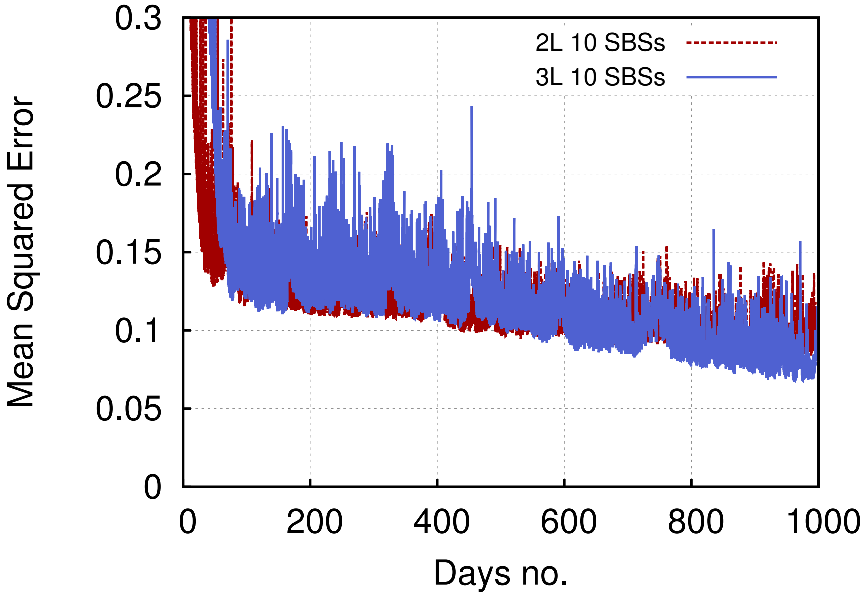

FIGURE 6.2: Mean squared error of the MFNN for different number of hidden layers.

cases that are correctly identified as such, in detail:

$$\text{sensitivity} = \frac{\text{true positive no.}}{\text{true positive no.} + \text{false negative no.}} \tag{6.6}$$

where define the false negatives as the cases when the MFNN does not estimate that the system is under-dimensioned (i.e., $\hat{L}^t_{\text{MBS}} \leq L^{\text{thrHigh}}_{\text{MBS}}$) but it is really in outage. Fig. 6.3 provides the sensitivity as a function of the day. From Fig. 6.3, we can observe that the MFNN with two hidden layers takes approximatively 50 days for reaching a stable behavior, whereas the one with three hidden layers takes 10 times longer and passes the 500 days.

Besides, the specificity measures the proportion of negative cases that are correctly identified as such, which corresponds to:

$$\text{specificity} = \frac{\text{true negative no.}}{\text{true negative no.} + \text{false positive no.}} \tag{6.7}$$

where false positives have been defined as the cases when the MFNN expects that the system in under-dimensioned (i.e., $\hat{L}^t_{\text{MBS}} > L^{\text{thrHigh}}_{\text{MBS}}$) but it is not in outage. Fig. 6.4 depict the specificity as function of the system evolution epochs. In this case, the MFNNs reach a stable behavior at 1500 days. However, the MFNN with two hidden layers presents less variance on the specificity. We can also note that the asymptotic value of the specificity is lower than the sensitivity. This is due to the fact that we have adopted a guard margin to guarantee the MBS not to be overloaded (i.e. $L^{\text{thrHigh}}_{\text{MBS}} = 0.85$). Therefore, some false positives are MFNN estimations that fall between $L^{\text{thrHigh}}_{\text{MBS}}$ and 1,

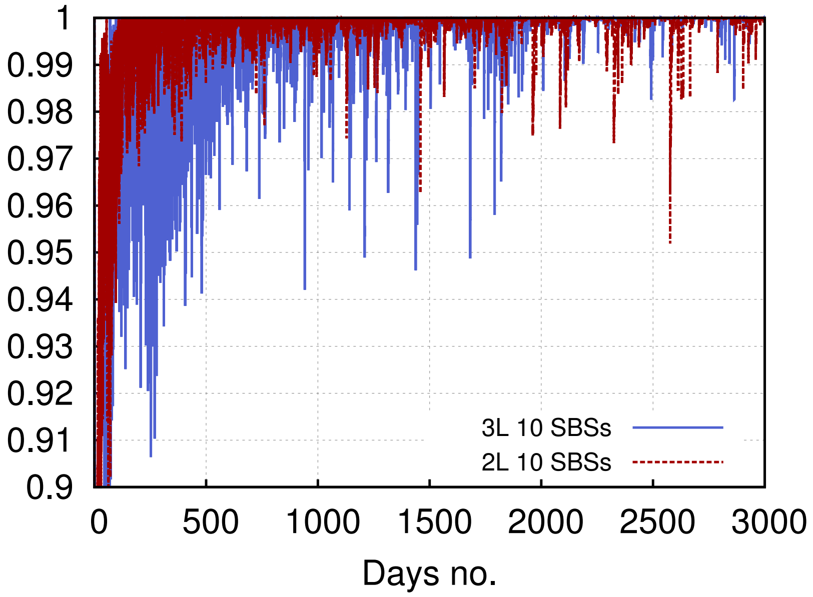

Figure 6.3: Sensitivity of the MFNN for different number of hidden layers.

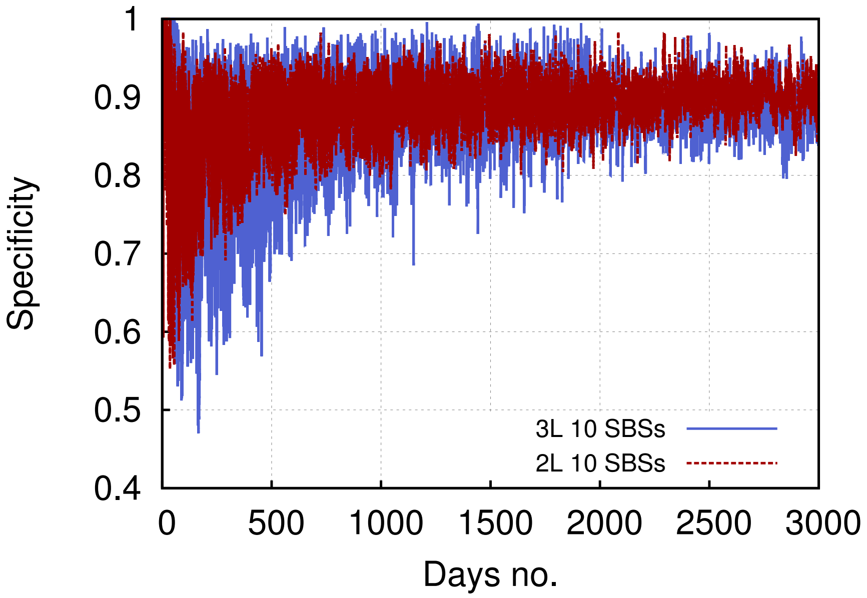

Figure 6.4: Specificity of the MFNN for different number of hidden layers.

which do not represent a system outage.

Based on the analysis in the above, the MFNN with two hidden layers has been used due to its better sensitivity and specificity, and a faster training phase.

6.5.3 Distributed Q-learning and Layered Learning Training Analysis

The training phases of both distributed Q-learning and Layered Learning algorithms have been evaluated considering the stability of the system to avoid conditions of *battery failure*, which we defined as the case when the battery level drops below the security threshold of the battery SOC $B_{\text{th}}^{\text{OFF}}$. The reason behind this choice is that we considered the energy as the most important parameter allowing the SBS to be operative and avoiding a rapid degradation of the batteries [135]. In detail, in the epoch t, a SBS i is said to be in battery failure if $B_t^i \leq B_{\text{th}}$. Then, the total battery failure time for SBS i over a period of time $T > 0$ is computed as $\int_0^T 1\{B_t^i \leq B_{\text{th}}\}dt$, where $1\{\cdot\}$ is the indicator function, which is one if the event in its argument is verified and zero otherwise. In a certain day, we define that the system is stable if the sum of the battery failure time of all the SBSs during the day is higher than 5%. An algorithm is said to have converged when is stable during a window of three consecutive days.

An example of the convergence behavior of QL and LL algorithms is shown in Fig. 6.5 and Fig. 6.6, where the hourly battery level of a SBS is plotted on a per hour basis for a scenario with 3 SBSs and different traffic profiles. The simulations start with the month of January and runs for 400 days spanning across the correspondent months. In both cases, the system starts with a short-sighted approach, since it is using the energy only according to the instantaneous availability, and drops frequently below the threshold. During this period, the agent is at the beginning of the exploration phase and has to gather information from the environment in order for its Q functions to stabilize. The resulting training phase is very shorter in case of the office traffic profile (almost 40 days for both 20% and 50% of heavy users) than the residential one that presents a duration of 50 and 80 for the case of 20% and 50% of heavy users, respectively. After these points, the battery level drops below B_{th} less often and the density of points starts becoming more prominent above the battery threshold. Similarly to what experienced with the duration of the training phase, the number of points falling below the threshold in case of office traffic profile are less with respect to the residential one. This phenomenon is due to the fact that the hour profile of the office traffic is more similar to the one of the harvested energy (i.e., both of them are concentrated during the daylight hours), which helps the MRL in finding a policy that avoids the battery failure problem, as will be also showed in the following sections. In such case, the improvement of the LL approach with respect to the QL one is more evident, as depicted in Fig. 6.6a and Fig. 6.6b. In fact, in Fig. 6.6a the LL is able to avoid that the battery level falls outside the ideal SOC window (i.e., below $B_{\text{th}}^{\text{OFF}}$), while QL presents many points below the battery security threshold starting from 300 days, which is approximatively the beginning of the winter season. The effect of the traffic demand can be appreciated in both Fig. 6.5 and Fig. 6.6.

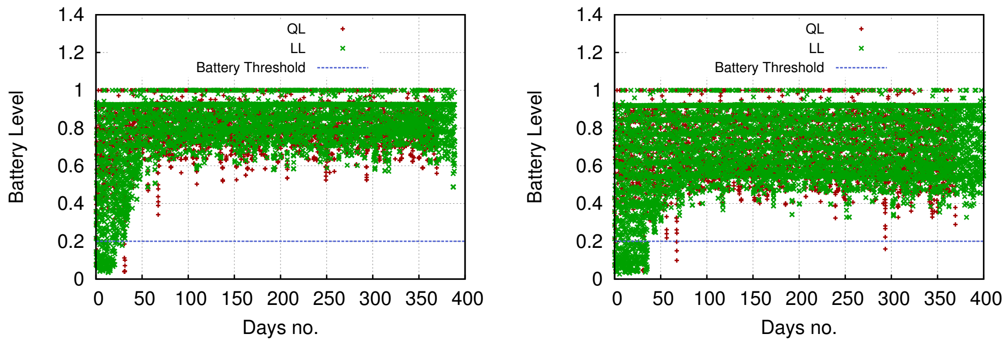

(A) 20% of heavy users (B) 50% of heavy users

Figure 6.5: Example of battery level of an SBS in a network of 3 SBSs with Office traffic profile. Scenario with 70 UEs per SBS with 20% and 50% of heavy users.

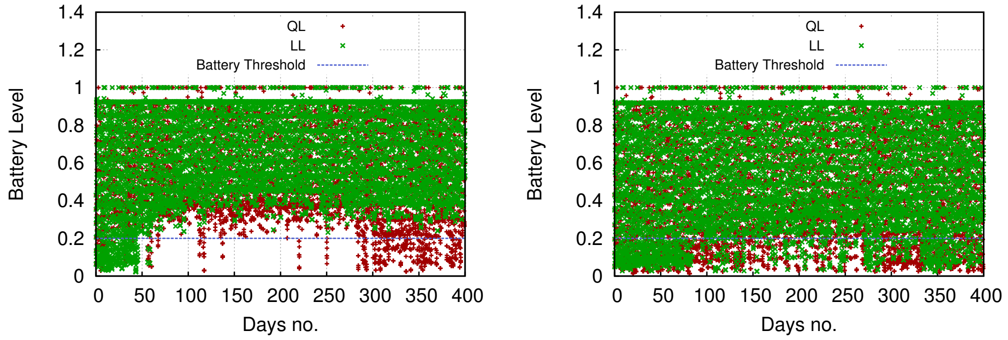

(A) 20% of heavy users (B) 50% of heavy users

Figure 6.6: Example of battery level of an SBS in a network of 3 SBSs with Residential traffic profile. Scenario with 70 UEs per SBS with 20% and 50% of heavy users.

In case of the Office traffic profile, the minimum average battery level decreases from 0.6 to 0.4. In case of the residential traffic profile, only the LL is able to guarantee the minimum battery level and only for the case of 20% of heavy users. Therefore, despite of converging as in the definition above, the system in the last case is less stable and presents still some problem in finding a solution that guarantees a longer battery lifetime. It is to be noted that, the system is dimensioned for the worst case scenario of working in the winter season. Thus, during the summer the energy reserves are abundant and, usually, both LL and QL have an easier task when optimizing the system.

6.5.4 ON/OFF Policies

In this section, we analyze the behavior of the switch ON/OFF policies of the LL solution. The LL policies are compared with optimal direct load control based on Dynamic Programming (DP) introduced in [93]. The policies have been evaluated across a full year of simulation with the HAMRL algorithm already trained offline. The results are presented separately for the *winter* and the *summer* periods, respectively termed "Win"

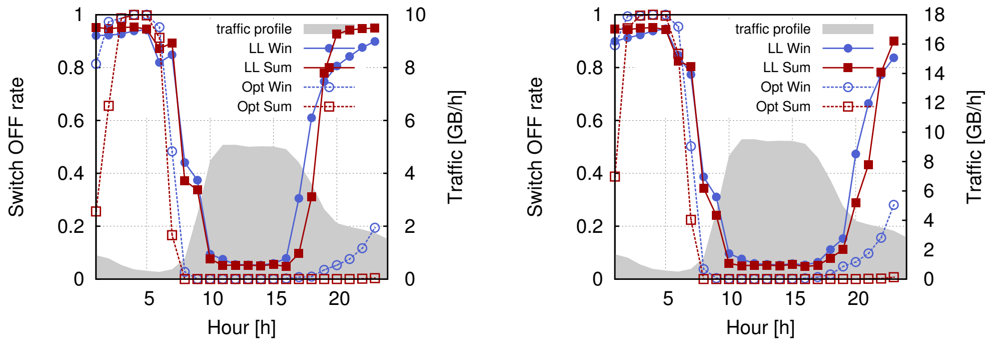

(A) 20% of heavy users

(B) 50% of heavy users

FIGURE 6.7: Daily average switch OFF rate for the LL and optimal solutions with Office traffic profile. Scenario with 70 UEs per SBS with 20% and 50% of heavy users.

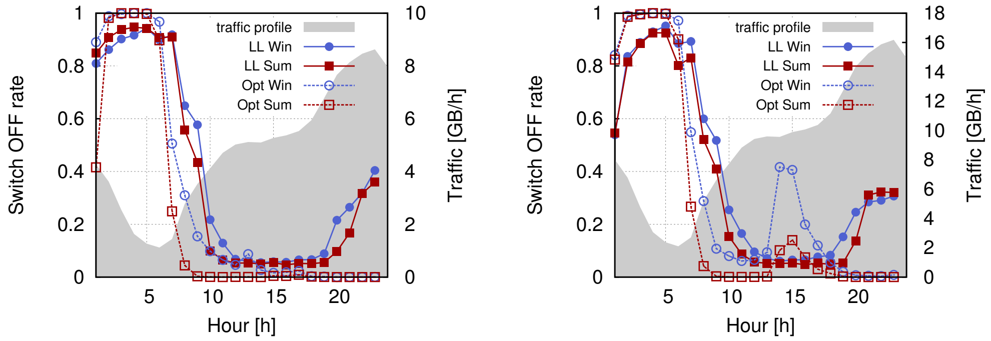

(A) 20% of heavy users

(B) 50% of heavy users

FIGURE 6.8: Daily average switch OFF rate for the LL and optimal solutions with Residential traffic profile. Scenario with 70 UEs per SBS with 20% and 50% of heavy users.

and "Sum" in the plots, since the harvesting process substantially differs for different seasons. January, February, October, November and December are considered *winter* months. Thus, it is impossible to evaluate the optimal solution over a full simulated year for networks with more than 3 SBSs. The daily average switch OFF rate of the SBSs for the LL and optimal policy with Office and Residential traffic profile is reported in Fig 6.7 and Fig 6.8, respectively, jointly with the total traffic requested by the 3 SBSs. Regarding the latter, it is to be noted that, the two traffic profiles considerably differ in the amount of traffic requested during the day. In fact, while the office traffic arrives to 61 GB/h for 20% of heavy users and to 115 GB/h for the case of 50% ones, the residential almost double the capacity requirements reaching up to 116 GB/h and 218 GB/h, respectively.

In Fig. 6.7 we observe that the policies substantially converge in having a high switch OFF rate during the night in order to save energy for the daily peak of traffic. However, the LL algorithm is more conservative with respect to the optimal one, i.e., it is starting the high switch OFF rate period already in the late afternoon (i.e., at 8 pm). The total amount of traffic in the network influences the policies of the LL algorithm moving the beginning of the high switch OFF zone from the 8 pm till 12 pm. Therefore, the main difference between the optimal and the LL solutions is in the duration of the high switch OFF period. The latter presents a more conservative approach and needs to switch OFF with higher intensity for being able to reach the design goals.

In Fig. 6.8 we observe that the policies have a similar behavior during the night and differs during the day. In fact, considering the case of high traffic in Fig. 6.8b, the optimal solution reports an extra switching OFF period during the afternoon in order to save energy for the peak of traffic during the night. On the contrary, LL is maintaining the behavior of the office traffic profile with only switch OFF period during the night. However, LL reacts to the higher traffic demand during the night by reducing of 50% the switch OFF rate with respect to the case of the office traffic profile.

6.5.5 Network Performance

In this section the LL framework is compared with a distributed QL solution and a greedy (GR) algorithm. The GR switches OFF an SBS when its battery is below a security threshold $B_{\text{th}}^{\text{OFF}}$, and reactivates it when the battery returns above the threshold. $B_{\text{th}}^{\text{OFF}}$ is set to 20% for maintaining the batteries in the correct SOC operative range and avoid to rapidly jeopardize the battery performance [135]. Results are obtained averaging simulations spanning over different months for an overall duration of 365 simulated days with framework already trained. Despite of the fact that the training is performed offline, the exploration phase is not stopped in order to be able to follow the slower dynamics of the harvesting energy process across the seasons. It is worth noting that, the performance behavior evaluated including the training phase does not change substantially, since the training phase is relatively short with respect to the assessment window. Moreover, the training can be reduced by using *offline* solution like the one presented in [137], where Q-tables are initialized with trained Q-values evaluated either with a simulation approach or obtained by other expert SBSs that have been already deployed, as in the transfer learning paradigm. As for Section 6.5.4, two representative periods are considered for presenting the results: winter and summer, respectively termed “Win” and “Sum”. We considered a high-traffic intensity involving 70 UEs (50% heavy), since the results with low-traffic present a similar behavior and will not presented for space reasons.

Fig. 6.9 presents the system average percentage gain in throughput of the LL and QL schemes with respect to the GR. The LL framework presents always a higher throughput. Moreover, the LL has better scalability than QL, which shows a degradation starting from 5 SBSs. This phenomenon is of particular intensity in case of residential traffic

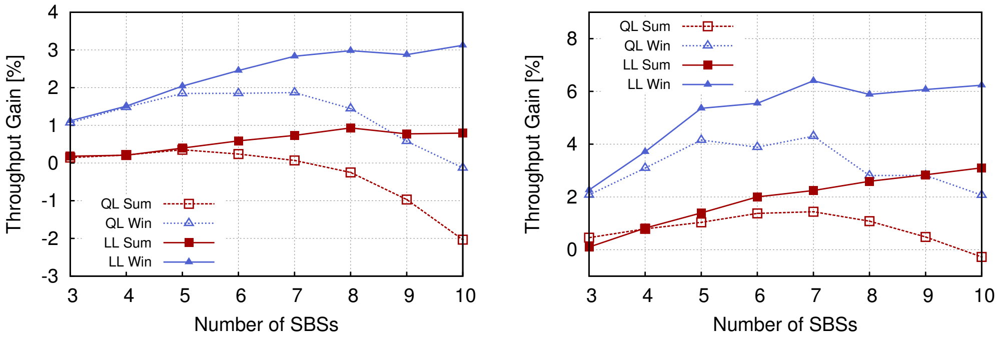

(A) Office Traffic Profile

(B) Residential Traffic Profile

FIGURE 6.9: Throughput [%] gain of the LL and QL solutions with respect to the GR one. Scenario with 70 UEs per SBS with 50% of heavy users with Office and Residential traffic profile.

profile, where it leads to a throughput lower than the GR in the summer period, as depicted in Fig. 6.9a. This is the typical problem of a distributed QL solutions, since the lack of coordination may generate conflicting behaviors among the agents. This issue may occur with higher probability for a higher number of agents, as clearly demonstrated by the QL performance in Fig. 6.9. It is to be noted that, during summer the gain in throughput is lower since the renewable source system has been dimensioned to provide the necessary energy in winter season. This implies that during summer the harvested energy is generous and both LL and QL have fewer margins for policy optimization.

Fig. 6.10 reports the average traffic drop rate of the three schemes and confirms the analysis in the above. The QL solution is able to reduce the drop rate with respect to the GR in most of the cases for the case of Residential traffic profile, where it has a higher drop rate only in case of 10 SBSs during the summer. However, the scalability issue with the drop rate is more clear in the case of the Office traffic profile, where the GR solution has better performance both in summer, starting from 8 SBSs, and in winter, in case of 10 SBSs. Alternatively, LL is able to always present the lowest traffic drop rate and to maintain it almost always below the HAMRL system drop rate threshold D_{th} of the 3%. The only exception is for the case of Residential traffic profile in the winter season, where the traffic drop rate reaches the 8%, which corresponds to approximately the half of the one experienced by the GR.

We now analyze the average daily performance during the summer and winter periods in the scenario with 10 SBS in order to highlight the differences between QL and LL in the most sensitive zones. In Fig. 6.11, we report the traffic drop rate of the LL, QL and GR solutions in a cluster of 10 SBSs varying the number of UEs per SBS. The LL solution is able to reduce the traffic drop rate of more than 50% with respect to GR. On the contrary, QL has always worst performance in summer period and also in the winter

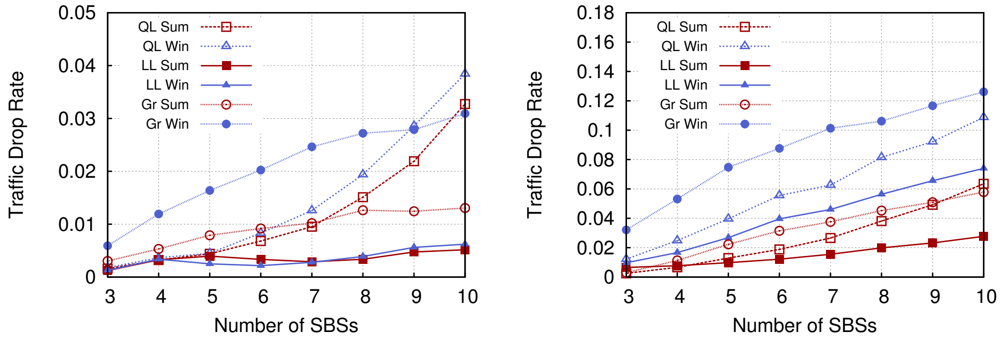

(A) Office Traffic Profile

(B) Residential Traffic Profile

Figure 6.10: Traffic drop rate of the LL, QL and GR solutions. Scenario with 70 UEs per SBS with 50% of heavy users with Office and Residential traffic profile.

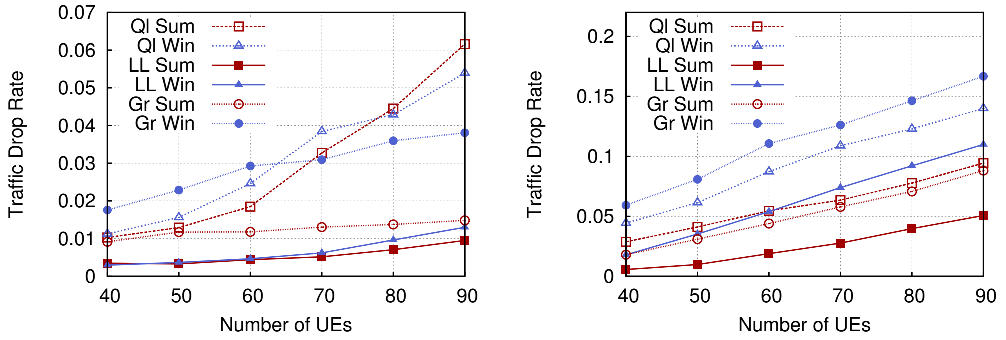

(A) Office Traffic Profile

(B) Residential Traffic Profile

Figure 6.11: Traffic drop rate of the LL, QL and GR solutions. Scenario with 10 SBSs and varying the number of UEs per SBS with 50% of heavy users with Office and Residential traffic profile.

one starting from 60 UEs per SBS when considering the Office traffic profile. Finally, Fig. 6.12 presents the average hourly traffic drop for the case of 70 UEs per SBS. It is clear that LL outperforms the other solutions during all the day and considering both traffic profiles. In detail, in case of the Office traffic profile, LL can meet the design goals on the system drop rate during the whole day, while GR and QL present high peaks in the early morning (9 am) and early night (from 8 pm to 12 pm). Regarding the residential traffic profile, it can be seen that LL is not able to maintain the traffic drop rate below D_{th} passing the 4% since it is not able to properly manage the high traffic peaks at late night and early morning, which are two sensitive periods as in both of them the system does not have high energy reserves.

6.5.6 Energy Assessment

Table 6.2 and Table 6.3 present the footprint of the two learning-based methods and of a baseline solution where both the MBS and the SBSs are powered with the grid.

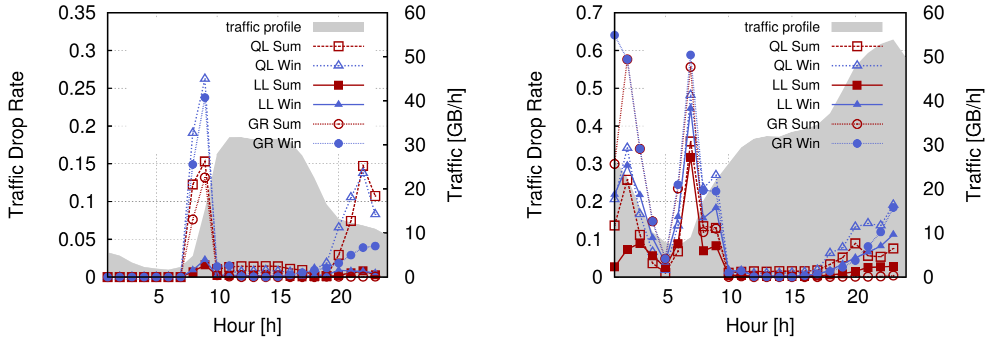

(A) Office Traffic Profile

(B) Residential Traffic Profile

FIGURE 6.12: Average hourly traffic drop rate of the LL, QL and greedy solutions. Scenario with 10 SBSs and 70 UEs per SBS with 50% of heavy users with Office and Residential traffic profile.

In particular, the comparison is performed in terms of grid energy consumption and carbon dioxide equivalent (CO2e) production for a scenario with 50% of heavy users. The CO2e has been evaluated by considering the average grid electricity CO2 intensity of UK in 2016, which corresponds to 320 gCO2eq/kWh [140]. In addition, the column excess energy reports the values of the harvested energy that cannot be used by the SBSs nor stored in the batteries, since the harvesting/storage system is dimensioned for the worst case (i.e., winter).

The learning solutions can reach energy and carbon savings of up to 50% during the summer, as for the scenarios with 10 SBSs. However, the savings are strongly affected by the number of SBSs deployed. In fact, for small numbers of SBSs, the energy footprints of the three methods are closer, and the savings are limited to $20 - 30\%$ for networks with 5 SBSs. The traffic profile is another important factor that influences the footprint, since it varies in the total amount of data exchanged in the network and in temporal dynamics, as discussed in Section 6.5.4. The energy savings for the scenarios with office traffic profile are in general 10% greater with respect to the ones obtained with the office traffic profile. The reason behind this fact is that the latter has a peak of traffic during the night (12 am), which is where the energy reserves are scarce and the learning solutions differ more with respect to the optimal and rely more on the MBS, as can be seen in the longer high switch OFF period depicted in Fig. 6.8. Considering the two learning methods, the amount of traffic delivered influences the behavior of the energy consumption, as expected. Thus, LL, that drops less traffic, usually consumes more energy with respect to the QL solution. However, the gap between them is almost null when considering scenarios with 10 SBSs, which is where QL experiences the highest drop error rate since it suffers of agents' coordination problem, as presented in Fig. 6.10.

Finally, looking at the excess energy values in Table 6.2 and Table 6.3, we can appreciate

Table 6.2: Energy consumption, carbon dioxide equivalence and exceed energy in the winter period for a network composed of 5 and 10 SBSs, and 70 UEs per SBS with 50% of heavy users.

Traffic	Solution	Energy Used (kWh)		CO2e (kg)		Excess Energy (kWh)	
		5 SBSs	10 SBSs	5 SBSs	10 SBSs	5 SBSs	10 SBSs
Off	grid	4784	6854	1435	2139	0	0
	QL	3320	3745	1066	1198	770	1499
	LL	3324	3647	1064	1167	776	1310
Res	grid	4921	7130	1574	2281		
	QL	3634	4180	1163	1338	501	999
	LL	3854	4200	1233	1344	536	949

Table 6.3: Energy consumption, carbon dioxide equivalence and exceed energy in the summer period for a network composed of 5 and 10 SBSs, and 70 UEs per SBS with 50% of heavy users.

Traffic	Solution	Energy Used (kWh)		CO2e (kg)		Excess Energy (kWh)	
		5 SBSs	10 SBSs	5 SBSs	10 SBSs	5 SBSs	10 SBSs
Off	grid	6871	9713	2199	3108	0	0
	QL	4584	5184	1455	1659	2662	5295
	LL	4592	5069	1469	1622	2651	5033
Res	grid	6975	10106	2232	3234	0	0
	QL	4923	5651	1575	1808	3912	6995
	LL	5188	5647	1660	1807	3941	7892

how the harvested energy process is abundant in summer, where the energy that cannot be used can be greater than the grid energy used by the system, as in the summer for the case of 10 SBSs. As for the energy savings, this circumstance occurs with particularly intensity with the residential traffic profile, that is the scenario in which the learning algorithms experience more difficulties in optimizing the system. The performance of QL and LL are similar in this case, expect for the case of summer with 10 SBSs, where the QL consumes 10% more of harvested energy despite of the fact that is dropping more traffic. This behavior confirms that LL scales better and is able to use more efficiently the available energy reserves, i.e., it utilizes less solar energy than QL and delivers more traffic.

In the light of the above results, future work need to consider enhancements in the decisions making process for enabling the system to reduce the exceed energy and work with the same performance under different traffic conditions. Moreover, tolerating an increment in the complexity of the problem, the exceed energy can be a new variable in an extended optimization problem than can control the process of sharing it with other network elements, as in a micro-grid scenario, and/or trading it, as done by the prosumers in the smart grid architecture.

6.6 Concluding Remarks

In this chapter we have presented a comprehensive framework for the management of two tiers networks with SBS powered with solar power. A Layered Learning approach to improve the EE of the system while maintaining the performance requirements has been proposed.

The first layer implements a MRL algorithm for learning the control policies locally at each SBS. Each agent (SBS) makes autonomous decisions to independently learn when switching ON/OFF for adapting to the dynamic conditions of the environment, in terms of energy inflow and traffic demand. Layer 2 is in charge of improving the Layer 1 policies through a MFNN-based solution by considering network-wide parameters and, in doing this, helping in mitigating the effects of the conflicting behavior of the agents. The interaction between the two layers is provided by the heuristically accelerated MRL paradigm.

We compared the policies with respect to an optimal offline solution based on dynamic programming, obtaining that the behaviors correspond in almost all cases, proving the fact the online learning can be a viable tool for managing dense network of SBSs. Then, we analyzed the training phase of both MFNN and MRL algorithms. The latter highlighted the improvements obtained thanks the introduction of the proposed LL approach with respect to a distributed MRL solution. The network performance of the proposed LL algorithm has been contrasted with respect to the one of a greedy and distributed MRL solutions. Simulations results show that the proposed solution outperforms the other ones in terms of throughput and drop rate. The energy savings achieved are considerable with respect to standard solution where both MBS and SBSs are powered with the grid, reaching up to the 50%. Moreover, the exceed energy is also abundant, which opens the door to the possibility of extending the problem for including it in the optimization framework.

Finally, there are several ways in which this work can be extended. The traffic model is deterministic due to the lack of models considering the geographical and temporal statistical distributions. However, HetNet scenarios are characterized for specific spatial distribution of users (i.e., hotspot) that varies during the day according to the zone (e.g., residential, office, transportation). The effect of these dynamics in the learning process is important to be evaluated for considering the deployment of this framework in real networks. The proposed solution has shown some stability problem for network of very dense SBSs with high traffic. The proposed heuristically accelerated RL together with the layered learning paradigm represent a good starting point, since they combine the flexibility of a distributed learning solution with the efficiency of a centralized one. Further work can be done for a deeper integration between the solutions adopted in the two layers. The results on the excess energy encourages to integrate its control in the optimization problem. In fact, the presence of abundant energy perfectly matches with Demand Response method of the smart grid, where the energy can be either shared among elements and/or traded with the energy operators.

Chapter 7

Conclusions and Future Work

The trend for the next generation of cellular network, the Fifth Generation (5G), predicts a 1000x increase in the capacity demand with respect to 4G, which leads to new infrastructure deployments. In order to deal with this huge demand, one of the most promising solution is to support macro BSs with small form scale factor BSs, which helps in improving the spectrum efficiency and provides broadband connection in hot spot manner. However, this will translate in a important increase in energy consumption. It is estimated that the energy footprint of the whole ICT ecosystem might reach the 51% of global electricity production by 2030, mainly due to mobile networks and services [5]. Consequently, the cost of energy may also become predominant in the OPEX of a mobile network operator and, cellular communication networks will have greater ecological impact in the coming years. Therefore, an efficient control of the energy consumption in 5G networks is not only desirable but essential.

The research community has been paying close attention to the energy efficiency (EE) of the radio communication networks, with particular emphasis on the dynamic switch ON/OFF of the base stations (BSs). However, only with the introduction of energy harvesting (EH) capabilities is possible to enable the needed energy savings, especially in scenario with dense deployments of SBSs. The objective of this Ph.D thesis is to present a solid contribution on the control of the SBSs by evaluating online switch ON/OFF policies based on ML tools. According to the study of the state-of-the-art literature, a set of new opportunities were identified on the field of online control solution, which has been recognized as novel topic that enable the optimization of the system considering a more realistic scenario, i.e., with accurate traffic and energy models.

The adoption of learning methods for the control of SBSs enables a highly adaptive and autonomous behavior, which is in-line with the paradigms of HetNet and self-organization of 5G wireless communications. The proposed framework is based on a multi-agent RL approach for controlling the SBS together with a Layered Learning paradigm to simplify the problem by decompose it in subtasks. The technical chapters of this thesis have hence been focused on the design of learning approaches analyzing MRL solutions and their extension with LL.

The novelties presented in this Ph.D thesis include not only the development of online switching ON/OFF algorithm for improving the EE of HetNet, but also, the definition of a methodology to model the energy inflow of solar panels as a function of time through stochastic Markov processes. Thus, the frameworks developed have been successfully applied to investigate realistic scenarios under different environmental conditions, such as traffic profiles of residential and office areas, and considering the different seasons of the year for what concern the energy harvesting process.

7.1 Summary of Results

The goal of this thesis is to contribute on making more sustainable the ICT ecosystem, by focusing on the next generation cellular networks. The focus has been put on the design and performance analysis and evaluation of new energy-efficient control algorithms HetNet with energy harvesting capabilities. The thesis is organized into one preliminary part and three main parts:

- Chapter 1, Chapter 2 and Chapter 3: introducing the problem, the state-of the art and the theoretical background.
- Chapter 4: presenting the first technical part on an accurate stochastic Markov processes for the description of the energy scavenged by outdoor solar sources.
- Chapter 5: presenting the second technical part on the definition and analysis of a control solution for SBSs powered with solar panels based on distributed MRL.
- Chapter 6: presenting the third technical part on the definition and analysis of a control framework for HetNet with EH capabilities based on LL.

In what follows, the contributions and conclusions of the three main technical parts are summarized.

7.1.1 Modeling Solar Sources through Stochastic Markov Processes

The research work presented in this Ph.D. thesis started by presenting a methodology to derive simple and accurate stochastic Markov processes for the description of the energy scavenged by outdoor solar sources. The proposed models are especially useful for the theoretical investigation and the simulation of energetically self-sufficient communication systems that include these devices. In fact, a large body of work has been published so far to mathematically analyze these facts considering deterministic, independent and identically distributed across time slots or time-correlated Markov models, which do not guarantee to estimate the effectiveness of the proposed strategies in realistic scenarios. The Markov models that we derived in this paper are obtained from extensive solar radiation databases, that are widely available online. Basically, from hourly radiance patterns, we derive the corresponding amount of energy (current and voltage) that is accumulated over time, and we finally use it to represent the scavenged energy in terms of its relevant statistics. Toward this end, two clustering approaches for the raw radiance data are described and the resulting Markov models are compared against the empirical distributions. Our results indicate that Markov models with just two states provide a rough characterization of the real data traces. While these could be sufficiently accurate for certain applications, slightly increasing the number of states to, e.g., eight, allows the representation of the real energy inflow process with an excellent level of accuracy in terms of first and second order statistics.

7.1.2 EH HetNet Control through Distributed Q-Learning

The massive deployment of SBS represents one of the most promising solutions adopted by 5G cellular networks to meet the foreseen huge traffic demand. The high number of network elements entails a significant increase in the energy consumption suggesting the usage of renewable energies for powering the SBSs for reducing both the environmental impact of mobile networks and enabling cost saving on operators' electric bills. In this work, we proposed an ON/OFF switching algorithm, based on reinforcement learning, that autonomously learns energy income and traffic demand patterns. The algorithm is based on distributed multi-agent Q-learning for jointly optimizing the system performance and the self-sustainability of the SBSs. We analyze the algorithm by assessing its convergence time, characterizing the obtained ON/OFF policies, and evaluating an offline trained variant. Simulation results demonstrate that our solution is able to increase the energy efficiency of the system with respect to simpler approaches. Moreover, the proposed method provides an harvested energy surplus, which can be used by mobile operators to offer ancillary services to the smart electricity grid. Nevertheless, there are various aspects that need to be further investigated. First, we would like to enhance the decisions made by the SBSs so that they will cooperatively compute optimal policies accounting for common (and global) performance objectives. Note that in the current algorithm this cooperation is only marginally achieved through the use of the global drop rate in the reward functions that are locally computed by the SBSs. Finally, we need to explore more scenarios considering different traffic profiles with different traffic demands for studying the behavior of the algorithm in more 5G operative cases.

7.1.3 EH HetNet Control through Layered Learning

In the last part of this Ph.D. thesis, we investigated techniques based on Layered Learning for the Radio Resource Management of dense cellular networks with SBSs powered solely by renewable energy. The goal of the proposed solution is to improve the system scalability, which has been demonstrated to be an issue in MRL system. In the first layer, reinforcement learning agents locally select switch ON/OFF policies of the SBSs according to the energy income and the traffic demand based on a heuristically accelerated RL paradigm similar to the one defined in Chapter 5. The second layer relies on an Artificial Neural Network that estimates the network load conditions to implement a centralized controller enforcing local agent decisions. The proposed framework has been compared with an optimal bound obtained offline based on dynamic programming. The resulting learned behavior of the SBSs matches quite well the optimal one, except in extreme cases as for high load with residential traffic profile. Simulation results prove that the proposed layered framework outperforms both a greedy and a completely distributed solution like the one presented in Chapter 5 both in terms of throughput and energy efficiency under various conditions and with different traffic demand profiles.

7.2 Future Work

The road toward the sustainability of wireless networks represents one of the main challenges for the future. This Ph.D dissertation aimed at starting the investigation on some open topics that have not been covered in the state-of-the-art, and some others have been identified through the course of the thesis. In the light of the conclusions presented above, multiple research lines have been left open for future work. In what follows, we summarize the most important ones.

7.2.1 Realistic Models of the Network Environment

In Chapter 4 we presented an accurate Markov model for the harvested energy by solar panels. The model is accurate and allows to have realistic energy harvesting profiles for different cities of US. However, such model is difficult to reproduce for other cities in the world and, nowadays, even for the same cities it has been developed. In fact, in order to maintain it flexibility in defining the solar panel type, it needs information like extraterrestrial radiation, dry-bulb temperature and of the dew point temperature which are not easily to find in the free available data-bases. Moreover, in order to have a good statistical confidence, the data set should span over several years, which is usually another constraint of the open data-bases. Future work includes to find a more simple methodologies to retrieve accurate model for the solar harvested energy and, possibly, also for other renewable energies source type. For example, clusterization and feature extraction methods represent tools that are suitable for solving this kind of problem.

The issues faced for the RES energy models are even more important for what concern the traffic demand ones. In fact, the models we adopted in the work carried out in this thesis, despite of proving a realistic representation of the real phenomenon, do not provide any specification on the geographical and temporal statistical distributions. In fact, HetNet scenarios are characterized for specific spatial distribution of users (i.e., hotspot) that varies during the day according to the zone (e.g., residential, office, transportation). The model in literature do not provide any reference to this respect. All the models define only the temporal variations of the total amount of traffic requested per hour basis. Therefore, it is impossible to reproduce realistic scenarios in which the traffic profiles have specific distributions for both the time and the space, instead of a deterministic value. In literature, the common solution is to make assumption on the spatial distribution and analyze the different profiles separately, has been done in this thesis. Further investigations to fill this gap remain a future work. Some preliminary work have been already performed on this field. For instance, in [141] an LTE sniffer capable of decoding the unencrypted LTE Physical Downlink Control Channel (PDCCH) has been used for analyzing the temporal and spatial analysis of the recorded traces and deriving the stochastic characterization for the daily-varying LTE traffic. However, the process of retrieving the needed data is long and, at the time of this writing, the model is limited only to a few cases.

7.2.2 Characterization of the RL based solutions

One of most important problem when using learning solutions in multi-agent systems is the duration of the training phase and the convergence to the point of equilibrium. As highlighted in chapter 6, the proposed solutions have still margin for improvement for both aspects.

The duration of the training is important in real network for enabling the rapid deployment of new SBSs and allowing the network to rapidly reconfigure and adapting to the new architecture. The offline training has been investigated in this thesis providing interesting results. However, it is not always possible to simulate offline a specific change in the network deployment. Therefore, solutions like transfer learning have to evaluated. Regarding the convergence, ML literature offers different algorithms that can find interesting solutions (e.g., NashQ [142] or DynaQ [28]). However, the space of possible solutions becomes too big, making unfeasible it usage in real network due to the increased time of training. Therefore, future work has to consider more research on multi-agent systems. The proposed heuristically accelerated RL together with the layered learning paradigm represent a good starting point, since they combine the flexibility of a distributed learning solution with the efficiency of a centralized one. Further work can be done for a deeper integration between the solutions adopted in the two layers. For example, the centralized controller can take directly part of the single SBS control process, by estimating the SBSs behavior in a more detail fashion. For instance deep learning and deep neural networks can be an interesting solution to exploit thanks to their abilities in predicting the relation among different patterns, in this case the ones of the energy income and the traffic demand.

The solutions proposed in Chapter 5 and Chapter 6 have been presented from a distributed perspective, for highlighting the advantages that these methods have in the problem studied. However, a comparison with the optimal bound has been carried out only partially, due to complexity of the problem. This aspect is important for having a quantitative evaluation of the gap of the learning solution with respect to the optimum. In fact, considering all the dynamics of system, it is impossible that the learning solutions found the optimal, as it is demonstrated in Chapter 6. Similarly, a comparison with a centralized solution is needed to quantify the gap of distributed solutions with respect to the centralized ones. In fact, centralized solution typically have better performance provided that they have complete knowledge of the system. This, in turns, translates in a high complexity due to the higher signaling and dimension of the problem. The centralized approach is of particular interest when considering the SDN/NFV-like approach, where, thanks to the SDN framework, the network can provide a large number of parameter in data centers. In addition, the layered learning paradigm can be a valuable architecture for distributed NFV approaches [143], where virtualized functions should be located where they are the most effective and least expensive. To this respect, future work included the development of more lightweight models for finding the optimal solution and the evaluation of centralized and distributed NFV-like solutions.

7.2.3 Integration with Smart Grids

The huge energy consumption estimation of mobile networks for the next future encourage their integration with the upcoming smart grid architectures. In fact, as showed in Chapter 5 and Chapter 6, the HetNet with EH capabilities can become a prosumer and share or trade the energy during the day, according to the energy incomes.

In case of sharing, the SBSs can either help other SBSs when running out of energy or provide energy to ancillary services. In this respect, Energy Packet Networks (EPN) are envisaged to be an interesting solution to be further explored for energy transfer among network nodes. In an EPN, discrete units of energy, termed *energy packets*, can be exchanged among network elements of the micro-grid.

Trading is a solution of the Demand Response (DR) family that aimed at helping in solving the problem of managing the peaks of energy demand in the smart grid, namely Demand-Side Management (DSM). As we introduced in [80], this solution will be interesting when a proper pricing schemes will be in place, which should incentivize BSs to sell their excess energy, while also making these transactions convenient for the electricity grid. In the next future, the energy price will depend on the cost of production and on the expected demand. In this scenario, future work can evaluate decision-making solutions to find the best energy-purchasing policies for the BSs taking into account: (i) current and forecast renewable energy income, (ii) current and forecast traffic load and (iii) the future evolution of the energy prices. In this scenario, BSs act as prosumers of the smart grids.

Bibliography

[1] EARTH: Energy Aware Radio and neTwork tecHnologies. D2.3: Energy efficiency analysis of the reference systems, areas of improvements and target breakdown. Project Deliverable D2.3, www.ict-earth.eu, 2010.

[2] Cisco Systems Inc. Cisco Visual Networking Index: Global Mobile Data Traffic Forecast Update, 2016 – 2021. White Paper, http://www.cisco.com/, February 2017.

[3] M. P. Mills. The Cloud Begins with Coal: Big Data, Big Networks, Big Infrastructure, and Big Power. Digital Power Group, August 2013.

[4] Ward Van Heddeghem, Sofie Lambert, Bart Lannoo, Didier Colle, Mario Pickavet, and Piet Demeester. Trends in worldwide ict electricity consumption from 2007 to 2012. *Computer Communications*, 50:64 – 76, 2014. ISSN 0140-3664. doi: https://doi.org/10.1016/j.comcom.2014.02.008. URL http://www.sciencedirect.com/science/article/pii/S0140366414000619. Green Networking.

[5] Anders S. G. Andrae and Tomas Edler. On global electricity usage of communication technology: Trends to 2030. *Challenges*, 6(1):117, 2015.

[6] Albrecht Fehske, J. Malmodin, G. Biczók, and Gerhard Fettweis. The Global Footprint of Mobile Communications: The Ecological and Economic Perspective. *IEEE Communications Magazine, issue on Green Communications*, 49(8):55–62, August 2011. ISSN 0163-6804. doi: 10.1109/MCOM.2011.5978416.

[7] Ericsson. 5G radio access: research and vision. White Paper, available on-line.

[8] Nokia Solutions Networks. Looking ahead to 5G. White Paper, http://nsn.com/innovative-thinking/technology-vision.

[9] ETSI. ES 203 208; Environmental Engineering (EE); Assessment of mobile network energy efficiency (v1.2.1), 2017.

[10] 3GPP. TR 21.866.; Study on Energy Efficiency Aspects of 3GPP Standards (Rel.14), 2017.

[11] European Council 23 and 24 October 2014 conclusions. 2030 climate and energy policy framework for the European Union. White Paper, available on-line.

[12] Z. Hasan, H. Boostanimehr, and V.K. Bhargava. Green cellular networks: A survey, some research issues and challenges. *Communications Surveys Tutorials, IEEE*, 13(4):524–540, Fourth 2011.

[13] F. Han, S. Zhao, L. Zhang, and J. Wu. Survey of Strategies for Switching Off Base Stations in Heterogeneous Networks for Greener 5G Systems. *IEEE Access*, 4:4959–4973, August 2016. ISSN 2169-3536. doi: 10.1109/ACCESS.2016.2598813.

[14] E. Palm, F. Heden, and A. Zanma. Solar powered mobile telephony. In *Proc. of EcoDesign, Second International Symposium on Environmentally Conscious Design and Inverse Manufacturing*, pages 219 –222, Tokyo, Japan, Dec. 2001.

[15] B. Lindemark and G. Oberg. Solar power for radio base station (RBS) sites applications including system dimensioning, cell planning and operation. In *Proc. of Int. Telecommunications Energy Conference, INTELEC*, pages 587 –590, Edinburgh, UK, Oct. 2001.

[16] David López-Pérez, Ming Ding, Holger Claussen, and Amir H Jafari. Towards 1 Gbps/UE in cellular systems: Understanding ultra-dense small cell deployments. *IEEE Communications Surveys & Tutorials*, 17(4):2078–2101, June 2015. ISSN 1553-877X. doi: 10.1109/COMST.2015.2439636.

[17] G. Auer, V. Giannini, C. Desset, I. Godor, P. Skillermark, M. Olsson, M.A. Imran, D. Sabella, M.J. Gonzalez, O. Blume, and A. Fehske. How much energy is needed to run a wireless network? *IEEE Wireless Communications*, 18(5):40–49, October 2011.

[18] P. Dini, M. Miozzo, N. Bui, and N. Baldo. A model to analyze the energy savings of base station sleep mode in lte hetnets. In *Green Computing and Communications (GreenCom), 2013 IEEE and Internet of Things (iThings/CPSCom), IEEE International Conference on and IEEE Cyber, Physical and Social Computing*, pages 1375–1380, Aug 2013.

[19] Giuseppe Piro, Marco Miozzo, Giuseppe Forte, Nicola Baldo, Luigi Alfredo Grieco, Gennaro Boggia, and Paolo Dini. HetNets Powered by Renewable Energy Sources. *IEEE Internet Computing*, 17(1):32–39, 2013.

[20] A. G. Tsikalakis and N. D. Hatziargyriou. Centralized control for optimizing microgrids operation. In *2011 IEEE Power and Energy Society General Meeting*, pages 1–8, July 2011. doi: 10.1109/PES.2011.6039737.

[21] M. Miozzo, D. Zordan, P. Dini, and M. Rossi. SolarStat: Modeling Photovoltaic Sources through Stochastic Markov Processes. In *IEEE Energy Conference (ENERGYCON)*, Dubrovnik, Croatia, May 2014.

[22] Open Networking Foundation. Software-Defined Networking: The New Norm for Networks. *ONF White Paper*, 2:2–6, April 2012.

[23] Yong Li and Min Chen. Software-Defined Network Function Virtualization: A Survey. *IEEE Access*, 3:2542–2553, December 2015. ISSN 2169-3536. doi: 10.1109/ACCESS.2015.2499271.

[24] M. Y. Arslan, K. Sundaresan, and S. Rangarajan. Software-defined networking in cellular radio access networks: potential and challenges. *IEEE Communications Magazine*, 53(1):150–156, January 2015. ISSN 0163-6804. doi: 10.1109/MCOM.2015.7010528.

[25] J. Pérez-Romero, O. Sallent, R. Ferrús, and R. Agustí. Knowledge-based 5g radio access network planning and optimization. In *2016 International Symposium on Wireless Communication Systems (ISWCS)*, pages 359–365, Sept 2016. doi: 10.1109/ISWCS.2016.7600929.

[26] J. Hoydis, M. Kobayashi, and M. Debbah. Green Small-Cell Networks: A Cost- and Energy-Efficient Way of Meeting the Future Traffic Demands . *IEEE Veh. Technol. Mag.*, Mar. 2011.

[27] K. P. Sycara. Multiagent systems. *AI Magazine*, 19(2):79–92, 1998.

[28] R. S. Sutton and A. G. Barto. *Reinforcement Learning: An Introduction.* MIT Press, 1998.

[29] Peter Stone and Manuela Veloso. *Using decision tree confidence factors for multiagent control*, pages 99–111. Springer Berlin Heidelberg, Berlin, Heidelberg, 1998.

[30] R. A. C. Bianchi, M. F. Martins, C. H. C. Ribeiro, and A. H. R. Costa. Heuristically-accelerated multiagent reinforcement learning. *IEEE Transactions on Cybernetics*, 44(2):252–265, Feb 2014. ISSN 2168-2267. doi: 10.1109/TCYB.2013.2253094.

[31] M. H. Alsharif, R. Nordin, and M. Ismail. Survey of green radio communications networks: Techniques and recent advances. *Journal of Computer Networks and Communications*, 2013:13, 2013.

[32] EARTH (Energy Aware Radio and neTwork tecHnologies). EU Funded Research Project FP7-ICT-2009-4-247733-EARTH, Jan. 2010 - Jun. 2012. `https://www.ict-earth.eu`.

[33] Dario Sabella, Damiano Rapone, Maurizio Fodrini, Cicek Cavdar, Magnus Olsson, Pal Frenger, and Sibel Tombaz. *Energy Management in Mobile Networks Towards 5G*, pages 397–427. Springer International Publishing, 2016. doi: 10.1007/978-3-319-27568-0_17.

[34] C-RAN: the road towards green RAN. *China Mobile Research Institute, White Paper*, 2011.

[35] NEC. NFV C-RAN for Efficient RAN Resource Allocation. `http://www.nec.com/en/global/solutions/nsp/sc2/doc/wp_c-ran.pdf`. Online White Paper; accessed on March 16, 2016.

[36] Small Cell Forum. Virtualization for small cells: overview. *White Paper (available on-line*, 2015.

[37] C. Desset, B. Debaillie, V. Giannini, A. Fehske, G. Auer, H. Holtkamp, W. Wajda, D. Sabella, F. Richter, M. J. Gonzalez, H. Klessig, I. Gódor, M. Olsson, M. A. Imran, A. Ambrosy, and O. Blume. Flexible power modeling of LTE base stations. In *2012 IEEE Wireless Communications and Networking Conference (WCNC)*, pages 2858–2862, April 2012. doi: 10.1109/WCNC.2012.6214289.

[38] N. Bartzoudis, O. Font-Bach, M. Miozzo, C. Donato, P. Harbanau, M. Requena, D. López, I. Ucar, A. A. Saloña, P. Serrano, J. Mangues, and M. Payaró. Energy footprint reduction in 5g reconfigurable hotspots via function partitioning and bandwidth adaptation. In *2017 Fifth International Workshop on Cloud Technologies and Energy Efficiency in Mobile Communication Networks (CLEEN)*, pages 1–6, June 2017. doi: 10.23919/CLEEN.2017.8045934.

[39] M. Miozzo, N. Bartzoudis, M. Requena, O. Font-Bach, P. Harbanau, D. López-Bueno, M. Payaró, and J. Mangues. Sdr and nfv extensions in the ns-3 lte module for 5g rapid prototyping. In *2018 IEEE Wireless Communications and Networking Conference (WCNC)*, April 2018.

[40] Nicola Baldo, Marco Miozzo, Manuel Requena-Esteso, and Jaume Nin-Guerrero. An open source product-oriented lte network simulator based on ns-3. In *Proceedings of the 14th ACM International Conference on Modeling, Analysis and Simulation of Wireless and Mobile Systems*, MSWiM '11, pages 293–298, New York, NY, USA, 2011. ACM. ISBN 978-1-4503-0898-4. doi: 10.1145/2068897.2068948. URL `http://doi.acm.org/10.1145/2068897.2068948`.

[41] Hong Zhang, Jun Cai, and Xiaolong Li. Energy-efficient base station control with dynamic clustering in cellular network. In *IEEE International Conference on*

Communications and Networking (CHINACOM), pages 384–388, Guilin, China, August 2013. doi: 10.1109/ChinaCom.2013.6694626.

[42] Sumudu Samarakoon, Mehdi Bennis, Walid Saad, and Matti Latva-aho. Dynamic Clustering and ON/OFF Strategies for Wireless Small Cell Networks. *IEEE Transactions on Wireless Communications*, 15(3):2164–2178, March 2016. ISSN 1536-1276. doi: 10.1109/TWC.2015.2499182.

[43] Shijie Cai, Limin Xiao, Haibin Yang, Jing Wang, and Shidong Zhou. A cross-layer optimization of the joint macro and picocell deployment with sleep mode for green communications. In *IEEE Wireless and Optical Communication Conference (WOCC)*, pages 225–230, Chongqing, China, May 2013. doi: 10.1109/WOCC.2013.6676373.

[44] Yutao Zhu, Zhimin Zeng, Tiankui Zhang, and Dantong Liu. A QoS-Aware Adaptive Access Point Sleeping in Relay Cellular Networks for Energy Efficiency. In *IEEE Vehicular Technology Conference (VTC Spring)*, pages 1–5, Seoul, Korea, May 2014. doi: 10.1109/VTCSpring.2014.7023152.

[45] Ran Tao, Jie Zhang, and Xiaoli Chu. An Energy Saving Small Cell Sleeping Mechanism with Cell Expansion in Heterogeneous Networks. In *IEEE Vehicular Technology Conference (VTC Spring)*, pages 1–5, Porto, Portugal, May 2016. doi: 10.1109/VTCSpring.2016.7504126.

[46] Alexandra Bousia, Elli Kartsakli, Luis Alonso, and Christos Verikoukis. Energy efficient base station maximization switch off scheme for LTE-advanced. In *IEEE International Workshop on Computer Aided Modeling and Design of Communication Links and Networks (CAMAD)*, pages 256–260, Barcelona, Spain, September 2012. doi: 10.1109/CAMAD.2012.6335345.

[47] Hakim Ghazzai, Muhammad Junaid Farooq, Ahmad Alsharoa, Elias Yaacoub, Abdullah Kadri, and Mohamed-Slim Alouini. Green Networking in Cellular HetNets: A Unified Radio Resource Management Framework With Base Station ON/OFF Switching. *IEEE Transactions on Vehicular Technology*, 66(7):5879–5893, July 2017. ISSN 0018-9545. doi: 10.1109/TVT.2016.2636455.

[48] Yuan Yuan and Ping Gong. A QoE-orientated base station sleeping strategy for multi-services in cellular networks. In *International Conference on Wireless Communications & Signal Processing (WCSP)*, pages 1–5, Nanjing, China, October 2015. doi: 10.1109/WCSP.2015.7341051.

[49] Feng Han, Zoltan Safar, and KJ Ray Liu. Energy-efficient base-station cooperative operation with guaranteed QoS. *IEEE Transactions on Communications*, 61(8):

3505–3517, August 2013. ISSN 0090-6778. doi: 10.1109/TCOMM.2013.061913.120743.

[50] Ying Wang, Yuan Zhang, Yongce Chen, and Rong Wei. Energy-efficient design of two-tier femtocell networks. *EURASIP Journal on Wireless Communications and Networking*, 2015(1):1, February 2015. ISSN 1687-1499. doi: 10.1186/s13638-015-0242-4.

[51] Anqi He, Dantong Liu, Yue Chen, and Tiankui Zhang. Stochastic geometry analysis of energy efficiency in HetNets with combined CoMP and BS sleeping. In *IEEE Annual International Symposium on Personal, Indoor, and Mobile Radio Communication (PIMRC)*, pages 1798–1802, Washington DC, USA, September 2014. doi: 10.1109/PIMRC.2014.7136461.

[52] Yong Sheng Soh, Tony QS Quek, Marios Kountouris, and Hyundong Shin. Energy Efficient Heterogeneous Cellular Networks. *IEEE Journal on Selected Areas in Communications*, 31(5):840–850, May 2013. ISSN 0733-8716. doi: 10.1109/JSAC.2013.130503.

[53] A. Bousia, A. Antonopoulos, L. Alonso, and C. Verikoukis. Green distance-aware base station sleeping algorithm in LTE-Advanced. In *IEEE International Conference on Communications (ICC)*, pages 1347–1351, June 2012. doi: 10.1109/ICC.2012.6364240.

[54] Hina Tabassum, Uzma Siddique, Ekram Hossain, and Md Jahangir Hossain. Downlink performance of cellular systems with base station sleeping, user association, and scheduling. *IEEE Transactions on Wireless Communications*, 13(10): 5752–5767, October 2014. ISSN 1536-1276. doi: 10.1109/TWC.2014.2336249.

[55] Chang Liu, Yi Wan, Lin Tian, Yiqing Zhou, and Jinglin Shi. Base Station Sleeping Control with Energy-Stability Tradeoff in Centralized Radio Access Networks. In *IEEE Global Communications Conference (GLOBECOM)*, pages 1–6, San Diego, CA, USA, Dec 2015. doi: 10.1109/GLOCOM.2015.7417363.

[56] D. Tsilimantos, J.-M. Gorce, and E. Altman. Stochastic analysis of energy savings with sleep mode in ofdma wireless networks. In *INFOCOM, 2013 Proceedings IEEE*, pages 1097–1105, April 2013.

[57] Y. S. Soh, T. Q.S. Quek, M. Kountouris, and H. Shin. Energy efficient heterogeneous cellular networks. *Selected Areas in Communications, IEEE Journal on*, 31 (5):840–850, 2013.

[58] K. Samdanis, T. Taleb, D. Kutscher, and M. Brunner. Self organized network management functions for energy efficient cellular urban infrastructures. *Mob. Netw. Appl.*, 17(1):119–131, February 2012. ISSN 1383-469X.

[59] E. Oh, K. Son, and B. Krishnamachari. Dynamic base station switching-on/off strategies for green cellular networks. *Wireless Communications, IEEE Transactions on*, 12(5):2126–2136, 2013.

[60] R. Li, Z. Zhao, X. Chen, and H. Zhang. Energy saving through a learning framework in greener cellular radio access networks. In *Global Communications Conference (GLOBECOM), 2012 IEEE*, pages 1556–1561, 2012.

[61] Khaled Al Haj Ismaiil, Bachir Assaf, Milad Ghantous, and Michel Nahas. Reducing power consumption of cellular networks by using various cell types and cell zooming. In *International Conference on e-Technologies and Networks for Development (ICeND)*, pages 33–38, Beirut, Lebanon, April 2014. doi: 10.1109/ICeND.2014.6991188.

[62] Zhisheng Niu, Yiqun Wu, Jie Gong, and Zexi Yang. Cell zooming for cost-efficient green cellular networks. *IEEE Communications Magazine*, 48(11):74–79, November 2010. ISSN 0163-6804. doi: 10.1109/MCOM.2010.5621970.

[63] Long Bao Le. QoS-aware BS switching and cell zooming design for OFDMA green cellular networks. In *IEEE Global Communications Conference (GLOBECOM)*, pages 1544–1549, Anaheim, CA, USA, December 2012. doi: 10.1109/GLOCOM.2012.6503333.

[64] Xiaodong Xu, Chunjing Yuan, Wenwan Chen, Xiaofeng Tao, and Yan Sun. Adaptive Cell Zooming and Sleeping for Green Heterogeneous Ultra-Dense Networks. *IEEE Transactions on Vehicular Technology*, 2017. doi: 10.1109/TVT.2017.2749058.

[65] Zujie Hu, Yifei Wei, Xiaojuan Wang, and Mei Song. Green relay station assisted cell zooming scheme for cellular networks. In *International Conference on Natural Computation, Fuzzy Systems and Knowledge Discovery (ICNC-FSKD)*, pages 2030–2035, Changsha, China, August 2016. doi: 10.1109/FSKD.2016.7603493.

[66] Yutao Zhu, Tian Kang, Tiankui Zhang, and Zhimin Zeng. QoS-aware user association based on cell zooming for energy efficiency in cellular networks. In *IEEE International Symposium on Personal, Indoor and Mobile Radio Communications (PIMRC Workshops)*, pages 6–10, London, UK, September 2013. doi: 10.1109/PIMRCW.2013.6707826.

[67] Gencer Cili, Halim Yanikomeroglu, and F Richard Yu. Cell switch off technique combined with coordinated multi-point (CoMP) transmission for energy efficiency in beyond-LTE cellular networks. In *IEEE International Conference on Communications (ICC)*, pages 5931–5935, Ottawa, Canada, June 2012. doi: 10.1109/ICC.2012.6364869.

[68] L.A. Suarez, L. Nuaymi, and J. Bonnin. Energy performance of a distributed bs based green cell breathing algorithm. In *Wireless Communication Systems (ISWCS), 2012 International Symposium on*, pages 341–345, 2012.

[69] H.S. Dhillon, R.K. Ganti, F. Baccelli, and J.G. Andrews. Modeling and analysis of k-tier downlink heterogeneous cellular networks. *Selected Areas in Communications, IEEE Journal on*, 30(3):550–560, 2012.

[70] S. Cho and W. Choi. Energy-efficient repulsive cell activation for heterogeneous cellular networks. *Selected Areas in Communications, IEEE Journal on*, 31(5): 870–882, 2013.

[71] L. Saker, S-E Elayoubi, R. Combes, and T. Chahed. Optimal control of wake up mechanisms of femtocells in heterogeneous networks. *Selected Areas in Communications, IEEE Journal on*, 30(3):664–672, 2012.

[72] I-Hong Hou and Chung Shue Chen. An energy-aware protocol for self-organizing heterogeneous lte systems. *Selected Areas in Communications, IEEE Journal on*, 31(5):937–946, 2013.

[73] S. Samarakoon, M. Bennis, W. Saad, and M. Latva-aho. Opportunistic sleep mode strategies in wireless small cell networks. In *Communications (ICC), 2014 IEEE International Conference on*, pages 2707–2712, June 2014.

[74] Chenlong Jia and Teng Joon Lim. Resource partitioning and user association with sleep-mode base stations in heterogeneous cellular networks. *IEEE Transactions on Wireless Communications*, 14(7):3780–3793, July 2015. ISSN 1536-1276. doi: 10.1109/TWC.2015.2411737.

[75] Yutao Zhu, Zhimin Zeng, Tiankui Zhang, Lu An, and Lin Xiao. An energy efficient user association scheme based on cell sleeping in LTE heterogeneous networks. In *International Symposium on Wireless Personal Multimedia Communications (WPMC)*, pages 75–79, Sydney, Australia, September 2014. doi: 10.1109/WPMC.2014.7014794.

[76] M.A. Marsan, S. Buzzi, D. Ciullo, and M. Meo. Multiple daily base station switch-offs in cellular networks. In *Communications and Electronics (ICCE), 2012 Fourth International Conference on*, pages 245–250, 2012.

[77] H. Al Haj Hassan, L. Nuaymi, and A Pelov. Renewable energy in cellular networks: A survey. In *Online Conference on Green Communications (GreenCom), 2013 IEEE*, pages 1–7, Oct 2013.

[78] J. Xu, L. Duan, and R. Zhang. Cost-aware green cellular networks with energy and communication cooperation. *IEEE Communications Magazine*, 53(5):257–263, May 2015. ISSN 0163-6804. doi: 10.1109/MCOM.2015.7105673.

[79] G. Piro, M. Miozzo, G. Forte, N. Baldo, L.A. Grieco, G. Boggia, and P. Dini. Hetnets powered by renewable energy sources: Sustainable next-generation cellular networks. *Internet Computing, IEEE*, 17(1):32–39, 2013.

[80] Davide Zordan, Marco Miozzo, Paolo Dini, and Michele Rossi. When telecommunications networks meet energy grids: Cellular networks with energy harvesting and trading capabilities. *IEEE Communications Magazine*, 53(6):117–123, June 2015. ISSN 0163-6804. doi: 10.1109/MCOM.2015.7120026.

[81] NREL, National Renewable Energy Laboratory. Renewable Resource Data Center. `http://www.nrel.gov/rredc/`, .

[82] NREL, National Renewable Energy Laboratory. Best Research-Cell Efficiencies. `http://www.nrel.gov/ncpv/images/efficiency_chart.jpg`, .

[83] Bloomerg New Energy Finance. World Energy Perspective – The Cost of Energy Technologies. World Energy Council's White Paper, `http://about.bnef.com`, October 2013.

[84] H.S. Dhillon, Ying Li, P. Nuggehalli, Zhouyue Pi, and J.G. Andrews. Fundamentals of heterogeneous cellular networks with energy harvesting. *Wireless Communications, IEEE Transactions on*, 13(5):2782–2797, May 2014.

[85] H.S. Dhillon, R.K. Ganti, and J.G. Andrews. A tractable framework for coverage and outage in heterogeneous cellular networks. In *Information Theory and Applications Workshop (ITA), 2011*, pages 1–6, Feb 2011.

[86] D. Valerdi, Qiang Zhu, K. Exadaktylos, Suhua Xia, M. Arranz, Rui Liu, and D. Xu. Intelligent energy managed service for green base stations. In *GLOBECOM Workshops (GC Wkshps), 2010 IEEE*, pages 1453–1457, Dec 2010.

[87] T. Han and N. Ansari. On greening cellular networks via multicell cooperation. *Wireless Communications, IEEE*, 20(1):82–89, 2013.

[88] Y.K. Chia, S. Sun, and R. Zhang. Energy cooperation in cellular networks with renewable powered base stations. In *Wireless Communications and Networking Conference (WCNC), 2013 IEEE*, pages 2542–2547, April 2013.

[89] M.A. Marsan, G. Bucalo, A. Di Caro, M. Meo, and Yi Zhang. Towards zero grid electricity networking: Powering bss with renewable energy sources. In *Communications Workshops (ICC), 2013 IEEE International Conference on*, pages 596–601, June 2013.

[90] National Renewable Energy Laboratory (NREL). PVWatts Simulator. `http://rredc.nrel.gov/solar/calculators/pvwatts/version1/`.

[91] G. Lee, W. Saad, M. Bennis, A. Mehbodniya, and F. Adachi. Online Ski Rental for ON/OFF Scheduling of Energy Harvesting Base Stations. *IEEE Transactions on Wireless Communications*, 16(5):2976–2990, May 2017. ISSN 1536-1276. doi: 10.1109/TWC.2017.2672964.

[92] M. Mendil, A. De Domenico, V. Heiries, R. Caire, and N. Hadj-said. Fuzzy Q-Learning based energy management of small cells powered by the smart grid. In *2016 IEEE 27th Annual International Symposium on Personal, Indoor, and Mobile Radio Communications (PIMRC)*, pages 1–6, Valencia, Spain, September 2016. doi: 10.1109/PIMRC.2016.7794880.

[93] Nicola Piovesan and Paolo Dini. Optimal direct load control of renewable powered small cells: A shortest path approach. *Internet Technology Letters*, pages e7–n/a, 2017. ISSN 2476-1508. doi: 10.1002/itl2.7. e7.

[94] A. P. Couto da Silva, D. Renga, M. Meo, and M. Ajmone Marsan. The impact of quantization on the design of solar power systems for cellular base stations. *IEEE Transactions on Green Communications and Networking*, 2(1):260–274, March 2018. doi: 10.1109/TGCN.2017.2762402.

[95] N. Baldo, P. Dini, J. Mangues, M. Miozzo, and J. Núñez. Small cells, wireless backhaul and renewable energy: a solution for disaster aftermath communications. In *4th International Conference on Cognitive Radio and Advanced Spectrum Management (COGART 2011)*, Barcelona, Spain, October 2011.

[96] W. Guo, S. Wang, C. Turyagyenda, and T. O'Farrell. Integrated cross-layer energy savings in a smart and flexible cellular network. In *Communications in China Workshops (ICCC), 2012 1st IEEE International Conference on*, pages 79–84, 2012.

[97] A. Galindo-Serrano and L. Giupponi. Downlink femto-to-macro interference management based on fuzzy q-learning. In *Modeling and Optimization in Mobile, Ad Hoc and Wireless Networks (WiOpt), 2011 International Symposium on*, pages 412–417, May 2011.

[98] Lorenza Giupponi, Ana M. Galindo-Serrano, and Mischa Dohler. From cognition to docition: The teaching radio paradigm for distributed & autonomous deployments. *Comput. Commun.*, 33(17):2015–2020, November 2010. ISSN 0140-3664.

[99] Christopher M. Bishop. *Pattern Recognition and Machine Learning (Information Science and Statistics)*. Springer-Verlag New York, Inc., Secaucus, NJ, USA, 2006. ISBN 0387310738.

[100] Dayan P. *Unsupervised learning.* The MIT Encyclopedia of the Cognitive Science, 1999.

[101] R. Bellman. *Dynamic Programming.* Princeton, NJ: Princeton Univ. Press, 1957.

[102] G. W. Brown. *Iterative solution of games by fictitious play, in: Activity Analysis of Production and Allocation*, chapter 24, pages 374–376. John Wiley and Sons, New York, 1951.

[103] D. Fudenberg and D. K. Levine. *The Theory of Learning in Games*, volume 1 of *MIT Press Books*. The MIT Press, June 1998.

[104] C. J. C. H. Watkins. *Learning from Delayed Rewards.* PhD thesis, King's College, Oxford, 1989.

[105] Christopher J.C.H. Watkins and Peter Dayan. Technical note: Q-learning. *Machine Learning*, 8(3):279–292, May 1992. ISSN 1573-0565. doi: 10.1023/A:1022676722315. URL https://doi.org/10.1023/A:1022676722315.

[106] Lucian Buşoniu, Robert Babuška, and Bart De Schutter. *Multi-agent Reinforcement Learning: An Overview*, pages 183–221. Springer Berlin Heidelberg, Berlin, Heidelberg, 2010. doi: 10.1007/978-3-642-14435-6_7. URL https://doi.org/10.1007/978-3-642-14435-6_7.

[107] Amy Greenwald and Keith Hall. Correlated-q learning. In *Proceedings of the Twentieth International Conference on International Conference on Machine Learning*, ICML'03, pages 242–249. AAAI Press, 2003. ISBN 1-57735-189-4. URL http://dl.acm.org/citation.cfm?id=3041838.3041869.

[108] Yoav Shoham, Rob Powers, and Trond Grenager. If multi-agent learning is the answer, what is the question? *Artif. Intell.*, 171(7):365–377, May 2007. ISSN 0004-3702. doi: 10.1016/j.artint.2006.02.006. URL https://doi.org/10.1016/j.artint.2006.02.006.

[109] Michael Bowling and Manuela Veloso. Rational and convergent learning in stochastic games. In *Proceedings of the 17th International Joint Conference on Artificial*

Intelligence - Volume 2, IJCAI'01, pages 1021–1026, San Francisco, CA, USA, 2001. Morgan Kaufmann Publishers Inc. ISBN 1-55860-812-5, 978-1-558-60812-2. URL `http://dl.acm.org/citation.cfm?id=1642194.1642231`.

[110] Michael Bowling. Convergence and no-regret in multiagent learning. In *Proceedings of the 17th International Conference on Neural Information Processing Systems*, NIPS'04, pages 209–216, Cambridge, MA, USA, 2004. MIT Press. URL `http://dl.acm.org/citation.cfm?id=2976040.2976067`.

[111] Reinaldo A. C. Bianchi and Ramón López de Màntaras. Case-based multiagent reinforcement learning: Cases as heuristics for selection of actions. In *Proceedings of the 2010 Conference on ECAI 2010: 19th European Conference on Artificial Intelligence*, pages 355–360, Amsterdam, The Netherlands, The Netherlands, 2010. IOS Press. ISBN 978-1-60750-605-8. URL `http://dl.acm.org/citation.cfm?id=1860967.1861038`.

[112] N. Morozs, T. Clarke, and D. Grace. Distributed heuristically accelerated q-learning for robust cognitive spectrum management in lte cellular systems. *IEEE Transactions on Mobile Computing*, 15(4):817–825, April 2016. ISSN 1536-1233. doi: 10.1109/TMC.2015.2442529.

[113] Peter Stone and Manuela M. Veloso. Layered learning. In *Proceedings of the 11th European Conference on Machine Learning*, ECML '00, pages 369–381, London, UK, UK, 2000. Springer-Verlag. ISBN 3-540-67602-3. URL `http://dl.acm.org/citation.cfm?id=645327.649544`.

[114] Shai Shalev-Shwartz and Shai Ben-David. *Understanding Machine Learning: From Theory to Algorithms*. Cambridge University Press, New York, NY, USA, 2014. ISBN 1107057132, 9781107057135.

[115] Y. LeCun, B. Boser, J. S. Denker, D. Henderson, R. E. Howard, W. Hubbard, and L. D. Jackel. Backpropagation applied to handwritten zip code recognition. *Neural Computation*, 1(4):541–551, Dec 1989. ISSN 0899-7667. doi: 10.1162/neco.1989.1.4.541.

[116] D. Gunduz, K. Stamatiou, N. Michelusi, and M. Zorzi. Designing intelligent energy harvesting communication systems. *Communications Magazine, IEEE*, 52(1):210–216, January 2014.

[117] O. Ozel, K. Tutuncuoglu, J. Yang, S. Ulukus, and A. Yener. Transmission with Energy Harvesting Nodes in Fading Wireless Channels: Optimal Policies. *IEEE Journal on Selected Areas in Communications*, 29(8):1732–1743, 2011.

[118] M. Gregori and M. Payaró. Energy-Efficient Transmission for Wireless Energy Harvesting Nodes. *IEEE Transactions on Wireless Communications*, 12(3):1244–1254, 2013.

[119] M. Gatzianas, L. Georgiadis, and L. Tassiulas. Control of wireless networks with rechargeable batteries. *IEEE Transactions on Wireless Communications*, 9(2): 581–593, 2010.

[120] N. Michelusi, K. Stamatiou, and M. Zorzi. Transmission Policies for Energy Harvesting Sensors with Time-Correlated Energy Supply. *IEEE Transactions on Communications, to appear*, PP(99):1–14, 2013.

[121] J.V. Dave, P. Halpern, and H.J. Myers. Computation of incident solar energy. *IBM Journal of Research and Development*, 19(6):539–549, November 1975.

[122] A. F. Zobaa and R. C. Bansal. *Handbook of Renewable Energy Technology.* World Scientific Publishing Co., 2011. Edited Book.

[123] F.A. Lindholm, J.G Fossum, and E.L. Burgess. Application of the superposition principle to solar-cell analysis. *IEEE Transactions on Electron Devices*, 26(3): 165–171, 1979.

[124] A. Luque and S. Hegedus. *Handbook of Photovoltaic Science and Engineering.* Wiley, 2003.

[125] F. Ongaro, S. Saggini, S. Giro, and P. Mattavelli. Two-dimensional MPPT for photovoltaic energy harvesting systems. In *IEEE Workshop on Control and Modeling for Power Electronics (COMPEL)*, Boulder, Colorado, USA, June 2010.

[126] D. P. Hohm and M. E. Ropp. Comparative study of maximum power point tracking algorithms. *Wiley Progress in Photovoltaics: Research and Applications*, 11(1):47–62, January 2003.

[127] D. Brunelli, L. Benini, C. Moser, and L. Thiele. An Efficient Solar Energy Harvester for Wireless Sensor Nodes. In *IEEE Design, Automation and Test in Europe (DATE)*, pages 104–109, Munich, Germany, March 2008.

[128] Jeffrey S. Simonoff. *Smoothing Methods in Statistics.* Springer-Verlag, 1996.

[129] Solarbotics Ltd. SCC-3733 Monocrystalline solar cells. `http://solarbotics.com/`.

[130] Solar-Stat: an Open Source Framework to Model Photovoltaic Sources through stochastic Markov Processes, 2013. URL `http://www.dei.unipd.it/~rossi/software.html`.

[131] M. Mezzavilla, M. Miozzo, M. Rossi, N. Baldo, and M. Zorzi. A lightweight and accurate link abstraction model for system-level simulation of lte networks in ns-3. In *Proc. of ACM MSWIM*, October 2012.

[132] Eyal Even-Dar and Yishay Mansour. Learning rates for q-learning. *J. Mach. Learn. Res.*, 5:1–25, December 2004. ISSN 1532-4435.

[133] 3GPP. TS 36.423; X2 Application Protocol (Rel.15), 2018.

[134] M. E. Harmon and S. S. Harmon. Reinforcement learning: A tutorial. 2000. URL `http://www.nbu.bg/cogs/events/2000/Readings/Petrov/rltutorial.pdf`.

[135] Languang Lu, Xuebing Han, Jianqiu Li, Jianfeng Hua, and Minggao Ouyang. A review on the key issues for lithium-ion battery management in electric vehicles. *Journal of Power Sources*, 226:272–288, 2013.

[136] Xi Li, G. Landi, J. Núñez-Martínez, R. Casellas, S. González, C. F. Chiasserini, J. Rivas Sanchez, D. Siracusa, L. Goratti, D. Jimenez, and L. M. Contreras. Innovations through 5g-crosshaul applications. In *2016 European Conference on Networks and Communications (EuCNC)*, pages 382–387, June 2016. doi: 10.1109/EuCNC.2016.7561067.

[137] M. Miozzo, L. Giupponi, M. Rossi, and P. Dini. Switch-on/off policies for energy harvesting small cells through distributed q-learning. In *2017 IEEE Wireless Communications and Networking Conference Workshops (WCNCW)*, pages 1–6, March 2017. doi: 10.1109/WCNCW.2017.7919075.

[138] Fengli Xu, Yong Li, Huandong Wang, Pengyu Zhang, and Depeng Jin. Understanding Mobile Traffic Patterns of Large Scale Cellular Towers in Urban Environment. *IEEE/ACM Trans. Netw.*, 25(2):1147–1161, April 2017. ISSN 1063-6692. doi: 10.1109/TNET.2016.2623950. URL `https://doi.org/10.1109/TNET.2016.2623950`.

[139] Paolo Dini, Nicola Piovesan, Dagnachew A. Temesgene, and Marco Miozzo. Toward the Energy Self-Sufficiency of Mobile Networks via Intelligent Traffic Load Management. *submitted to IEEE Communications Magazine - Green Communications and Computing Networks Series.*

[140] Earth Notes. On Variations in GB Grid Electricity CO2 Intensity. `http://www.earth.org.uk/note-on-UK-grid-CO2-intensity-variations.html`.

[141] H. D. Trinh, N. Bui, J. Widmer, L. Giupponi, and P. Dini. Analysis and modeling of mobile traffic using real traces. In *2017 IEEE 28th Annual International Symposium on Personal, Indoor, and Mobile Radio Communications (PIMRC)*, pages 1–6, Oct 2017. doi: 10.1109/PIMRC.2017.8292200.

[142] J. Hu and M. P. Wellman. Nash Q-learning for general-sum stochastic games. *Journal on Machine Learning Research*, 4:1039–1069, 2003.

[143] A. Aissioui, A. Ksentini, A. M. Gueroui, and T. Taleb. Toward elastic distributed sdn/nfv controller for 5g mobile cloud management systems. *IEEE Access*, 3: 2055–2064, 2015. doi: 10.1109/ACCESS.2015.2489930.